MODELING OF A MEMBRANE MICRO-CHANNEL REACTOR FOR A WATER GAS SHIFT REACTION

A DISSERTATION

Submitted in partial fulfilment of the requirements for the award of the degree of

MASTER OF TECHNOLOGY

in

CHEMICAL ENGINEERING

(With Specialization in Computer Aided Process Plant Design)

By

SUSHMABEN RAMASHANKAR GUPTA

DEPARTMENT OF CHEMICAL ENGINEERING
INDIAN INSTITUTE OF TECHNOLOGY ROORKEE
ROORKEE -247 667 (INDIA)
JUNE, 2008

CANDIDATE'S DECLARATION

I hereby declare that the work which is being presented in this dissertation entitled **"MODELING OF A MEMBRANE MICRO-CHANNEL REACTOR FOR A WATER GAS SHIFT REACTION"**, in partial fulfillment of the requirements for the award of the degree of **Master of technology** in **Chemical Engineering** with specialization in "**Computer Aided Process Plant Design(CAPPD)**", and submitted in the **Department of Chemical Engineering** of **Indian Institute of Technology, Roorkee**, is an authentic record of the work carried out by me during the period July 2007 to June 2008, under the guidance of **Dr. SURENDRA KUMAR, Professor and Dr. AMIT K. DHIMAN, Lecturer** of Chemical Engineering Department, Indian Institute of Technology Roorkee, Roorkee.

The matter embodied in this dissertation work has not been submitted by me for the award of any other degree of this or any other Institute/ University.

Date: June-2008
Place: ROORKEE

Sushmaben 23/6/08
(SUSHMABEN RAMASHANKAR GUPTA)

CERTIFICATE

This is to certify that the above statement made by the candidate is correct to the best of my knowledge.

Amit 23/6/08
(Dr. AMIT K. DHIMAN)
Lecturer

23/6/08
(Dr. SURENDRA KUMAR)
Professor

Department of Chemical Engineering,
Indian Institute of Technology, Roorkee
ROORKEE-247667 (INDIA)

ACKNOWLEDGEMENT

The gratitude is the memory of the heart and in carrying out this dissertation work, persistent inspiration, unflinching support and encouragement of countless persons have served as the driving force.

I am greatly indebted to my guide **Dr. SURENDRA KUMAR,** Professor and **Dr. AMIT K. DHIMAN,** Lecturer of Chemical Engineering Department, Indian Institute of Technology Roorkee, for their guidance and support during the entire course of the work. Their cooperation and in depth knowledge have made my work possible. I would like to sincerely acknowledge their valuable guidance, relentless support, discerning thoughts and loads of inspiration that led me forward to delve deeper into the issue.

I wish to express my profound sense of gratitude to **Dr. (Mrs.) SHASHI,** Assistant Professor of Chemical Engineering Department, Indian Institute of Technology Roorkee, for her constructive suggestions, moral support and constant encouragement during the course of this dissertation work.

I would like to thank **Dr. SHRI CHAND,** Prof. and Head of the Department and DRC Chairman for providing various facilities during the course of this dissertation work.

I would like to especially thank to Ms. Tripta Garg for her kind cooperation and pleasant manner. Special thanks are also due to Sh.Mange Ram, Mr. Rahman of Reaction Engineering Research (RER) Lab, Sh.Akhilesh Kumar of the CAD centre of Department.

I would like to thank all of my friends and well wishers for their suggestion and help in completion of this dissertation work.

Last but not least, I sincerely acknowledge the support and guidance of my parents for their encouragement and moral support.

23/6/08

(SUSHMABEN RAMASHANKAR GUPTA)

ABSTRACT

Micro-channel reactor offer unique possibilities for temperature control of chemical reaction due to the strong coupling of channel and wall temperature. For the reformation of hydrocarbons for fuel-cell applications a low CO conversion of the product gas is desired. For every gas composition arising during the reaction process an optimum temperatures exists at which the reaction rate is highest. We have demonstrate that this optimum temperature profile to a good approximation can be achieved in a single step water gas shift reactor by controlling the temperature via cooling gas flowing in parallel to the reformate. Here, we have discusses the development of an integrated reaction and heat exchange approach to micro-channel reactor design that enhances the reaction yields. We detail the formulation of one-dimensional models for micro-channel reactor with and without heat conduction through the wall-channel and apply these models to study WGS reaction. The parametric study investigated the sensitivities of design parameters of the micro-channel reactor. Results from study are presented and discussed, and the optimized operating parameters are identified for the both case of micro-channel reactor. We also detail the formulation of one-dimensional models for membrane micro-channel reactor with the consideration of heat conduction through the wall-channel and apply these models to WGS reaction. We also considered the case of membrane micro-channel reactor without the heat conduction through the wall-channel and also with and without heat exchange stream-cooling medium i.e. air. For this case, we have used the optimized parameters to study WGS for the three case of membrane micro-channel reactor. Here, we have considered palladium as membrane for this study which has an infinite selectivity towards H_2 against any other species. The synthesis gases from a steam reformer or autothermal reactor are used as the feed gas, while we have considered there is no sweep gas. A published WGS reaction rate with the commercial 5 wt. % copper on alumina catalyst is incorporated into the model. From our study, we have seen that we need small micro-channel reactor length with heat conduction as compared to without heat conduction through wall-channel.

NOMENCLATURE

ATR	Auto thermal reforming
HTS	High temperature shift conversion
LTS	Low temperature shift conversion
MMCR	Membrane micro-channel reactor
MMR	Micro-channel reactor
PEMFC	Polymer electrolyte membrane fuel cells
POX	Catalytic partial oxidation reaction
PrOX	Non-catalytic partial oxidation reaction
SR	Steam reforming
WGSR	Water-gas shift reaction
μTAS	Micro-total analytical system

Symbols

E	Activation energy (kJ/mol)
R	Universal gas constant (8.314 J/mol K)
T	Absolute temperature (K)
a	Aspect ratio of channel i (dimensionless)
ΔH	Heat of reaction (kJ/mol)
ΔV	Incremental volume (m^3)
Δz	Incremental z (m)
A	Cross-sectional area of reaction-channel (m^2)
A_2	Cross-sectional area of wall-channel (m^2)
b	Width of rectangular channel (mm)
b_2	Fin thickness of wall-channel (mm)
C_i	Concentration of i^{th} species (kPa)
C_p	Heat capacity (J/kg K)

D	Diffusivity of hydrogen through palladium (m^2/s)
D_0	Diffusivity pre-exponential coefficient (m^2/s)
d_i	Hydraulic diameter of channel i (m)
dz	Derivative with respect to the z coordinate (m^{-1})
E_D	Activation energy for diffusion (kJ/mol)
F_i	Molar flow rate of i^{th} species (mol/s)
h_1	Cooling channel height (mm)
h_2	Wall channel height (mm)
$h_3 = R_2$	Reaction channel height or inside diameter of the shell (mm)
$h_{c,i}$	Surface convective heat transfer coefficient of channel i ($W/m^2 K$)
J	Permeation flux (mol/ m^2 s)
K	Sievert's constant ($kPa^{0.5}$ m^3 / mol)
k_3	Specific reaction rate (mol g^{-1} s^{-1} kPa^x)
K_3	Equilibrium constant (dimensionless)
k_{cat}	Thermal conductivity of the catalyst (W/ m K)
k_e	Effective thermal conductivity of the reactant (W/ m K)
k_f	Thermal conductivity of the fluid (W/ m K)
mw	Average molecular weight of the reactant stream (gm/mol)
Nu	Nusselt number (dimensionless)
P	Pressure (kPa)
$P_{H_2,SW}$	Pressure of hydrogen in the shell side (kPa)
P_i	Partial pressure of i^{th} species (kPa)
Q	Permeation coefficient (mol/ $kPa^{0.5}$ m s)
Q_i	Heat flow in channel i (W)
r	Reaction rate (mol/ m^3 s)
r'	Reaction rate per weight of catalyst (mol g^{-1} s^{-1})
R_1	Outside diameter of tube (mm)
T_4	Permeation Stream temperature (K)

T_i	Temperature in channel i (K)
U	Overall heat transfer coefficient (W/ m^2 K)
u_1	Heat exchange stream velocity i.e. air (m/s)
U_i	Heat transfer coefficient of channel i (W/ m^2 K)
U^M	Overall heat transfer coefficient through the membrane (W/ m^2 K)
V_i	Volumetric flow rate in channel i (m^3/s)
W_i	Heat capacity flow rate in channel i (W/K)
w_i	Circumference of channel i (m)
X_{co}	Conversion of carbon monoxide
y_i	Mole fraction of i^{th} species (dimensionless)
Z	Length of micro-channel Reactor (mm)
z	Coordinate along channel (m)

Greek letters

δ	Thickness of membrane (nm)
ε	Porosity of the reactant bed (dimensionless)
λ_2	Thermal conductivity of the wall (W/ m K)
ρ	Density (kg/ m^3)
ρ_b	Bulk catalyst density (kg/ m^3)
υ_i	Stoichiometric coefficient of i^{th} species (dimensionless)

Subscripts

f	Fluid
i	Reactant species i
M	Membrane
0	Condition at the inlet (z = 0)
1	Heat exchange stream: cooling channel
2	Wall channel
3	Reactant stream: reaction channel

CONTENTS

LIST OF FIGURES

LIST OF TABLES

CHAPTER 1

INTRODUCTION

1.1. WATER GAS SHIFT REACTION

1.1. 1. INTRODUCTION

WGS reactor is one of the critical components of a multi-reactor fuel processing system that supports distributed energy production through the use of a fuel cell [75]. Fuel cell is an efficient energy conversion device for both transportation and stationary power generation. It converts chemical energy directly into electrical energy, which is about two times more efficient than internal combustion engine in terms of gas mileage [75]. On the other hand, fuel cell is also an environmental friendly device; water is the only emission when hydrogen is the fuel. Although pure hydrogen is a superior fuel cell, currently there are issues on its storage and distribution [16]. As a more practical way, hydrogen used in an automotive fuel cell is suggested to be produced by reforming reactions of the available fuels, such as methanol, natural gas, gasoline and diesel [35]. The fuel processor produces hydrogen-rich streams from hydrocarbon based feed stocks in a multi-step process (fuel vaporizer, primary conversion reactor that produces synthesis gas, water gas shift reactor, and CO clean-up reactor). Several fuel processors are currently under industrial development. One option for a complete fuel processing system is described in Fig.1.1. Additional primary conversion reactors are also under investigation. The options for the production of synthesis gas from a gaseous or liquid hydrocarbon fuel include catalytic partial oxidation (POX), non-catalytic partial oxidation (PrOX), steam reforming (SR), and auto-thermal reforming (ATR). In SR, steam reacts with hydrocarbon over a catalyst to form H_2, CO and CO_2 at around 750–800°C since this reaction is strongly endothermic. In POX, the hydrocarbon reacts with a deficient amount of oxygen or air to produce H_2, CO and CO_2 while a large amount of heat is generated. ATR integrates these two processes together by feeding the hydrocarbon, water, and air together into the reactor at the same time. The SR reaction absorbs most of the heat generated by the POX reaction, and an overall process takes place slightly exothermally [10].

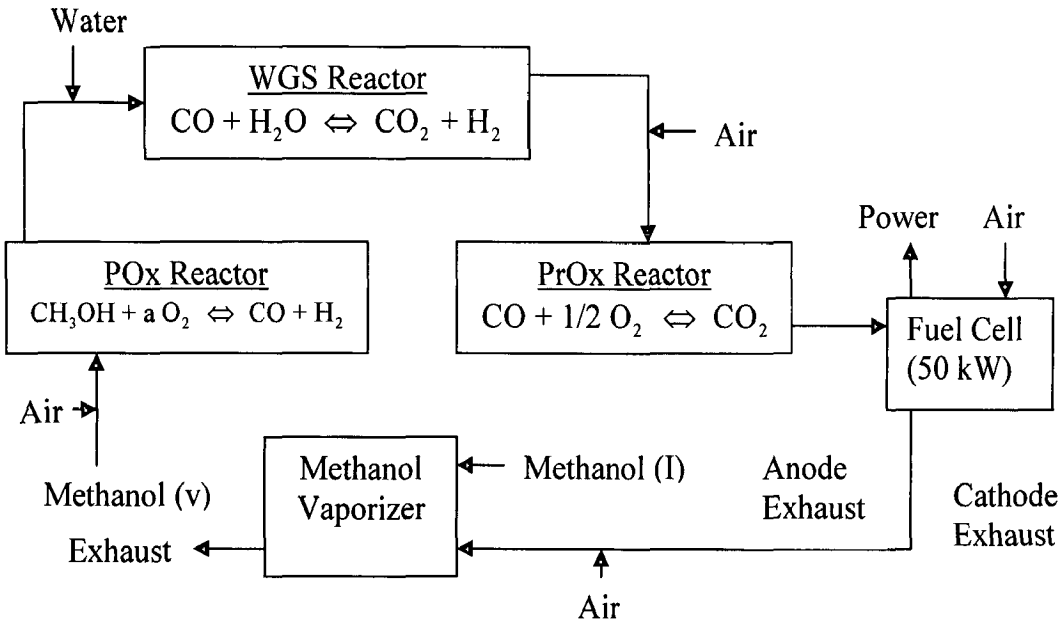

Fig.1.1. Complete fuel processing system

The inlet of the water gas shift reactor is the effluent of the primary conversion reactor, upon whose product composition served as the basis for selection of water gas shift feed conditions [75]. To design an efficient fuel reformer and to optimize its operating conditions, knowing the kinetics for steam reforming and water gas shift is critical. In most hydrocarbon processors, the water gas shift reactor is the biggest and heaviest component because the reaction is relatively slow compared to the other reactions and is inhibited at higher temperatures by thermodynamics. Therefore, reducing the size of the water gas shift reactor is an important issue. For fuel cell applications, a compact, efficient and reliable fuel processor is highly desirable. To design a compact fuel reformer system using process simulation and optimization, WGS reaction kinetics are a required and key component [19]. Being reversible and exothermic, the WGS reaction in the traditional fixed bed reactor is not efficient [35]. Recently, a renewed interest in the water-gas shift reaction has occurred, arising from the need for pure hydrogen production in conjunction with the development of fuel-cell power systems. Moreover, the WGS reaction is also one of the key steps involved in automobile exhaust processes, since the hydrogen produced is a very effective reductant for NO*x* removal [6]. The water gas shift reaction is an historical and industrially important reaction in the fuel reformer because of the reactor's size. It is

important to include the effects of other reactions in the reforming system: hydrocarbon reforming and CO selective oxidation, when designing the WGS reactor. In particular, research activity is growing in catalyst characterization, kinetic and reactor modeling and new catalyst formulation [19].

The Water Gas Shift Reaction is typically a heterogeneous reaction of gas phase reactant and solid phase catalyst, which is usually in the form of pellets through which the reactant stream flows. It catalytically converts carbon monoxide (CO) (produced in the primary conversion stage of the fuel processor) [75] and water (H_2O) to produce hydrogen (H_2) and carbon dioxide (CO_2). It is a weakly exothermic [indicated by the negative heat load (ΔH)], reversible reaction in accordance with the following equation:

$$CO + H_2O \Leftrightarrow CO_2 + H_2 \qquad \Delta H^{\circ}_{298} = -41 \text{ kJ/mol} \tag{1.1}$$

At low temperatures, the reaction favors the forward shift reaction, while at high temperatures the reverse reaction dominates [46]. In view of its industrial importance, the water-gas shift reaction has been the subject of numerous theoretical and mechanistic studies. At present, when the production of high-purity hydrogen is required the water-gas shift reaction is carried out in two distinct stages, using catalysts that have been specifically designed for each stage. The first step involves a high-temperature conversion (HTS) (300-400°C) using an iron-chromium spinel catalyst, which decreases the CO concentration from an initial value of 35-40 mol% to 3 mol%. Conversion of the remaining carbon monoxide is carried out in a lower-temperature (LTS) process stage (200-250°C) since the equilibrium CO concentration decreases with decreasing reaction temperature. The catalyst used in this second step is a high-activity copper-zinc oxide. LTS are preferred in most cases, due to equilibrium conditions and low-temperatures of hydrocarbon and methanol reforming [16]. The formulations of both these catalysts have been optimized for the conversion of CO/H_2 feed-stocks, derived from hydrocarbon steam reforming, which are relatively free from sulphur impurities [37, 64].

1.1.2. APPLICATIONS

The water gas shift reaction has many applications and some of them are as follows:

1. The water-gas shift reaction is one of the most important industrial reactions for future energy technologies [26, 29]. This reaction can take place whenever carbon monoxide and water are present and therefore it may be an important step or side reaction in many processes [42]. Demand for hydrogen, a product of the shift reaction, will undoubtedly become even greater in the future, since new uses for hydrogen are expected to appear, such as in coal liquefaction and gasification, hydro treatment of heavier petroleum and shale oil liquids, and its use as a direct fuel [5].
2. After the development of the low temperature shift catalyst composed of copper and zinc oxide during the 1960s, the main application of WGS reaction has been hydrogen production for ammonia synthesis or other industrial processes such as hydro- treating of petroleum stocks. However, recently a new application for the WGS reaction is in reforming systems for fuel cells [19].
3. The chemical industry utilizes considerable quantities of hydrogen in the production of chemical products and intermediates, e.g., ammonia synthesis from the reaction of nitrogen with hydrogen or methanol synthesis from carbon monoxide hydrogenation. The hydrogen is primarily obtained, in most locations, by the steam reforming of methane or higher hydrocarbons, a reaction which produces CO and H_2 as the principal products. For most applications the hydrogen concentration of the product gases is insufficient and in this case, the WGS reaction is extensively used to adjust the CO/H_2 ratio for the subsequent synthesis gas i.e. methanol, to produce hydrogen for ammonia synthesis and to detoxify gases [37, 42]. As it is used to increase the H_2 content in synthesis gas, is an important part of ammonia or a hydrogen plant [61].
4. For transportation fuel cell applications, one of the key issues is the purity of hydrogen. Even a very small amount of CO in the hydrogen, e.g., >10 ppm, will deteriorate the fuel cell performance by poisoning platinum, which works as the electro-catalyst in polymer electrolyte membrane fuel cells. WGSR is one of the steps in the overall process of producing hydrogen and ammonia from natural gas.

The role of WGSR is to reduce carbon monoxide levels and obtain additional hydrogen [46, 29, and 5].

5. In a steam reformer, methanol and steam react to produce hydrogen and carbon dioxide, and also significant amounts of carbon monoxide as byproduct. Carbon monoxide poisons the catalyst in fuel cells and therefore, the reformate stream needs to be further treated to remove CO. While high temperature fuel cell membranes that are tolerant to CO are currently being investigated, in general, purifying the hydrogen stream using a micro-membrane remain important design options in micro-reformers [59, 19]. It is possible to use micro-structured reactors in secondary hydrogen cleaning systems [31].

1.1.3. DIFFERENT CATALYSTS

The water-gas shift reaction is usually carried out on a metal oxide catalyst. Depending on the reaction temperature, various catalysts are used. Catalyst texture and structure and feed mixture composition are strongly affect the kinetics and mechanism of the WGSR. The WGSR is a reversible and exothermic reaction, many materials being capable of catalyzing it. A large number of metals, metal oxides and mixed oxides have been proposed and patented to catalyze the water-gas shift reaction (Fe, Cu, Zn, Cr, Co, Ni oxides and combinations of these oxides). In industry Fe_3O_4-Cr_2O_3 and $Cu/ZnO/Al_2O_3$ are used almost exclusively [18].

1.1.3.1 Copper-based shift catalysts

Copper-based shift catalysts arise from a more recent development which has gained wide industrial acceptance. These are the so-called low-temperature shift catalysts, operating from 453 to 523 K. These catalysts have good activity at low temperature and are therefore attractive, since equilibrium is more favorable at lower temperature. In addition to higher activity, another advantage claimed for the low-temperature shift catalysts is higher selectivity and fewer side reactions at high pressures [5]. Model catalysts based on Cu single crystals have very well-controlled surface cleanliness and geometric structure. WGSR is a structure-insensitive reaction, as the specific reaction rate r_o (mol CO/h/g Cu) is always proportional to the copper metal surface area irrespective of changing the Al/Zn

ratio, the mean copper crystallite size, and/or the copper loading. Preparation of mixed oxides with a high copper dispersion is therefore required for obtaining more active catalysts. Because copper exhibits a high activity and selectivity as compared to other metals, Cu-based catalysts are preferentially used to catalyze this reaction at low temperatures (443-523 K) and low concentrations of carbon monoxide, in the so called low-temperature CO-shift process.

1.1.3.2 Cu-Zn-Al mixed oxide catalyst

Binary CuO/ZnO and ternary $CuO/ZnO/Al_2O_3$ mixed oxide catalysts have been widely employed commercially since the early 1960s in WGSR. The low temperature Cu/ZnO catalysts are widely used which has the high-surface-area [26]. The commercial $Cu/ZnO/Al_2O_3$ catalyst is the most active catalyst of the catalysts examined at low temperatures, e.g. at 160-250 °C. The $Cu/ZnO/Al_2O_3$ mixed oxides should contain CuO in a finely dispersed phase in order to obtain WGS catalysts exhibiting superior activity. In $Cu/ZnO/Al_2O_3$ catalysts copper provides the active sites for catalysis. For a given copper loading, $Cu/ZnO/Al_2O_3$ catalysts are substantially more active than Cu/ZnO catalysts. The addition of aluminium, although inactive for the WGS reaction, is required for improving the catalyst performance [29].

1.1.3.3 Gold-based catalysts

A number of gold-based catalysts on different supports have been successfully used in these reactions at low temperatures. The prerequisite for the synthesis of a highly active gold supported catalyst is not only to obtain a high dispersion of gold particles but also to choose an appropriate support for the reactions. The activity and especially the stability of the gold catalysts depend on both the state and structure of the support and the specific interaction between gold and the support [6].

1.1.3.4 Cobalt-based oxide catalyst

Cobalt molybdenum oxide catalysts are more active than the iron chromium oxide or copper-zinc oxide catalysts in the temperature range 350-400°C to design a high-activity catalyst suitable for use with sulphur-containing feedstock. The cobalt manganese oxide

catalyst is particularly effective for the conversion of high inlet carbon monoxide concentrations and, hence, may be more useful for the conversion of coal-derived CO/H_2. A cobalt chromium oxide is used as catalysts for a broad range of reactions including ammonia oxidation, hydrocarbon oxidation, and automobile exhaust pollution control. Cobalt chromium oxide catalyst demonstrated very little catalytic activity below 250°C, and in general, catalytic activity increased markedly between 250 and 350°C. The cobalt chromium oxides are classified as high-temperature shift catalysts [37].

1.1.3.5 Iron-oxide catalyst

Iron oxides- Fe_3O_4-Cr_2O_3 catalysts are used at 300-400 °C where equilibrium effects the composition of the product gas. Therefore, in industry this reaction is often run in two stages to guarantee the total conversion of carbon monoxide to carbon dioxide. The catalyst used in the second state is $Cu/ZnO/Al_2O_3$, which is active already at 200-250 °C and the reaction is thus not equilibrium limited [42]. The iron-chromium oxide as high-temperature water-gas shift catalyst is originally formulated for use with coal-derived CO/H_2 and in the sulphided form this catalyst retains about half the activity of the non-sulphided material.

1.1.4. DIFFERENT MECHANISMS

Although numerous studies of the reaction kinetics and mechanism for the water gas shift reaction have been reported during the past few decades, there are still disagreements and contradictory reports over the active site and the reaction mechanism. Reduced particle size leads to significant pressure drop that should be accounted for in the analysis of the rate constant [19].

1.1.4.1 Formate mechanism

In which surface hydroxyls (OH_a) produced from dissociatively adsorbed H_2O combine with adsorbed CO (CO_a) to produce a surface formate intermediate ($HCOO_a$), which then decomposes to 1/2 H_2 and CO_2 [26].

$$H_2O \rightarrow OH_{(a)} + \tfrac{1}{2} H_2 \quad (1.2)$$

$$CO_{(a)} + OH_{(a)} \rightarrow HCOO_{(a)} \quad (1.3)$$

$$HCOO_{(a)} \rightarrow CO_2 + \tfrac{1}{2} H_2 \quad (1.4)$$

1.1.4.2 Surface redox or regenerative mechanism

The surface redox mechanism is based on the adsorption and dissociation of water on the catalytic surface. Here, dissociation of adsorbed water is the controlling rate [5]. It used to successfully describe the kinetics of the forward water-gas shift over Cu [29].

$$H_2O + Red \rightarrow H_2 + Ox \quad (1.5)$$

$$CO + Ox \rightarrow CO_2 + Red \quad (1.6)$$

where, Red represents a reduced site and Ox an oxidized site.

The regenerative mechanism is the cycling of two steps [reactions (1.5) and (1.6)]. In the first step, water adsorbs and dissociates on reduced sites of catalyst surface to produce hydrogen while oxidizing a site. In the following step, CO is oxidized to CO_2 on these oxidized sites [19]. The structure-sensitivity of the WGS reaction on copper would therefore be related to the water dissociation for producing O_x and hydrogen. The step 1 is not sensitive to modifications of catalyst parameters, at least under the standard reaction conditions [29].

1.1.4.3 Adsorptive mechanism

In the adsorptive mechanism, CO and H_2O adsorb on the catalyst surface and form an intermediate which results in desorbed hydrogen and CO_2 [19].

$$H_2O + CO \rightarrow CO_{(ads)} + H_2O_{(ads)} \rightarrow [int^*] \rightarrow CO_2(ads) + H_2(ads) \rightarrow CO_2 + H_2 \quad (1.7)$$

1.1.4.4 Langmuier Hinshelwood mechanism

An alternating oxidation-reduction process could be significant at the beginning of the transient reaction period on the activated catalyst, but the main reaction path probably consists of a Langmuier-Hinshelwood mechanism [5] involve a surface formate intermediate [29]. In Langmuier-Hinshelwood mechanism, dissociation of adsorbed water

is the determining step. It involves a surface formate intermediate. Langmuir-Hinshelwood model, which considers the adsorption of four species (CO, CO_2, H_2 and H_2O) and the surface reaction as the controlling step, adequately describes the reaction behavior at the given temperature and concentration ranges. It is useful in designing industrial low temperature converters [5].

1.1.4.5 Dissociative mechanism

Dissociative mechanism proceeding via a lattice or adsorbed oxygen intermediate, in this mechanism water dissociates to form a surface-adsorbed oxygen species which subsequently reacts with CO to form CO_2.

$$H_20_{(g)} + * \rightarrow H_2 + O_{(a)} \quad (1.8)$$

$$CO_{(g)} + O_{(a)} \rightarrow CO_2 \quad (1.9)$$

where * is a vacant surface site.

The reaction (1.8) may occur via a hydroxyl intermediate [37].

1.1.4.6 Associative mechanism

Associative mechanism involves an adsorbed formate intermediate. For the associative mechanism, adsorbed CO reacts with a surface hydroxyl species to form an adsorbed formate intermediate which subsequently decomposes to CO_2 and H_2. [37]

1.1.5. VARIOUS RATE EXPRESSIONS

Different mechanisms, various elementary reaction paths, and different rate determining steps and assumptions as to the active sites of the catalyst, create numerous rate expressions. Table.1.1 presents the different rate expressions reported in the literature.

Table 1.1 Different rate expressions reported in the literature

S. No.	Description	Rate expression
1.	Derived from LangmuierHinshelwood model with assumption of surface reaction is rate controlling [19].	$r_{CO} = k \dfrac{\left(p_{H_2O}p_{CO} - \dfrac{p_{H_2}p_{CO_2}}{K_P}\right)}{[1 + K_1p_{CO} + K_2p_{H_2O} + K_3p_{CO_2} + K_4p_{H_2}]^2}$ (1.10)
2.	Derived from Adsorptive mechanism with assumption of single path reaction mechanism [19].	$r_{CO} = k \dfrac{\left(p_{H_2O}p_{CO} - \dfrac{p_{H_2}p_{CO_2}}{K_P}\right)}{[1 + K_1p_{H_2O} + K_3p_{CO_2}]}$ (1.11)
3.	Derived from redox mechanism and confirmed its validity using Cu-Zn-Cr catalysts [19].	$r_{CO} = k \dfrac{\left(p_{H_2O}p_{CO} - \dfrac{p_{H_2}p_{CO_2}}{K_P}\right)}{[p_{H_2O} + p_{CO}]}$ (1.12)
4.	Derived from redox mechanism with assumption of single path reaction model [19]	$r_{CO} = \dfrac{k_1k_2\left(p_{H_2O}p_{CO} - \dfrac{p_{H_2}p_{CO_2}}{K_P}\right)}{[k_1p_{H_2O} + k_2p_{CO} + (k_{1-} + k_{2-})\, p_{CO_2}]}$ (1.13)
5.	Simple reversible rate expression for CO conversion which do not consider any mechanism [19].	$r_{CO} = k\left(p_{H_2O}p_{CO} - \dfrac{p_{H_2}p_{CO_2}}{K_P}\right) = kp_{CO}p_{H_2O}(1-\beta)$ (1.14) where, $\beta = \left(\dfrac{p_{H_2}p_{CO_2}}{p_{H_2O}p_{CO}Keq}\right)$, (1.15) and empirical rate expression given by, $r_{CO} = 1.85 \times 10^{-5} \exp\left(12.88 - \dfrac{1855.5}{T}\right)p_{CO}p_{H_2O}(1-\beta)$ (1.16)

6.	Power-law type rate expression with consideration of WGSR is not a simple order reaction, especially at higher steam/CO ratios [19].	$r_{CO} = k\, p^{n}_{CO} p^{m}_{H_2O} (1-\beta)$ (1.17)
7.	Derived from the numerical fitting [19].	$r_{CO} = 2.96 \times 10^{5} \exp\left(-\frac{47400}{RT}\right)\left(p_{CO}p_{H_2O} - \frac{p_{CO_2}p_{H_2O}}{Ke}\right)$ (1.18)
8.	This rate expression is proposed by Mann et al. which clearly validates the experimental results [59].	$r_{CO} = \frac{K\exp\left(\frac{p_{H_2O}p_{CO}}{p_{H_2}^{1/2}}\right)\left(1 - \frac{p_{H_2}p_{CO_2}}{Keq\, p_{H_2O}p_{CO}}\right)}{\left[+k_1 p_{CO_2} p_{H_2}^{1/2} + k_2\left(\frac{p_{H_2O}}{p_{H_2}^{1/2}}\right)\right]^2}$ (1.19) where, $K_1 = \exp\left(9.12 - \frac{4870}{T}\right)$, $K_2 = \exp\left(-3.28 + \frac{854}{T}\right)$, $K = K\exp\left(1 + \frac{636 p_{CO\text{-}av}}{T}\right)^2$ (1.20)
9.	This rate expression proposed by Mizsey et al. with 5% cu on alumina catalyst which we have used for our work [59].	$r_{CO} = k_3 p_{CO} p_{H_2O}\left(1 - \frac{p_{CO_2}p_{H_2}}{K_3 p_{CO} p_{H_2O}}\right)\left(\frac{mol}{g\text{-}cats}\right)$ (1.21) where, $Keq \cong \left(\frac{p_{CO_2}p_{H_2}}{p_{CO}p_{H_2O}}\right)$ or $Keq = \exp\left(\frac{4577.8}{T} - 4.33\right)$ (1.22)

1.1.6. EQUILIBRIUM CONSTANT

According to thermodynamic properties and relations the equilibrium constant for the water gas shift reaction is give by the following equation:

$$\ln(\mathrm{Keq}) = \frac{5693.5}{T} + 1.077 \ln \mathrm{T} + 5.44 \times 10^{-4} T - 1.125 \times 10^{-7} \mathrm{T}^2 - \left(\frac{49170}{T^2}\right) - 13.148 \qquad (1.23)$$

$$\text{where, Keq} \cong \left(\frac{p_{CO_2} p_{H_2}}{p_{CO} p_{H_2O}}\right) \qquad (1.24)$$

Simpler equation for *K*eq is given by Moe [21]:

$$\mathrm{Keq} = \exp\left(\frac{4577.8}{\mathrm{T}} - 4.33\right) \qquad (1.25)$$

According to the above equations [Eqs. 1.23-1.25], the equilibrium constant of WGSR is 210 at 200 °C and 38.8 at 300 °C. Very low CO exiting concentrations requires very low temperatures and/or high water to CO ratios [19]. WGSR is not a simple first-order reaction in the carbon monoxide activity. However, the first-order rate equation describes the phenomenon quite well. For the commercial catalysts examined, the power-law rate model where the concentration exponent of carbon monoxide is close to one and the concentration exponent of water is a small positive number close to zero gives the best results [42].

1.1.7. VARIOUS PARAMETERS

The design of a WGS reactor used to generate fuel cell grade hydrogen must choose several operating parameters subject to several constraints. Five critical design constraints include: (1) the inlet gas composition, (2) the inlet gas flow rate, (3) the temperature exiting the reforming reactor, (4) the exiting CO concentration constraint of the down stream processes, and (5) the water requirements for proper operation of the fuel cell. For the case of methanol steam reforming, the gas typically contains H_2 and CO in a ratio between 2 and 3, with some residual water. The WGS reactor design parameters used to meet these constraints include: (1) reactor temperature; (2) water addition rate; and (3) reactor size (weight of catalyst) [59, 19].

1.1.8. LIMITATIONS

Applying the empirical kinetic relationship in a simple isothermal plug flow model shows that to maintain a constant CO and water concentration exiting the reactor requires controlling the reactor temperature and the water addition rate closely. These two exiting compositions are important to maintain steady operation of the fuel cell. Large variations in CO concentration will make downstream oxidation of CO more difficult to control, resulting in fluctuating CO concentrations entering the fuel cell, which will result in fluctuating current and voltages. Large variations in water exiting the WGS reactor will make controlling the moisture needed for proper PEM operation more difficult [19].

1.2. MICRO-CHANNEL REACTOR

1.2.1. INTRODUCTION

The micro0reaction technology is now a days one of the most innovative and rapid developing fields in chemical engineering, synthesis and process technology [45]. By using the tools of micro-fabrication, several novel reactor configurations can be fabricated allowing different designs that would not have been possible with conventional packed beds. Such systems, referred to as micro-channel reactors or micro-reactors, typically have dimensions in the sub-millimeter range, the effect being a reduction in diffusive transport limitations [55]. The micro-reactor is usually a continuous flow reactor (contrast with/to a batch reactor). For a reaction engineer, the term "micro-reactor" traditionally has meant a small tubular reactor for testing catalyst performance, but with the widening use of micro-fabrication technologies, the "micro" prefix generally designates chemical systems fabricated with techniques originally developed for electronic circuits. Such systems have feature sizes in the sub-millimeter range and reaction components are usually integrated with sensors and actuators [39]. A micro-reactor is a reactor whose dimension is of the order of 100 μm [60]. These small reactors are already used in testing process chemistries; for example, catalyst testing often employs small tubular reactors formed by filling powdered catalysts into glass tubes [39]. Areas that have attracted most research to date have centered on gas and liquid phase reactions covering heterogeneous and homogeneous catalysis, catalytic oxidation, heterocyclic synthesis, and photochemical reactions [66]. As the distance between the heat source and the heat sink is reduce, the corresponding

contribution of slow conduction and diffusion to the heat exchange or catalyst surface is reduced [59].

1.2.2. ADVANTAGES AND DISADVANTAGES

1.2.2.1. ADVANTAGES

Micro-reactor systems due to their small characteristic channel dimensions of several tenth to hundreds micrometers show several advantages over conventional laboratory-scale reactor systems. Micro-reactors have been mainly applied in the fields of fine chemistry, pharmaceuticals and chemical engineering [66, 39].

1. Two major advantages are: excellent mass transfer and heat transfer [8]. The first is based on the small channel diameters, which results in a reduction of mixing times even at a laminar flow regime due to short diffusion path length, the latter is due to the large surface-to-volume ratio, which results in heat transfer rates of up to 25000 $W/(m^2h)$ [66]. The high heat and mass transfer rates possible in microfluidic systems allow reactions to be performed under more aggressive conditions with higher yields with more uniform temperature that lead to a higher level of reaction control [66].
2. The outstanding property of a micro-reactor is its extremely large surface-to-volume ratio [66]. Even very fast and very exothermic reactions can, therefore, be performed isothermally and in the case of multiphase reactions the mass transfer path is minimal and selectivity is high [59].
3. Because of the small amount of injected chemicals and the high rate of heat transfer, the systems are especially suited for reactions with highly toxic, flammable and explosive chemical compounds [39].
4. Micro-reactor technology increases the safety, reliability and quality of chemical and biochemical processes [75].
5. A micro-reactor makes use of diffusive mixing in the laminar flow state [14] that makes possible the production of high quality chemical and pharmaceutical products [60].
6. The removal of potentially significant large-scale plant accidents associated with thermal runaway could also be envisaged due to the inherent thermal dissipation possible in micro-reactor devices. Indeed, it has been demonstrated that reactions can

be performed beyond their current explosive limits by adopting micro-reactor technology [33].

7. Even if a micro-reactor fails, the small quantity of chemicals released accidentally could be easily contained. Moreover, the presence of integrated sensor and control units could allow the failed reactor to be isolated and replaced while other parallel units continued production [39].
8. Micro-channel reactors would clearly require less space, utilities, and produce less waste. Such system reduces the size of conventional chemical reactors without lowering the throughput under controlled conditions [28, 39].
9. Scale-up to production by replication of micro-reactor units used in the laboratory would eliminate costly redesign and pilot plant experiments, thereby shortening the development time from laboratory to commercial production [77]. That is advantageous for the fine chemical and pharmaceutical industries, where production amounts are often small less than a few metric tons per year [39].
10. It can be optimized through a scale-out methodology creating a safe and efficient approach to chemical discovery and production [28].
11. It is cheaper to operate in terms of material and man-power, capital cost is usually lower, small flammable liquid and gas inventories, relative ease of product and effluent disposal are being more compact, micro-reactors are generally safer to operate [20].
12. Micro-reactors typically have heat exchanger coefficients of at least 1 MW m^{-3} K^{-1}, up to 500 MW m^{-3} K^{-1} vs. a few kilowatts in conventional glassware. Thus, micro-reactors can remove heat much more efficiently than glass vessels and even critical reactions such as nitrations can be performed safely at high temperatures [34].
13. Hot spot temperatures as well as the duration of high temperature exposition due to exothermicity decreases remarkably. Thus, micro-reactors may allow better kinetic investigations using only small amounts of chemicals [66], because local temperature gradients affecting reaction rates are much smaller than in any batch vessel [82].
14. Heating and cooling a micro-reactor is also much quicker and operating temperatures can be as low as -100 °C. As a result of the superior heat transfer, reaction temperatures may be much higher than in conventional batch-reactors. Many low temperature reactions as organo-metal chemistry can be performed in micro-reactors at

temperatures of -10°C rather than -50°C to -78°C as in laboratory glassware equipment [34].

15. Micro-reactors are normally operated continuously. This allows the subsequent processing of unstable intermediates and avoids typical batch workup delays [34].
16. Continuous operation and mixing causes a very different concentration profile when compared with a batch process. This may be an advantage or disadvantage depending on the reaction mechanism - it is important to be aware of such different concentration profiles [34].
17. Pressurisation of materials within micro-reactors (and associated components) is generally easier than with traditional batch reactors. This allows reactions to be increased in rate by raising the temperature beyond the boiling point of the solvent. Pressurisation may also allow dissolution of reactant gasses within the flow stream [34].
18. In addition, micro-channel reaction systems provide large surface and interface areas, which are advantageous for many chemical processes such as extractions and catalytic reactions [57].
19. The quest for micro-reaction technologies will lead to better process intensification and efficient analytical methods [57].
20. New reaction pathways deemed too difficult in conventional microscopic equipment, e.g., direct fluorination of aromatic compounds, could be pursued [39].
21. Micro-chemical systems for combinatorial synthesis and screening of small molecules and systems for nucleic acid synthesis and detection have already used for drug discovery in pharmaceutical companies [39].
22. It is recognized that micro-reactors can provide better energy and material utilization leading to more efficient chemical production and less pollution [74, 77].
23. The micro-reactors offers the facility of rapid and precise control of temperature, which is helpful in obtaining heat-unstable compounds, high reaction rates, high yield of reaction products [60].
24. Besides these striking advantages, benefits such as small reaction volumes, less consume of space and material and the possibility of a modular integration of micro-reactors in complete systems favour the application of micro-reactors [69].

1.2.2.2. DISADVANTAGES

The following are the disadvantages to micro-channel reactor:

1. The very low flow rates can lead to significant heat transfer and mass transfer effects which may mean that the kinetic data cannot be accurately obtained [20].
2. The small scale of operation may result in poor reproducibility; both because of the kinetic data cannot be accurately obtained and sampling difficulties [20].
3. Only small amounts of product are produced and hence testing is limited to methods requiring only small quantities of material, e.g. gas chromatography [20].
4. High levels of technical skill are generally required for operation [20].
5. Typically, reactions performing very well in a micro-reactor encounter many problems in vessels, especially when scaling up [34].
6. Micro-reactors are well suitable for fast and exothermic reactions (traditional semi-batch application) but cause trouble as soon as particles (i.e. unsoluble/unexpected side-products) are involved [34].

With modern instrumentation many of the disadvantages can be overcome and with the advent of micro-processor control, catalyst evaluation can be automated to the point where micro-reactors are an indispensible item in catalyst research laboratories [20].

1.2.3. APPLICATIONS

The strong advantages offered by micro-reaction devices are useful, particularly in the development of micro-reaction systems for commercial purposes. Once a micro-reactor is optimized, it can be easily introduced into an industrial scale plant [57].

1. First applications of micro-reactor have been for analytical purposes. In this case, the sample to be analysed undergoes chemical transformations, so that the final product can be easily detected. Miniaturization of analytical systems can improve reliability, decrease analysis time, and reduce sample size and reagent consumption. The pharmaceuticals industry is the main driving force for developing this technology. This is because it will greatly improve and speed up high-throughput screening of combinatorial libraries, clinical diagnostics, DNA analysis and drug discovery [28].

2. As mass transfer path is minimal, micro-reactors have the possibility of being used for inherently safe production and measurement of intrinsic rate constants.
3. The advantages of micro-total analytical system [μTAS] are efficient thermal control, short response times, defined flow characteristics, large surfaces, small volumes that reduce inertia and small amount of samples required. So, that liquid/ liquid isomerization and gas/liquid asymmetric hydrogenation is carried out using a static micro-mixer [28].
4. Micro-reactors with efficient heat exchange have been used for carrying out high temperature oxidation processes in the explosive regime. A micro-reactor with cross-flow heat exchanger and Pt/Al_2O_3 catalyst used to perform catalytic oxidation of hydrogen. Explosive reaction mixtures with concentration of hydrogen and oxygen up to 50 % by volume are operated safely and complete conversion of hydrogen to water is obtained without explosion. Thin-wall micro-reactors have been successfully to carry out oxidation and partial oxidation reactions of hydrogen, ammonia and ethane in the flammable regime. The heat dissipation can be controlled by varying the thickness and the thermal conductivity of the top wall, enabling the micro-reactor to access a wider temperature of operation conditions and milder oxidation conditions than can be achieved in conventional systems [28].
5. Micro-reactors with good residence time control used to carried out the catalytic dehydrogenations of isopropanol with periodic operation. It is also investigated for selective gas phase hydrogenation of unsaturated hydrocarbons like c,t,t-1,5,9-cyclododecatriene(CDT), 1,5-cyclopctadiene (COD) and benzene to their corresponding cyclic moloalkene with micro-channel reactors using palladium and ruthenium/ zinc catalysts [28].
6. Micro-reactor with efficient mass transfer and heat exchange used for the catalytic partial oxidation of methane to syngas. In conventional processes, due to slow heat conductivity of ceramic supported catalyst, high hot-spot temperatures may cause a fast degradation of the noble-metal catalyst. This metallic micro-structured catalyst promoted heat transfer in the direction of flow and would help to minimize hot-spot formation. It is also investigated for the direct oxidation of propylene to propylene oxide, liquid-liquid nitrations [28].

7. Although the solution-phase reaction is not a favourable process due to the large volume of enzymes required. Enzymatic oligosaccaride synthesis is performed using β-galactosidase in a continuous-flow micro-reactor. The reaction is performed by the separate loading, into inlets, of the enzyme in phosphate buffer solution and the substrate solution in acetonitrile, and is terminated by heating the recovered solution. The reaction in the micro-channel is approximately five times faster than that in the batch reaction [57].
8. A biphasic continuous-flow micro-reaction, dehalogenation reaction is studied in a chip-type glass micro-reactor using laccase by separately loading an aqueous solution of the enzyme, and the substrate solution in organic solvent. The reaction kinetics in of a biphasic stream in a micro-channel depends on the diffusion of the substrate into the aqueous phase [57].
9. Esterification hydrolysis reactions are an important process in industry that has also been performed in a micro-channel system. Hydrolysis of the ester is conducted in Lipase-immobilized micro-reactors using ceramic micro-reactor and glass micro-capillaries. Both micro-reactors showed 1.5 times better yield than the batch wise reaction using the same volume and enzyme ratios. This could have resulted from an increase in contact due to the larger surface area of micro-channel systems [57].
10. Esterification of diglycerol with lauric acid is performed using a monolytic micro-reactor tethering protease P for the bioconversion process. Transesterification of glycidol and vinyl n-butyrate is also performed using this micro-reaction device but the conversion depended on the amount of immobilized enzymes [57].
11. Micro-channel devices can be useful in imitating biological reaction apparatus, such as cellular surface and vascular system, by providing the advantages of reduced space and laminar flow compared with conventional reactor [57].

1.2.4. LIMITATIONS

The following are the general limitations to micro-channel reactor:

1. The range of reactions that could be performed in micro-reactors would be seriously limited without combining heterogeneous catalysis with micro-reactor systems. Whatever method is used to immobilise the catalyst, it will prove to be important to

appreciate that catalysts have different structures and that careful preparation and handling is vital [34].

2. Although there have been reactors made for handling particles, micro-reactors generally do not tolerate particulates well, often clogging. Gas evolved may also shorten the residence time of reagents by pushing out material much faster than anticipated (though the application of backpressure can solve this issue) [34].
3. Pumping by mechanical may generate a pulsating flow which can be disadvantageous. A continuous flow solution is electro-osmotic flow (EOF) [60].
4. Experimentation at the conventional bench scale is limited by high costs of reagents and safety concerns that the small volumes and inherent safety characteristics of micro-reactors could effectively eliminate [82].
5. The introduction of new chemicals is also limited by the risk and high capital costs of scaling from laboratory to production plant [39].

1.2.5. MATERIALS OF CONSTRUCTION

Important factors in the choice of material include the necessary fabrication equipment, chemical compatibility and internal surface characteristics [4]. Noble metal devices are suitable for fast exothermic heterogeneously catalyses reactions and this has been successfully demonstrated for the partial oxidation of methane to synthesis gas using a honeycomb, structured rhodium catalyst device [33]. Silicon has generated a great deal of interest due to the small feature size. The numerous advantages of using silicon are negated by the high cost of material and fabrication in clean rooms. This fact becomes significant as the size of the unit becomes larger. Thus, commercially viable micro chemical units may not necessarily use silicon as the principal material of construction [4]. Glass is a well-suited material for prototyping micro scale hand held chemical devices. Various methods of machining glass cheaply outside the clean room exist. Glass is transparent and allows easy visual inspection and spectroscopic reaction studies. Glass is also chemically inert to most reagents with the exception of hydrofluoric acid, hot phosphoric acid and hot alkali. And finally, as compared to metals, polymers or ceramics, glass has the distinct advantage of being compatible with silicon and can be readily bonded to silicon wafers and devices, thereby providing integrated functionality. The two major

reasons because of plastic are very desirable materials in the micro-fabrication of devices in contact with biological systems. First, plastics offer a broad spectrum of adaptable fabrication technologies for product development and large-scale production. Second, given the large number of polymeric materials available based on the chemical and morphological composition, plastics offer a broad spectrum of physical and chemical properties available for the design of biocompatible systems. Ceramic reactors would be useful for high-temperature and high-corrosive environments [39]. Fig.1.2. shows the interaction between the micro-channel reactor design parameters and its operating characteristics.

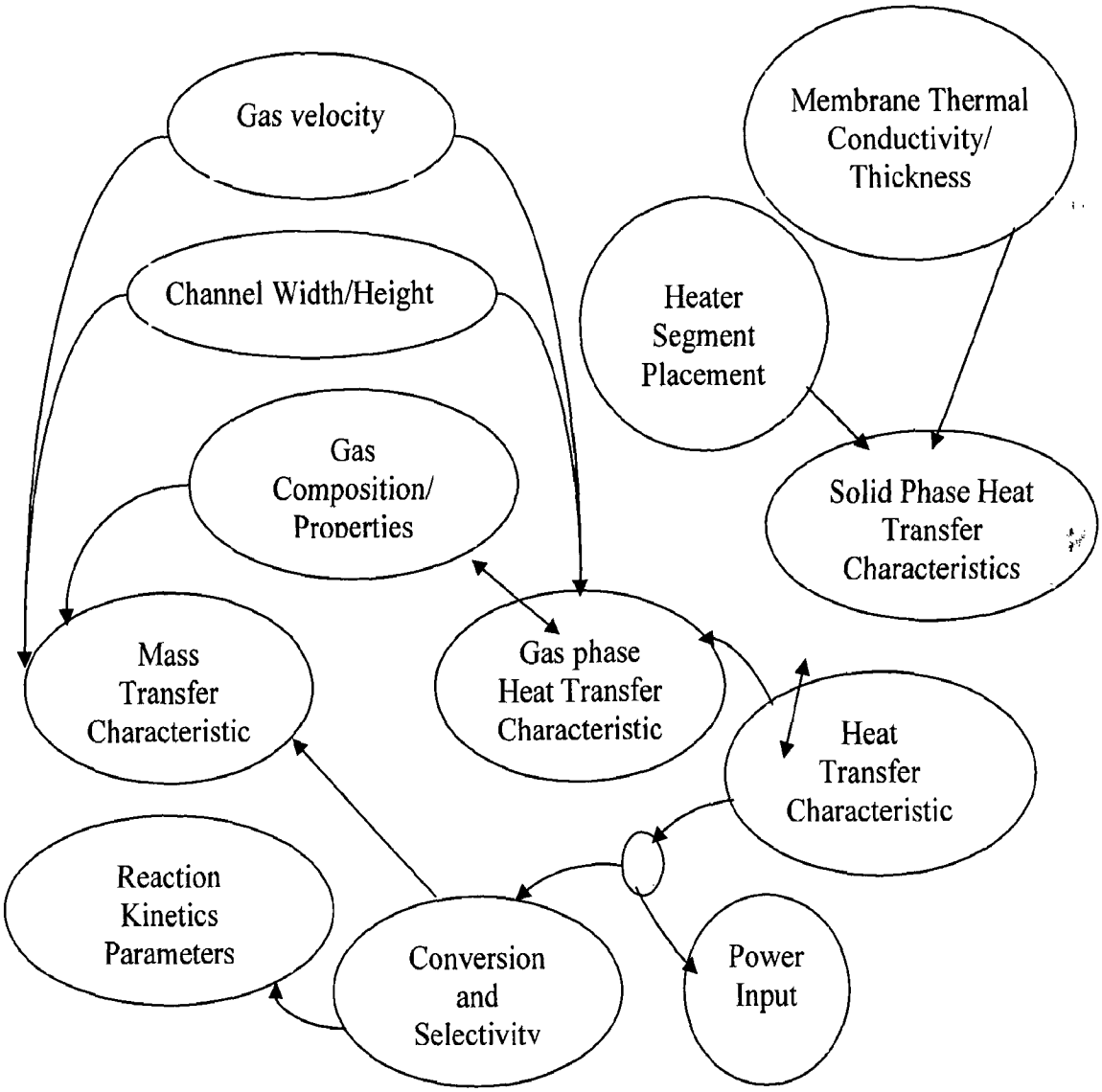

Fig.1.2. Graph showing the interaction between the micro-channel reactor design parameters and its operating characteristics

1.3. MEMBRANE MICRO-CHANNEL REACTOR

1.3.1. INTRODUCTION

Membrane reactors have found utility in a broad range of applications including biochemical, chemical, environmental, and petrochemical systems. The variety of membrane separation processes, the novel characteristics of membrane structures, and the geometrical advantages offered by the membrane modules have been employed to enhance and assist reaction schemes to attain higher performance levels compared to conventional approaches [68]. Membrane-based micro-reactors are an important class of micro-reactors that can combine reaction and separation in one single micro-device. Examples of membrane micro-reactors include the dehydrogenation of cyclo-hexane to benzene, hydrogen generation by oxidative coupling of methane, the production of moisture-free formaldehyde by the dehydrogenation of methanol and hydrogen separation/ water gas shift reaction. Recent approaches in gas phase separation have involved the use of membrane micro-channel reactors that used for micro-fuel cell applications as shown in Fig.1.3. Ultra thin palladium membranes selectively separate H_2 from a reformate gaseous mixture of CO, CO_2, H_2O and CH_3OH and can also be possibly combined with catalytic surfaces or packed bed configurations to perform shift reforming [2].

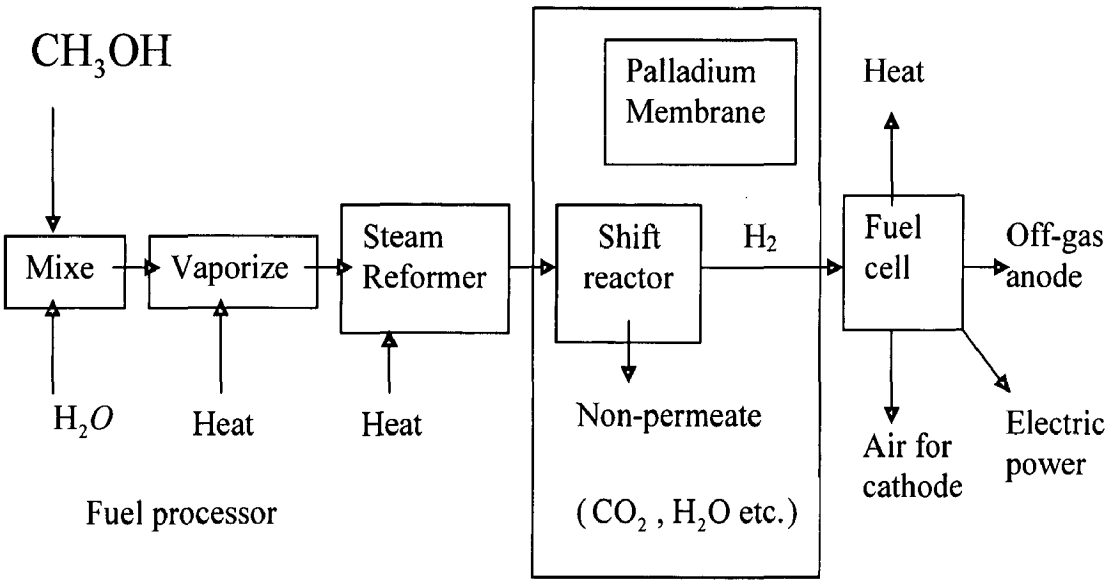

Fig.1.3. Schematic diagram of micro-reformer [2]

The practical use of hydrogen as a secondary source of clean and recyclable energy has been extensive. Practical use, however, involves solving problems such as storage and transport of the hydrogen. Among various methods for the storage of hydrogen, storage as liquid organic hydrides is a preferable candidate for practical use. It is especially attractive that the liquid organic hydrides are transportable in pipelines with no change in status. In terms of weight and volume for storage, this method is comparable to other methods such as storage in metal hydrides. When Pd membranes apply to chemical processes in which hydrogen species participate in certain reactions, a Pd membrane plays a role in permeating hydrogen selectively and generating active species to improve reaction efficiency, as well as a role of a reaction catalyst. These advantages of a Pd membrane can be utilized in hydrogen storage processes with liquid organic hydrides. The application of a micro chemical process is expected to enhance the performance of a Pd membrane reactor used in hydrogen storage processes. Narrowing a reaction channel is a potential method to improve efficiency of the hydrogen storage process. Such narrow channels mean that a micro-reactor must be constructed for these processes [33].

1.3.2. MEMBRANE FUNCTIONS

An extraordinary variety of membranes are available. The membranes can be catalytic/non-catalytic, polymeric/inorganic, and ionic/nonionic. It has different physical/chemical structures and geometries. Membranes are employed in gross physical forms as flat films, hollow fibers, tubules, and tubes, while their physical structures can be as follows: micro-porous symmetric and asymmetric membranes, nonporous membranes and composite membranes. Membranes can be of the polymeric variety or be inorganic in nature, which would include zeolitic, ceramic and metallic membranes. Membranes can also conduct electrical charges and can be chosen from one of following categories: ion-exchange membranes, bipolar membranes, mixed conducting membranes, proton-conducting membranes, etc. In many cases, the membranes have catalysts incorporated in their porous structure or on the surfaces. The membranes in such cases are termed as catalytic membranes. Of course, the membrane can be catalytic by itself without the addition of any catalyst materials from external sources. The term catalytic membrane

reactor sometimes includes the above cases as well as a catalytic reactor enclosed by a membrane, which is non-catalytic [68].

An understanding of these various membrane functions will be quite useful in future development and commercialization of membrane reactors. Various functions of the membranes in a reactor can be categorized according to the essential role of the membranes. They can be employed to introduce/separate/purify reactant(s) and products, to provide the surface for reactions, to provide a structure for the reaction medium, or to retain specific catalysts. The functions of the membrane in a reaction can be enhanced or increased also by the use of multiple membrane-based schemes. More importantly, the membrane inside the reactor has served a variety of functions. Frequently, a membrane (or two membranes) incorporated in a reactor serves more than one desired function, only one of which may involve a membrane separation process where membrane flux and selectivity are important. The introduction of another membrane into the reactor can increase the number of generic membrane functions in the reactor or achieve the same generic membrane function vs. some other species.

A list of the generic membrane functions performed by a membrane or two in a reactor is provided [68]:

1. Separation of products from the reaction mixture.
2. Separation of a reactant from a mixed stream for introduction into the reactor.
3. Controlled addition of one reactant or two reactants.
4. Non-dispersive phase contacting (with reaction at the phase interface or in the bulk phases).
5. Segregation of a catalyst (and cofactor) in a reactor.
6. Immobilization of a catalyst in (or on) a membrane.
7. Membrane is the catalyst.
8. Membrane is the reactor.
9. Solid-electrolyte membrane supports the electrodes, conducts ions, and achieves the reactions on its surfaces.
10. Transfer of heat.
11. Immobilizing the liquid reaction medium.

1.3.3. WORKING PRINCIPLE

The principle of a hydrogen perm-selective membrane reactor equipped with a packed-bed of catalyst and surrounding palladium-based membrane has been illustrates by Fig.1.4. The dehydrogenation occurs on the packed-bed catalyst, and the produced hydrogen is withdrawn through the membrane. The transport through the membrane is driven by the hydrogen partial pressure difference between retentate side and the permeate side. Three different possibilities exist to create the driving force [22]:

1. Use of an inert sweep gas in the permeate compartment (e.g. nitrogen, argon, etc.).
2. Application of a pressure difference between retentate and permeate compartment (if necessary by evacuation of the permeate).
3. Use of a reactive sweep gas to consume the permeated hydrogen (e.g. oxygen, air, carbon monoxide, unsaturated hydrocarbons, etc.).

Which of these possibilities is the best depends on the particular situation. In general, the worst case is the inert sweep gas because this has to be provided and compressed and a diluted hydrogen gas is produced which can be used only as a fuel gas with low calorific value.

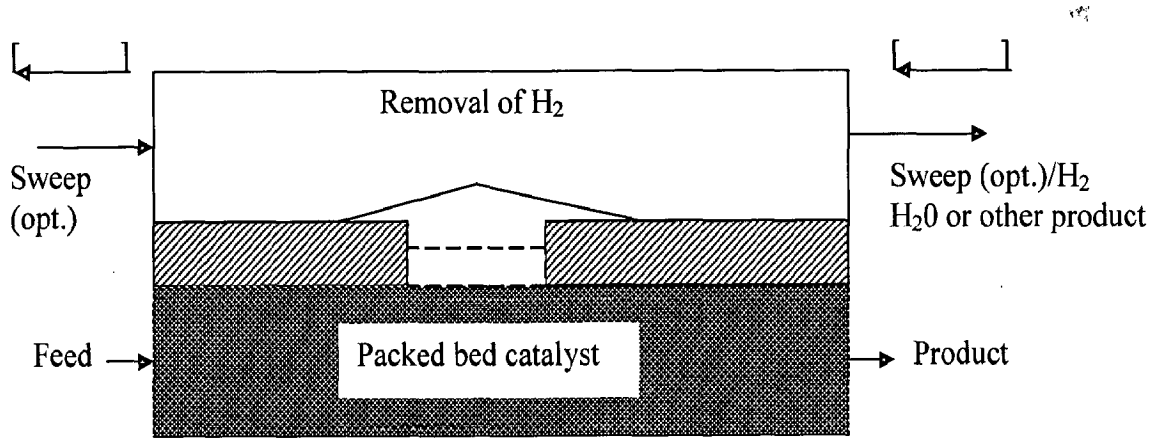

Fig.1.4. Working principle of membrane reactor

If the kinetics of the hydrogen producing reaction do allow an operation at elevated pressure, for instance in the range of 1–3 MPa, this becomes an attractive option because then the pressure difference is sufficiently large to flush out the permeated hydrogen. The advantages are that no sweep gas is required and that pure hydrogen is obtained as a marketable product. On the other hand, the feed gas has to be compressed but the produced hydrogen is obtained at low pressure, which limits its usability and could make a recompression necessary. If pure hydrogen, e.g. for a fuel cell, is the target product of the membrane reactor, then an operation at elevated retentate pressure is the only viable option. The third option, i.e. reacting the permeated hydrogen with the sweep gas, is promising because it avoids the disadvantages of the other two. Moreover, since hydrogen producing reactions are endothermic in most cases (hydrocarbon dehydrogenation and hydrocarbon steam reforming), it is favourable to generate the required heat right in the permeate compartment. An exothermic hydrogen-consuming reaction can be carried out for this purpose, if possible employing the palladium membrane surface as a catalyst. Hydrogen oxidation with air or hydrogenation of an organic compound is candidates, if they fit with the required reactor temperature. The disadvantage of hydrogen oxidation is that a high-valued product is used to heat the dehydrogenation. The other case, coupling of the dehydrogenation process to a second synthesis is difficult to run at optimised conditions in a commercial-scale reactor because of the reduced degree of freedom [22].

1.3.4. PALLADIUM MEMBRANE

Palladium membrane provides an excellent perm-selectivity to hydrogen [30]. When Pd membranes apply to chemical processes in which hydrogen species participate in certain reactions, a Pd membrane plays a role in permeating hydrogen selectively and generating active species to improve reaction efficiency, as well as a role of a reaction catalyst. These advantages of a Pd membrane can be utilized in hydrogen storage processes with liquid organic hydrides [27]. Palladium as a noble metal with exceptional hydrogen permeation properties and, at the same time, broad applicability as a catalyst, first of all for hydrogenation, is part of many of these developments. Dense palladium composite membranes can be used for hydrogen separation from packed-bed catalysts in gas-phase hydrocarbon dehydrogenation reactions. Dense palladium and palladium alloy membranes

are permeable for hydrogen only. Two main possibilities arise from this feature to employ these in membrane reactors, namely [22]:

1. To promote a dehydrogenation reaction by removal of the produced hydrogen from a dehydrogenation catalyst through the membrane, i.e. preventing the establishment of the chemical equilibrium, or
2. To carry out a hydrogenation reaction on the palladium surface with supply of hydrogen through the membrane.

The purpose of the use of the palladium membrane as well as its function differs considerable in both types of applications. In case (1), the aim is to increase the conversion of an equilibrium limited reaction by removal of one of the products. The dehydrogenation occurs in the gas phase over a conventional catalyst (e.g. a packed-bed) which is surrounded by the palladium membrane. In principle, the palladium surface could act as a dehydrogenation catalyst too, but then the reaction rate would be too small due to the low surface area. Hence, the membrane has no primary catalytic function. In case (2), the purpose can be two-fold: to promote a selective hydrogenation by deliberately dosing hydrogen through the membrane or to utilize an existing diluted hydrogen gas to perform the hydrogenation. In both situations, the palladium membrane has a catalytic function. From an engineering point of view case (2) has a limited potential, at least for gas-phase hydrogenations [22].

It is true that palladium is a versatile hydrogenation catalyst, but the reaction rate normally is proportional to the surface area of the catalyst, provided no diffusion limitation occurs and the active sites are uniformly distributed over the surface. Conventional hydrogenation catalysts have the palladium in highly dispersed form, e.g. as nano-scale metal clusters inside a porous pellet and hence do offer a large palladium surface area. Compared to this the accessible surface area of a dense palladium membrane is small. If the hydrogenation is to be performed in the liquid phase the situation may be different because then the reaction rate is often controlled by the kinetics of hydrogen mass transfer and the available active surface inside the porous catalyst is utilised anyway only in part. Liquid-phase hydrogenations are carried out at high pressure due to the poor solubility of hydrogen in most organic liquids. Palladium membranes would allow for a simplification

of the process design, as they could take over both the catalytic function and the task of dosing hydrogen. High pressure operation could then be avoided. Combined with a clear benefit in selectivity there might be interesting applications of this concept in the fine chemicals area. However, most palladium-based membranes are aimed at hydrogen removal from packed-bed catalysts either to boost the yield of industrially important dehydrogenation reactions (propane, isobutane/n-butane, ethyl-benzene, etc.) or to provide pure hydrogen (steam reforming of methane or methanol, water-gas-shift reaction), e.g. for use in low-temperature (PEM) fuel cell stacks [22].

Palladium-based membranes have been used for decades to provide ultra-pure hydrogen, e.g. in the semiconductors industry and for the operation of fuel cells. They are exploited to extract tritium from liquid-metal tritium breeders. In recent years, there has been a growing interest in the industrial application of palladium-based membranes for hydrogen producing reactions. Extensive investigations are conducted for the employment of palladium-based membranes for hydrogen removal to shift thermodynamic (equilibrium) limitations towards higher conversions, e.g. during dehydrogenation of hydrocarbons, steam reforming of methane and the water-gas-shift reaction. Hydrogen feeding through palladium membranes can improve the selectivity of hydrogenation reactions. Key requirements for the successful development of palladium-based membranes are low costs as well as high hydrogen permeability and perm-selectivity combined with good mechanical/thermal and long-term stability [22].

1.3.5. DESIGN CONCEPT

The micro-reactor design emphasizes on flexibility and ease of use. It consists of a micro-reactor plate and stainless steel housing. The micro-reactor plates have three functional elements namely, micro-fluidic components, the active catalyst and the separation membrane; while the housing unit provides a convenient interface between the micro-reactor and the macro-scale laboratory environment. The modular design enables the rapid fabrication and testing of different micro-reactor architectures, catalysts and membranes. Fig.1.5. summarizes the preparation and test procedures for the two types of multi-channel micro-reactor plates [77].

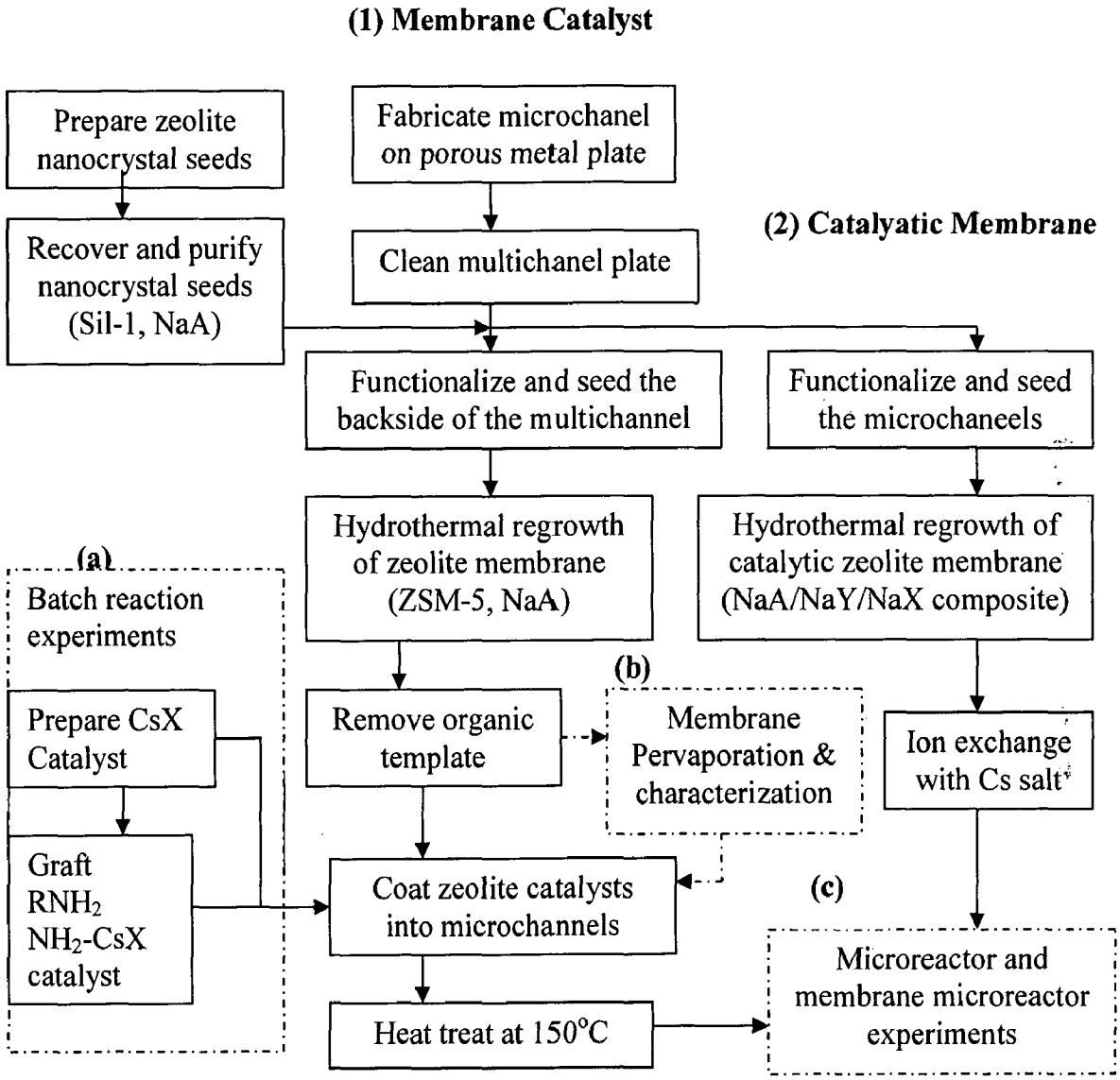

Fig.1.5. Process flow diagram for the preparation of membrane-catalyst and catalytic membrane plates [77]

1.4 ORGANIZATION OF THE THESIS

In chapter 1, we have introduced about the WGSR and we have discussed various industrial applications, different mechanisms, various rate expressions, equilibrium constants and various parameters to be considered and limitations for WGSR. Also, we have introduced about the micro-channel reactor. In which, we have discussed the various advantages, disadvantages, limitations, applications and various materials of construction. Further, we have introduced about membrane in the micro-channel reactor and we have discussed the various generic membrane functions performed by a membrane and basic working principle of membrane in a reactor. Also we have discussed about the palladium membrane and design concept of membrane micro-channel reactor.

The Chapter 2 summarizes the precious literature available on modeling, simulation and experimental studies for WGS reaction in different types of reactor such as fixed-bed reactor, membrane reactor, micro-channel reactor, and membrane micro-channel reactor. Based on these literature review, objective of the thesis have been made.

In chapter 3, we detail the formulation of one-dimensional models for micro-channel reactor and also membrane micro-channel reactor with the consideration of heat conduction through the wall-channel and apply these models to study WGSR. We also considered the case of micro-channel reactor without the heat conduction through the wall-channel and for the membrane micro-channel reactor without the heat conduction through the wall-channel and also with and without heat exchange stream-cooling medium i.e. air.

In chapter 4, we carried out the parametric study of the sensitivities of design parameters of the micro-channel reactor. The results from study are presented and discussed and the optimized operating parameters are identified for the both case of micro-channel reactor. For the membrane micro-channel reactor, we used these optimized operating parameters to study the WGS reaction for the three case of membrane micro-channel reactor.

Finally, chapter 5 includes the conclusions from our study and provides recommendation for the future work.

CHAPTER 2

LITERATURE REVIEW

In the open literature, many modeling, simulation and experimental studies of WGS reaction in different types of reactor such as fixed-bed reactor, membrane reactor, micro-channel reactor, and membrane micro- channel reactor are presented.

Alfadhel and Kothare (2005a) studied the development of a mathematical model that describes isothermal micro-fluidic steady flow in a membrane micro-reactor, i.e., a silicon micro-reactor that houses a permeable membrane in one wall. The model employs the Navier–Stokes equation with appropriate boundary conditions for fluid permeation through the membrane and velocity slip at the walls to account for high Knudsen number. The model equations are solved analytically using finite Fourier transforms. The model solution is used to evaluate the effect of fluid permeation through the membrane and the Knudsen number on the velocity profile and pressure drop. For the simplified cases of no permeation and/or no slip, the derived solution is in excellent agreement with published experimental and theoretical results available in the literature. The utility of the model is illustrated by applying the results to a membrane micro-separator used to separate hydrogen from the other effluents in a micro-reformer [2].

Alfadhel and Kothare (2005b) studied the problem of modeling multi-component concentration profiles in a membrane-based micro-reactor. Using basic constitutive laws of mass balance, they derive a low order model of a generic membrane micro-reactor, incorporating chemical reaction and permeation through a selective micro-membrane and utilizing a pressure distribution formula for slipping flows. Without loss of generality, the model can address non-isothermal conditions and can be extended to allow flow compressibility. They study the utility of the model in evaluating the optimal design and operation of a palladium-based membrane micro-reactor for conducting hydrogen purification and water gas shift (WGS) reforming in micro-fuel processing applications [3].

Baier and Kolb (2007) identified the Micro-channel reactors offer unique possibilities for temperature control of chemical reactions due to the strong coupling of channel and wall temperatures. This may be applied to all chemical reactions which require a certain temperature profile to achieve an optimum yield. For the reformation of hydrocarbons for fuel cell applications a low CO concentration of the product gas is desired. In conventional systems, this is achieved by sequentially processing the reformate through a high and low temperature water gas shift reactor because increased temperature enlarges the reaction rate while lower temperature shifts the equilibrium to the desired small CO concentrations. However, for every gas composition arising during the reaction process an optimum temperature exists at which the reaction rate is highest. They demonstrate that this optimum temperature profile to a good approximation can be achieved in a single step WGS reactor by controlling the temperature via cooling gas flowing in counter current to the reformate. Furthermore, the effect of water addition (steam injection) was analysed for a conventional two-step adiabatic reactor system and the possible size reduction in an integrated heat-exchanger reactor under comparable conditions was validated. Finally, the effect of diffusion limitations at various channel dimensions was investigated applying a two-dimensional model which allows a trade-off between pressure drop or respective reactor size and performance when dimensioning a real system in future [8].

Basile et al. (1996) experimental studied the water gas shift (WGS) reaction considered as a particular application of a catalytic membrane reactor (CMR). Experiments on the WGS reaction were carried out using a composite palladium membrane obtained by coating an ultrathin double-layer palladium film on the inner surface of the support of a commercial tubular ceramic membrane by a so-called co-condensation technique. The best operating conditions were determined at various $H_20/C0$ molar ratios, temperature, PI_{lumen}, gas feed flow and with and without nitrogen sweep gas. For a non-porous stainless steel tube and for the commercial ceramic membrane having the same geometrical dimensions, the conversion results are always lower than the equilibrium value. For the composite palladium membrane, the conversion also depends on the flow of the sweep gas utilized. For example, using a nitrogen sweep gas flow of 28.2 cm^3/min, the maximum conversion

value reaches 99.89%. The study of the effect of temperature on conversion of carbon monoxide in the WGS reaction shows that at higher reaction temperature, the thermodynamic equilibrium conversion of CO decreases. In contrast for the catalytic membrane reactor considered in this work, there is a maximum conversion value around 600 K. This value is a compromise between the kinetic rate of the reaction (which increases with increasing temperature) and thermodynamic considerations for the WGS reaction. The effect of the time factor (W/F) on conversion of CO, with and without sweep gas at three different temperatures (595, 615 and 633 K) shows that at greater W/F, there are correspondingly higher values of the CO conversion for each temperature considered. For each temperature there is a slight effect of the sweep gas, and this is higher at 595 K. The good performance of the composite ceramic-palladium membrane is confirmed by a comparison with experimental results recently presented in the literature for the same reaction. Reaction tests have been carried out for a feed mixture also. In this case, however, the resulting values are always below the equilibrium ones [12].

Basile et al. (2001) studied the water gas shift reaction performance in terms of complete conversions. The behaviour of a membrane reactor (MR) consisting of a tubular micro-porous ceramic within a thin palladium membrane was compared with a membrane reactor using a palladium/silver membrane. Membranes were developed in order to obtain a metallic layer thick enough to avoid any defects of the metallic layer and ensure infinite hydrogen selectivity with respect to other gases. The lumen of both membrane reactors was filled with the catalyst. The experiments were carried out by using nitrogen as inert gas in the streep having a flow rate ranging between 1×10^{-4} and 4×10^{-4}mols^{-1} in co-current and counter-current mode in the temperature range 331–350°C and in the feed molar flow range 3.05×10^{-5}–7.1×10^{-5} mol s^{-1}. Hydrogen was the only one gas passing through both membranes. A complete separation of hydrogen from the other gases of the reaction system was obtained. The water gas shift reaction conversion was close to 100% by using the Pd/Ag membrane. A mathematical model was developed to interpret the experimental data. It described the system under isothermal conditions and considered an axial differential mass balance in terms of partial pressure for each chemical species. The simulation study and the experimental results show a satisfactory agreement and both

highlight the possibility to shift towards 100% the conversion of the considered reaction [11].

Basile et al. (2003) estimated the performances of a membrane reactor (MR) when both shell side stream (sweep gas) and lumen side stream are continuously either in parallel flow configuration (co-current mode) or in counter-flow configuration (counter-current mode). Two mathematical models had been formulated and steady-state mass-balance gave two-dimensional differential equations, which were solved by using the orthogonal collocation technique. Simulation results for both co-current mode and counter-current mode had been compared in terms of hydrogen molar fraction (in the shell side) vs. axial co-ordinate at different hydrogen permeances, temperatures, and lumen pressures. At the operative conditions considered, a very similar CO conversion value has been obtained for both modes [13].

Bell and Edgar (1991a) describes the development and verification of a non-linear, steady-state model of a laboratory-scale water-gas shift reactor. The objective of the work was to develop a model of the laboratory reactor for use in simulation and model-based control strategies. Heat transfer parameters were determined from the experiments without reaction. Parameter estimates for the pre-exponential factor, the activation energy and the coefficient for heat transfer between the catalyst bed and reactor wall were determined from experiments with reaction. Non-linear optimization with a least-squares objective function was used to determine the parameter values. With six fitted parameters, the simplified reactor model accurately predicted the performance of the laboratory reactor system. A second-order reversible rate expression successfully modelled the water-gas shift reaction over a cobalt-molybdenum catalyst [14].

Bell and Edgar (1991b) discusses the modelling of variable catalyst activity in a packed-bed reactor described by Bell and Edgar. In addition, the performance of the dynamic model is compared with laboratory data. For the conditions used in this work, the reactor performance was found to be very sensitive to catalyst activation methods. A variable pre-exponential factor in the standard Arrhenius rate constant was required to

accurately model the catalyst activity. The results presented here provide a more comprehensive understanding of previously reported activity variations experienced with cobalt-molybdenum shift catalysts. The dynamic reactor model accurately predicted the reactor response to changes in inlet heater power input and inlet gas flow-rates and composition. The model also accurately predicted the change in sign of the gain associated with the steam flow-rate - carbon monoxide conversion relationship [15].

Brunetti, Caravella, et al. (2007) studied WGS in a Pd-alloy membrane reactor (MR) by means of a non-isothermal mathematical model using, as main parameter, Damkohler's number (*Da*), the ratio of characteristic times of flow rate and reaction, in a temperature range of 220–320 °C. Two different reactant equimolecular feed streams were considered: one containing only CO and H_2O, the other containing also H_2 and CO_2 of higher industrial interest. The permeation driving force was generated by feed pressure ranging 200–1500 kPa which allows a good H_2 recovery index (up to 95%) and a retentate stream rich (up to 80%) in CO_2. No sweep gas was used, therefore, a pure H_2 stream is obtained as permeate. CO conversion, H_2 recovery index and its partial pressure are the main variables used for analysing the MR performance and showing its advantages with respect to a TR in the large feed pressure range. In addition, the volume index and conversion index were introduced for the first time and proposed as simple tools analysing the volume reduction or improved conversion shown by MRs, both lead to the catalyst amount and reactor size being reduced. The two new indexes proposed by membrane engineering open a window on the analysis of MRs for H_2 production and CO_2 separation for the process intensification strategy. This paper describes a modelling analysis of a packed-bed membrane reactor involving dense Pd–Ag commercial perm-selective membrane [17].

Brunettia, Barbieria et al. (2007) analysed the water gas shift (WGS) reaction in a membrane reactor (MR) using a porous stainless steel supported silica membrane and a CuO/CeO_2 based commercial catalyst in a temperature range of 220–290°C up to 600 kPa. The reaction pressure effect on the CO conversion and permeate stream composition was followed with special attention paid to the significant performance improvement in the

MR. The best operating condition for the MR was identified as 280°C and 400 kPa, obtaining a CO conversion of 95% with an increment of 8% with respect to TR. Furthermore, the membrane permeance (H_2: 9.7.29; CO: 0.3.1.1; CO_2: 0.4.1.5 nmol/m^2.s.Pa) and selectivity (H_2/CO, H_2/CO_2 ranging from 15 to 40) and the influence of other gases on H_2 permeation were evaluated before and after reaction testing. No inhibition effect of other gases on the hydrogen flux in all cases was observed. An MR using silica membranes was successfully employed in the WGS reaction, obtaining always higher conversion than with a traditional reactor (TR) and also (at T >250 °C) exceeding the TR equilibrium conversion (TREC) [18].

Choi and Stenger (2003) studied the kinetics of the water gas shift reaction to evaluate existing reaction mechanisms, test various rate expressions and simulate the performance in a methanol fuel processor for fuel cell applications. The reaction was carried out in a micro-reactor testing unit using a commercial Sud-Chemie Cu/ZnO/Al_2O_3 catalyst between 120 and 250 °C with a range of feed rates and compositions. Using non-linear least squares optimization, the parameters in five rate expressions was fit to the experimental data. Based on a review of published work on the WGSR mechanism, a rate expression derived from a regenerative mechanism and another rate expression derived from adsorptive mechanism fit the experimental data equally well. Numerical integration of a one-dimensional PFR model was used for this parameter fitting. An empirical rate expression, $r_{CO} = kP_{CO}P_{H2O}(1 - \beta)$ with activation energy of 47.4 kJ/mol was also obtained from the experimental data which gives high degree of accuracy. Reactor performance was simulated to determine catalyst loadings required to achieve specific CO conversions as a function of temperature and water feed rate. These results are useful in studying the design trade offs available to reformer systems [19].

Damle et al. (1994) developed simplified process model to simulate a catalytic membrane water gas shift (WGS) reactor. A number of computer simulations were conducted to determine the potential of increased carbon monoxide (CO) conversion in WGS reaction due to simultaneous separation of product hydrogen (H_2) from the reactant

mixture. Gas separation factors based on Knudsen diffusion were used in these simulations to assess the feasibility of inorganic and ceramic membranes in a high-temperature, high-pressure (HTHP) coal gasification environment. The simulations indicated that although the increase in CO conversion and hydrogen concentration in a single membrane reactor stage was significant, a multistage membrane separation system would be needed to increase the hydrogen product concentration above 90%. As expected, increasing the feed pressure to permeate pressure ratio was found to increase the CO conversion and the product hydrogen concentration. At low feed to permeate pressure ratios, the model predicted a much better membrane reactor performance with a countercurrent feed and permeate flow scheme when compared with a concurrent flow scheme. The membrane performance, of course, depends strongly on the gas separation factors. With gas separation factors lower than the ideal Knudsen diffusion separation factors (e.g. H_2 to COP separation factor of 2 instead of the ideal Knudsen value of 4.7), the model simulation predicted a much smaller increase in CO conversion and product hydrogen concentration [21].

Dongho and Laud (2003) developed a simple two-step micro-kinetic model for the high-temperature water-gas shift was using existing experimental data. This two-step redox model uses only three adjustable parameters, and it is capable of predicting the inhibitory effect of CO_2 on the kinetics of the reaction. It was used to simulate the performance of an adiabatic membrane reactor for the water-gas shift where the membrane is based on Pd. The simulations show that excess steam in the feed is desirable to control the adiabatic temperature rise, 3:1 ratio of steam to carbon monoxide was found to be near optimum. The simulations further suggest that the rate of reaction is the limiting process in the membrane reactor, not the permeation of hydrogen through the membrane. At 90% hydrogen yield, finding a perfect membrane would only reduce the reactor size by 12%, whereas eliminating the inhibitory effect of CO_2 would reduce the reactor size by 76% [23].

Dupont et al. (2007) presented the specificities of micro-structured reactors as compared to conventional fixed-bed reactors through two case studies devoted to (i)

hydrogen production by methanol steam reforming, (ii) hydrogen purification by water-gas shift (WGS). This also features characteristic of micro-structured reactors in kinetic studies on the water-gas shift (WGS) reaction. Key features like catalyst coating stability, temperature and pressure management, effects of operating conditions (residence time, pressure drops, etc.) are well identified as controlling the micro-reactor performances for methanol reforming. These devices are also shown to be excellent tools for fast access to reaction kinetics as exemplified for the WGS reaction, subject to operating conditions carefully chosen to ensure proper hydrodynamics, in order to use conventional plug flow reactor models for extracting rate constants [24].

Goto et al. (2003) were simulated and compared three types of membrane micro-reactors for production of electric power by fuel cells with methane feed, i.e. (1) Pd membrane micro-reactor (Pd-MMR) followed by polymer electrolyte fuel cell (PEFC), (2) oxide-ion conducting solid oxide fuel cell (SOFC) and (3) proton conducting solid oxide fuel cell (H ± SOFC). The Pd-MMR followed by PEFC is the most effective system for electric power generation compared with the other two types of SOFC although the system is rather complex. However, the performances are dependent on the permeation properties of membranes (Pd, YSZ, perovskite) as well as kinetics of catalysts [32].

Huang and Winston (2005) had proposed the CO_2-selective WGS membrane reactor to decrease CO concentration in reforming synthesis gases and obtain high-purity H_2 products. Using a CO_2-selective membrane reactor shifts the reaction towards the product side, which enhances the conversion of CO and increases the purity of the H_2 product at a high pressure. The simultaneous reaction and transport process in the countercurrent WGS hollow-fiber membrane reactor was simulated by using a one-dimensional non-isothermal model and the effect of several system parameters including CO_2/H_2 selectivity, CO_2 permeability, and sweep-to-feed molar flow rate ratio were investigated. The synthesis gases from both auto-thermal reforming and steam reforming were used as the feed gas, while heated air was used as the sweep gas. A published WGS reaction rate expression with the commercial Cu/ZnO catalyst was incorporated into the model. The modeling results show that a CO concentration of less than 10 ppm, a H_2

recovery of greater than 97%, and a H_2 concentration of greater than 54% (on the dry basis) are achievable from auto-thermal reforming syngas. If steam reforming syngas is used as the feed gas, H_2 concentration can be as high as 99.64% (on the dry basis) along with a reduced membrane area requirement. Both auto-thermal reforming and steam reforming syngases showed similar trends with respect to the three system parameters. As the CO_2/H_2 selectivity increased, the recovery of H_2 increased, without affecting the membrane area requirement and the low CO attainment significantly. Higher membrane permeability resulted in the reduction of the required membrane area. Increasing sweep-to-feed ratio enhanced the permeation driving force but decreased the feed-side temperature and thus the reaction rate, resulting in a net effect balanced between them and an optimal ratio of about 1. The modeling study showed that both the WGS reaction rate and the CO_2 permeation played an important role on the overall reactor performance [35].

Huang and Winston (2008) proposed a CO_2-selective WGS membrane reactor, developed a one-dimensional non-isothermal model to simulate the simultaneous reaction and transport process and verified the model experimentally under an isothermal condition. Further modeling investigations were made on the effects of several important system parameters, including inlet feed temperature, inlet sweep temperature, feed-side pressure, feed inlet CO concentration, and catalyst activity.

Iyoha et al. (2007) conducted the high-temperature, water-gas shift reaction in 100 wt%Pd and 80 wt%Pd–20 wt%Cu (Pd80 wt%Cu) shell-and-tube membrane reactors at 1173 K with a 241 kPa (35 psig) trans-membrane pressure differential in the absence of heterogeneous catalyst particles. The tube bundle consisted of four parallel 15.25 cm long, 3.175 mm OD Pd-based tubes with a wall thickness of 125 μm. The modest catalytic activity of the Pd-based membrane surface for the forward WGSR, the high rate of hydrogen extraction through the Pd-based membranes, and the long residence times (1–5s) resulted in a dramatic shift in carbon monoxide conversions of 93% at 1173 K and a 1.5:1 steam-to-carbon monoxide feed ratio—a value well above the equilibrium value of 54% associated with a conventional (non-membrane) reactor. Carbon monoxide conversions decreased from 93% to 66% and hydrogen recovery from 90% to 85% at a residence time

of 5 s when the Pd was replaced with Pd80 wt%Cu, due to the lower permeance of the Pd 80 wt%Cu alloy. SEM-EDS analysis of the membrane tubes suggested that the water-gas shift environment caused pinhole formation in the retentate surfaces of the Pd and Pd 80 wt%Cu after approximately 8 days of operation [38].

Karnik et al. (2003) studied the design, fabrication and performance evaluation of a palladium based micro-membrane reactor for hydrogen gas separation as well as future possible shift reaction in a proposed micro-reactor to produce hydrogen by the reaction of methanol with steam in presence of a catalyst. The micro-membrane structure is built in a silicon substrate, using standard micro electro mechanical system (MEMS) micro-fabrication processes. Four layers, viz. copper, aluminum, spin-on-glass (SOG) and palladium form the composite membrane. Copper, aluminum and SOG layers provide structural support for the palladium film. Copper can act as catalyst in the water gas shift reaction that converts unwanted carbon monoxide gas into hydrogen. Palladium is used to separate hydrogen from other gases present. The novelty of this structure is that they had integrated the water gas shift reactor as well as the hydrogen gas separator in the same structure. This is because copper can act as a membrane support as well as a catalyst in the water gas shift reaction. The mechanical strength of the micro-membranes with various combinations for the thicknesses of the component Cu–Al-SOG-Pd layers was measured. Higher Al and Pd thicknesses aided the mechanical strength of the micro-membranes. The micro-membrane selectively separates hydrogen from 20:80 hydrogen: argon gas mixture by weight even at room temperature. A micro-membrane with 66 nm Cu, 200 nm Al, 500 nm SOG, and 200 nm Pd withstood a maximum pressure gradient of 1 atm before failure. The hydrogen flux through the palladium micro-membrane was measured and it was found that the flux increased with temperature as well as the hydrogen partial pressure gradient across the membrane, following the Sievert's law. This work was focused on studying and characterizing the water-gas shift reaction capabilities of the proposed micro-reactor/micro-separator. Future applications of this micro-membrane for simultaneous water gas shift reaction and hydrogen separation were also discussed [41].

Kim et al. (2005) discusses the development of an integrated reaction and heat exchange approach to micro-reactor design that enhances reaction yields by allowing the reactant stream to follow optimal reactant temperature profiles. The integrated design enables the integration among various components in a system through a heat exchange medium. The paper details the formulation of both one-dimensional (1-D) and two-dimensional (2-D) models for the integrated reaction and heat exchange reactor design, and applies these models to a parametric study of micro-reactor designs for the water gas shift (WGS) reaction. The parametric study investigated the sensitivities of design parameters (wall thermal conductivity, heat exchange medium, inlet temperature and velocity) for both the parallel flow and counter flow configurations of the integrated reaction and heat exchange design. Results from the study were presented and discussed, and the preferred operating ranges of the parameters to achieve CO conversion of at least 85% were identified for both configurations. For both parallel and counter flow reactor, there existed an optimal range of wall thermal conductivity. However, the range of acceptable thermal conductivities for the parallel flow configuration was narrow and limited to application of insulating materials. Thus, when considering mass production of the micro-reactors, the counter flow arrangement is favorable since the resultant extension of the range of optimal thermal conductivities enables the selection of traditional engineering materials, thereby lowering material costs and improving producibility. The integrated micro-reactor design showed significantly different behavior with liquid water as the heat exchange medium. For both parallel and counter flow, heat exchange stream temperature and velocity had little effect on the CO conversion. Required wall thermal conductivity was also very small, around 0.005 W/m K, to achieve CO conversion level of 90%. In addition, the integrated micro-reactor approach achieved higher catalyst utilization noted by a marked reduction in catalyst amount (of the order of 50%) when compared to a conventional adiabatic micro-reactor operating at the same level of conversion efficiency [46].

Kolb et al. (2005) applied the wash-coated alumina catalysts introduced into micro-channels for the water-gas shift reaction. The application standing behind this work was catalytic CO clean-up of reformate with the aim of hydrogen generation for mobile fuel cell systems. Bimetallic $Pt/CeO_2/Al_2O_3$, $Pt/Rh/CeO_2/Al_2O_3$, $Pt/Pd/CeO_2/Al_2O_3$ and

$Pt/Ru/Al_2O_3$ catalysts were tested in a standard screening protocol under the conditions of high temperature shift (9.1% CO, 290, 315 and 340 °C reaction temperature) and low-temperature shift (2.6% CO, 290, 315 and 340 °C reaction temperature) at water hourly space velocity (WHSV) of 100 N dm^3/(h.gcat). Methane, was formed as the only by-product. $Pt/CeO_2/Al_2O_3$ was identified as the best candidate concerning selectivity and activity. The optimum platinum content was found to range between 3 and 5 wt.%, whereas the optimum ceria content ranged between 12 and 24 wt.%. The calcination temperature and platinum metal salt solution applied during catalyst preparation had a drastic effect on the activity of the $Pt/CeO_2/Al_2O_3$ catalyst [47].

Kroll et al. (2007) were presented a straight forward procedure for membrane functionalization. The broad application of hollow fiber micro-bioreactors in various areas of biotechnology is still restricted due to a limited functionality of the membranes. Different commercially available polyethersulfone (PES) and polysulfone (PS) hollow fiber membranes were chemically modified by reacting terminal hydroxyl groups with ethylene glycol diglycidyl ether (EGDGE) to produce terminal epoxy groups. For increasing loading capacity hydroxyethyl cellulose polymers (HEC) were bound to the epoxy groups. Second epoxidation produced final polymers containing reactive epoxy groups on the hollow fiber surface. From this modified PES and PS respectively a wide variety of N-containing reagents (e.g. iminodiacetic acid (IDA)) can be bound to the epoxy groups. The different reactions were proved by acid orange II assay and phenol sulfuric assay. To assure intact hollow fiber surface after membrane modification scanning electron microscopic analyses were performed. The chelating IDA-membranes were complexed with different divalent metal ions (Cu^{2+}, Ni^{2+}, $Co^{2+,}$ and Zn^{2+}). Immobilized metal ion affinity PES hollow fiber membranes were used for purification of a recombinant protein (GFP-His) from Escherichia coli, which carried a polyhistidine sequence (His_6-tag). Determination of bound and unbound GFP-His_6 was performed by fluorescence spectroscopy, Bradford assay and SDS-PAGE [48].

Lai et al. (2003) was tested the performance of a membrane micro-reactor and compared with that of a micro-reactor, a packed bed reactor (PBR) and a packed bed

membrane reactor (PBMR) for the Knoevenagel condensation reaction of benzaldehyde and ethyl cyanoacetate to produce ethyl 2-cyano-3-phenylacrylate. Cs-exchanged NaX faujasite zeolite was used as the base catalyst for this equilibrium-limited reaction. Hydrophilic ZSM-5 membranes were employed in both the membrane micro-reactor and the PBMR for the selective removal of water byproduct from the reaction. The product yield per pass was low for the packed bed reactor. Higher yields were observed for the micro-reactor and PBMR, but the best performance belongs to the membrane micro-reactor, which displayed both supra-equilibrium conversion and better product purity. The synthesis gases from both auto-thermal reforming and steam reforming were used as the feed gas. As the inlet feed temperature increased, the required membrane area reduced because of the higher WGS reaction rate. Increasing the inlet sweep temperature decreased the required membrane area more significantly, even though the required membrane area increased slightly when the inlet sweep temperature exceeded about 160 °C. Higher feed-side pressure decreased the required membrane area as a result of the higher permeation driving force and reaction rate. A potentially more active catalyst could make the membrane reactor more compact because of the enhanced reaction rate. The modeling results have shown that a CO concentration of less than 10 ppm is achievable from syn.gases containing up to 10% CO [36].

Mukherjee et al. (2007) were designed, fabricated and characterized micro scale glass reactor with Water Gas Shift Reaction (WGSR). The fabrication procedure was quick, uncomplicated, template-free and inexpensive and did not require any special clean room facility, making it ideal for first generation prototyping. The fabricated unit was able to withstand pressure and temperature of 1.65 MPa and 260 °C respectively. An important reaction in micro scale fuel processing, namely WGSR, was carried out in this microreactor using a packed bed of 50–75 mm commercial catalyst particles at 185–250 °C. The design sizing was based on a CO flow of 0.06 mol/h. For this study, the low temperature $CuO/ZnO/Al_2O_3$ catalyst from ICI-Synetix was used. Experimental results were used to develop a kinetic model of the reaction. The goal of them are: (1) explore the use of glass as a material for fabrication of low cost, first generation micro-reactor prototypes, (2) fabricate and characterize the glass micro-reactor and micro-fluidic inter-

connector using template free, cheaper fabrication tools, and (3) characterize the rate expression for Water Gas Shift Reaction in the fabricated glass micro-reactor to facilitate future micro-reactor designs [59].

Tiggelaar et al. (2005) were evaluated critical steps in the fabrication process of a micro-reactor for high-temperature catalytic partial oxidation gas phase reactions. The micro-reactor contains a flow channel etched in silicon, capped with an ultrathin composite membrane consisting of silicon and silicon nitride layers, on which on the top-side thin-film heaters and sensors, and on the other side a thin-film catalyst patch are placed. The membrane is designed to have specific heat conductivity and mechanical properties. The paper focuses on three fabrication issues: definition and etching of sub-micron uniform single-crystalline silicon membranes, deposition of well-defined heater structures and temperature sensors on a thin composite membrane, and deposition of well-defined catalytic patches on the same membrane. For the latter two processes novel micro-machined shadow masks were developed. Preliminary experiments on the controlled oxidation of hydrogen gas in the explosive regime are discussed, which experiments confirm that heat management in the micro-reactor is excellent [73].

Tosti et al. (2003) obtained Pd–Ag thin wall permeators by coating ceramic porous tubes with thin Pd–Ag metal foils (50μm). A procedure of cold rolling and annealing has been used for producing thin metal foils. These membranes and membrane reactors have been proposed to recover hydrogen (and its isotopes) from tritiated water by using the water gas shift reaction and by the reverse reaction (CO_2 conversion) for applications in the fusion reactor fuel cycle. The rolled membranes have been tested at 135–360 °C with a hydrogen transmembrane pressure in the range 130–180 kPa and hydrogen flow rates up to 1.02×10^{-4} $mols^{-1}$. Both complete hydrogen selectivity and a good chemical and physical stability had been observed through long-term tests. The tests on the membrane reactors had been carried out at the temperature of 325–330 °C with a feed pressure of 100 kPa; in particular, reaction conversion values close to 100% (well above the equilibrium value, about 80%) have been attained with the water gas shift reaction. These tests had demonstrated their applicability to the fusion fuel cycle as well as to the hydrogenation or

dehydrogenation processes involving the use or the production of highly pure hydrogen [76].

Wan et al. (2001) had demonstrates that zeolites (i.e., Sil-1, ZSM-5 and TS-1) can be employed as catalysts, membrane or structural materials in miniature chemical devices. Traditional semiconductor fabrication technology was employed in micro-machining the device architecture. The fabricated miniature zeolite-based structures find applications as catalytic micro-reactors and membrane micro-separators. Four strategies for the manufacture of zeolite catalytic micro-reactors were discussed: zeolite powder coating, uniform zeolite film growth, localized zeolite growth and etching of zeolite-silicon composite film. These zeolites were deposited either as film or discrete islands with controlled particle size, crystal morphology, layer thickness (3-16 μm) and film orientation. Crystal intergrowth was also manipulated through the use of growth inhibitors. Sil-1 was also prepared as free-standing membrane for zeolite membrane micro-separators [77].

Yamamoto et al. (2006) was constructed a micro-reactor by inserting a stainless-steel rod into a Pd membrane tube reactor to investigate the effects of micro-channel size on the dehydrogenation of cyclohexane to benzene. The Pd membrane, having selective permeability for hydrogen, was coated onto the surface of an α-alumina porous tube. The dehydrogenation of cyclohexane was carried out at 573 K and atmospheric pressure. The yield of benzene was affected by varying the diameter of the stainless-steel rod and the yield with the thickest rod was approximately two times higher than that without any rods. The application of the micro-channels apparently increased the surface area per volume of the Pd membrane and thus, increased the catalytic reaction on the Pd membrane [81].

Table 2.1 summarized the different type of the catalyst reported in literature for WGSR at low and high temperature.

Table 2.1: Different type of catalysts reported in the literature

S. No.	Catalyst	Operating range of temperature (K)	References
Low temperature Catalyst			
1.	5 wt.% Cu on Al	621-710	Mizsey et al.[27]
2.	$Cu/ZnO/Al_2O_3$	393-523	Choi and Stenger [19], Keiski et al.[42], and Figueiredo et al.[27]
3.	$CuO/ZnO/Al_2O_3$	458-523	Andreeva et al.[6] and Mukherjee et al.[59]
4.	Cu/ZnO with different supports	423-523	Yahiro et al.[80]
5.	Cu/CeO_2	423-523	Zerva and Philippopoulos [83]
6.	Mo_2C/Mo [also applicable at high temperature]	500-631	Rebrov et al.[63]
7.	Au/CeO_2	413-623	Sandoval et al.[65], Gorke et al.[31] and Andreeva et al.[6]
8.	Au/TiO_2	50-400	Sandoval et al.[65]
9.	Ru/ZrO_2	523-573	Tonkovich et al.[75] and Gorke et al.[31]
High temperature Catalyst			
1.	Fe_3O_4/Cr_2O_3	600-723	Keiski et al.[42]
2.	$Rh/Fe_3O_4/Cr_2O_3$	573-673	Lei et al.[50-52]
3.	Co/Mo	573-723	Bell and Edgar [14-15]
4.	$Pt\text{-}ZrO_2$	523-673	Xue et al.[79]
5.	$CoCrO_2$	523-673	Hutchings et al.[37]

Table 2.2: Experimental study reported in the literature

S. No.	Reactor Type	Catalyst Type	Membrane Type	References
1.	Micro-membrane reactor	Cu along with Al and Spin-on-glass support	Palladium	Karnik et al. [41]
2.	Micro-reactor	Ru/ZrO_2 and Au/CeO_2	-----	Gorke et al. [31]
3.	Micro-glass reactor	$CuO/ZnO/Al_2O_3$	-----	Mukherjee et al. [59]
4.	Micro-reactor	5 wt.% Ru/ZrO_2	-----	Tonkovich et al. [75]
5.	Catalytic membrane reactor	α-Al_2O_3 and γ-Al_2O_3	Composite Pd and Commercial ceramic membrane	Basile et al. [12]
6.	Membrane reactor	Cu (20%) and Cu (0%)	Pd (80%) and Pd (100%)	Iyoha et al. [38]
7.	Membrane reactor	CuO/CeO_2	Porous stainless steel supported silica	Brunettia et al. [18]
8.	Membrane reactor	-----	Tubular microporous ceramic within a thin Pd [70 μm] and Pd/ Ag	Basile et al. [11]
9.	Membrane reactor	-----	Pd/ Ag	Tosti et al. [76]

Table 2.3: Modeling and simulation study reported in the literature

S. No.	Reactor Type	Catalyst Type	Membrane Type	Model Type	References
1.	Micro-channel reactor [integrated]	$CuO/ZnO/Al_2O_3$ [N_2 as heat exchange stream]	-----	Steady-state, 1-D, non-isothermal, BVP	Baier and Kolb [8]
2.	Micro-channel reactor [integrated]	5 wt.% Cu on Al [Air and Water as heat exchange stream]	-----	Steady-state 1-D, 2-D, non-isothermal	Kim et al. [46]
3.	Membrane micro- reactor	$CuO/ZnO/Al_2O_3$	Pd	Steady-state, 1-D, non-isothermal	Alfadhel and Kothare [3]
4.	Membrane reactor	----- [reaction is shell-side and no sweep gas]	Pd-Ag commercial permselective membrane	Steady-state, non-isothermal	Brunetti et al. [46]
5.	Membrane reactor	Cu/ZnO [reaction is tube-side and heated air as sweep gas]]	Hollow fiber module [CO_2-selective]	Steady-state, 1-D, non-isothermal, BVP	Huang et al. [35]
6.	Membrane reactor	$CuO/ZnO/Al_2O_3$ [reaction is tube-side and heated air as sweep gas]	Hollow fiber module [CO_2-selective]	Steady-state, 1-D, non-isothermal, BVP	Huang et al. [35]

7.	Membrane reactor	----- [reaction is tube-side and N_2 as sweep gas]	-----	Steady-state, 2-D, isothermal, IVP -BVP	Basile et al. [13]
8.	Fixed-bed reactor	$Cu/Zn/Ba/Al_2O_3$	-----	Un steady-state, 1-D, non-isothermal	Giunta et al. [30]
9.	Fixed-bed reactor	Co/Mo	-----	Steady-state, 2-D, non-isothermal	Bell and Edgar [14]
10.	Fixed-bed reactor	Co/Mo	-----	Un steady-state, 2-D, non-isothermal	Bell and Edgar [15]

2.1 OBJECTIVE OF PRESENT WORK

On the basis of the above literature review, limited studies on WGS reaction in micro-channel reactor with and without consideration of heat conduction through the wall-channel are reported in the literature.

Therefore, the following objectives have been aimed in the present study:

1. To develop mathematical model for an integrated reaction and heat exchange micro-channel reactor with heat conduction through the wall-channel and also for the membrane micro-channel reactor. Further, this has been used as a special case in which it has been verified by considering the case of without heat conduction through the wall-channel.
2. To study the effect of various operating conditions and parameters on the performance of micro-channel reactor and membrane micro-channel reactor.

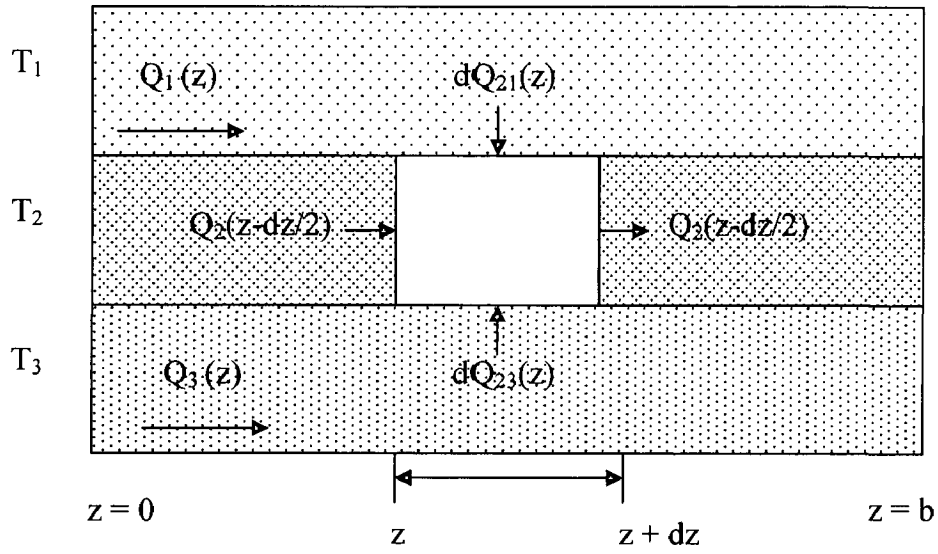

Fig.3.2. Schematic diagram of the energy conservation

3.1.2. Assumptions

The model equations are developed on the basis of following assumptions:

1. Micro-reactor is operated under steady-state conditions.
2. Plug flow model has been assumed for the reactant and heat exchange stream.
3. There is no pressure drop through the channel.
4. We have assumed constant properties for the heat exchange medium, i.e., air.
5. There is no phase change.
6. For the reactant stream, heat capacity flow changes due to the changing composition of the gas and change in heat capacity due to the temperature change is neglected.
7. Constant heat capacity flow through the heat exchange channel.

3.1.3. Material balance

Based on the volume element from z to $z + \Delta z$, mole balances equation for any reactant (or product) can be expressed by the following equations:

In – Out + Generation = Accumulation (3.1)

$$F_z - F_{z+\Delta z} - \left(-r\left(c_i, T_3\right)\Delta V\right) = 0 \tag{3.2}$$

After dividing Eq. (3.2) by ΔV and taking limit as $\Delta V \to 0$, we arrive at the differential form of the mole balance for a plug flow reactor:

$$\frac{dF_i}{dz} = r\left(c_i, T_3\right) A \tag{3.3}$$

The main purpose of the water gas shift reaction is to reduce carbon monoxide levels. So, we have converted this material balance equation in terms of the carbon monoxide conversion that will be given by the following equation:

$$\frac{dX_{co}}{dz} = \frac{-r\left(c_i, T_3\right) A}{Fco^0} \tag{3.4}$$

The relationship between CO conversion and molar flow rate are given by the following equations:

$$F_{co} = F_{co}{}^0 - (F_{co}{}^0 \times X_{co}) \tag{3.5}$$

$$F_{co_2} = F_{co_2}{}^0 + (F_{co}{}^0 \times X_{co}) \tag{3.6}$$

$$F_{h_2} = F_{h_2}{}^0 + (F_{co}{}^0 \times X_{co}) \tag{3.7}$$

$$F_{h_2o} = F_{h_2o}{}^0 - (F_{co}{}^0 \times X_{co}) \tag{3.8}$$

3.1.4. Energy balance

The convective heat flow in channel i is the product of the volumetric flow rate V_i, the density ρ_i, the specific heat capacity at constant pressure C_{pi} and the temperature T_i in the channel

$$Q_i = V_i \rho_i c_{pi} T_i = W_i T_i \tag{3.9}$$

where, W_i stands for the heat capacity flow rate.

In channel 1, we have assumed that a constant heat capacity flow (W_1) through the heat exchange channel. Since, heat transport by conduction is small compared to the convective transport term, the change in the heat flow rate along the heat exchange stream is given by

$$\frac{dQ_1}{dz} = W_1 \frac{dT_1}{dz} = -U_1 (T_1 - T_2) w_1 \tag{3.10}$$

In channel 3, the exothermic WGS reaction is assumed to take place, releasing energy $\Delta Hr(c_i, T_3)$, where r is the rate of the reaction (dependent on the concentrations C_i in the gas composition and the temperature T_3). The heat capacity flow (W_3) in channel 3 changes due to the changing composition of the gas (the change in heat capacity due to the temperature change is neglected). So, the change in the heat flow rate along the reactant stream [channel-3] is given by

$$\frac{dQ_3}{dz} = W_3 \frac{dT_3}{dz} = -U_3(T_3 - T_2)w_3 + \Delta H A r(c_i, T_3) \tag{3.11}$$

Here, we describe the fact that the heat vanishing from a channel is transported to the wall. U_i are the heat transfer coefficients, T_2 is the wall temperature and w_i is the "width" of the channel–wall interface, i.e., the circumference of the channel given by

$$w_i = 2(b + h_i) \tag{3.12}$$

The heat flowing inside the wall material in longitudinal direction, i.e., along the wall in the direction of fluid flow, is given by

$$Q_2 = -\lambda_2 A_2 \frac{dT_2}{dz} \tag{3.13}$$

where, the wall cross-section is given by

$$A_2 = 2bh_2 + b_2(h_1 + 2h_2 + h_3) \tag{3.14}$$

Now, we have applied energy conservation in the region illustrated by the broken rectangle of extension dz in Fig.3.2, i.e.,

$$\left(\frac{dQ_1}{dz}dz\right) + \left(\frac{dQ_3}{dz}dz\right) + Q_2\left(z - \frac{dz}{2}\right) - Q_2\left(z + \frac{dz}{2}\right) = 0 \tag{3.15}$$

where, $\frac{dQ_1}{dz} = -U_1(T_1 - T_2)w_1$ and $\frac{dQ_3}{dz} = -U_3(T_3 - T_2)w_3$ are the heat transferred from the fluid to the wall per unit length.

Using Taylor expantion for $Q_2\left(z \pm \frac{dz}{2}\right)$ we get,

$$\frac{dQ_2}{dz} = -\lambda_2 A_2 \frac{d^2T_2}{dz^2} = -U_1(T_1 - T_2)w_1 - U_3(T_3 - T_2)w_3 \tag{3.16}$$

Note that in writing the energy conservation Eq. (3.16) as above, the wall does not impose a resistance to heat flow in transverse direction. The model as stated in this form thus only applies where the resistance at the interface between fluids and wall dominates the total resistance across the wall. In all practical situations, the reactor design should fulfill this assumption. In cases, where this assumption does not apply the model can easily be extended according to Baier, T. et al. (2007) [8].

Energy balance equations constitute a system of three coupled ordinary differential equations for the three temperatures T_1, T_2, and T_3 of which two are of first order while one is of second order.

3.1.5 Boundary conditions

In order to solve the system we have to supply following boundary conditions:

$$X_{co(z=0)} = 0 \tag{3.17}$$

$$T_{1(z=0)} = T_{10} \tag{3.18}$$

$$T_{3(z=0)} = T_{30} \tag{3.19}$$

$$\left.\frac{dT_2}{dz}\right|_{z=\{0,L\}} = 0 \tag{3.20}$$

where, the second and third conditions are the inlet temperatures of the heat exchange stream [cold] and reactant stream [hot] fluid respectively and the fourth condition relate to the fact that heat cannot flow out of the front and rear ends of the wall, i.e., they ensure that the longitudinal heat flow inside of the wall vanishes at end of the reactor.

The second-order differential equations can be converted into the two 1-order equations by following way:

$$\frac{dT_2}{dz} = P_2 = 0 \tag{3.21}$$

$$\frac{d^2T_2}{dz^2} = \frac{dP_2}{dz} = \frac{U_1 w_1}{\lambda_2 A_2}(T_1 - T_2) + \frac{U_3 w_3}{\lambda_2 A_2}(T_3 - T_2) \tag{3.22}$$

The heat transfer coefficients (U_1 and U_3) are calculated from the parameterisation of the Nusselt number in the laminar flow regime according to Kim G.P. et al. (2005) [46] that is given by:

$$Nu = \frac{U_i d_i}{\lambda_2} = -1.047 + 9.326 \frac{1 + a_i^2}{(1 + a_i)^2} \tag{3.23}$$

where, d is the hydraulic diameter of the channel (defined as 4 times the cross-section divided by the wetted perimeter) given by [34]

$$d_i = \frac{(2\, h_i b)}{(h_i + b)} \tag{3.24}$$

And a is aspect ratio of the channel [dimensionless] given by [46]

$$a_i = \frac{h_i}{b} \tag{3.25}$$

For the study of WGS reaction in micro-channel reactor, we have considered the following two cases:

CASE-1: WGS micro-channel reactor with heat conduction through the wall-channel.

For this case, we have to solve five (5)-first order differential equations simultaneously, of which, four (4)-first order differential equations for the temperatures -- one for each channel; two for the wall-channel, since the original equations here is of second order and one (1)-first order differential equations for the reaction progress. We have solved these five (5)-first order differential equations using the MATLAB Ordinary Differential Equations toolbox.

CASE-2: WGS micro-channel reactor with neglecting heat conduction through the wall-channel.

This is the special case of the problem under consideration. For this case, we are neglecting the heat conduction through the wall-channel, we have to simplify the system of energy balance equations i.e. replace T_2 in energy balance equation of the heat exchange stream and reactant stream by the temperature of reaction-channel and cooling-channel respectively. Also w_1 and w_2 are same; otherwise we don't get heat conservation.

Furthermore, instead of U_1 and U_3 in energy balance equations of the heat exchange steam and reactant stream, we have to use overall heat transfer coefficient, U which can be written in the form [46]:

$$U = \frac{1}{\frac{1}{h_{c,1}} + \frac{h_2}{\lambda_2} + \frac{1}{h_{c,3}}} \tag{3.26}$$

where, $h_{c,i}$ is the surface-convective heat transfer coefficient and λ_2 the wall thermal conductivity.

For the heat exchange stream, the surface-convective heat transfer coefficient is given by [34]:

$$h_{c,1} = \frac{N_{u1} k_{f,1}}{D_h} = \frac{N_{u1} k_{f,1}}{4h_1} \tag{3.27}$$

For the reactant stream, the surface-convective heat transfer coefficient is given by [46]:

$$h_{c,3} = \frac{N_{u3} k_e}{D_h} = \frac{N_{u3} k_e}{4h_3} \tag{3.28}$$

where, D_h is the hydraulic diameter. For the parallel plate geometry of the micro-reactor, in the case of uniform wall temperature and constant heat flux, the Nusselt numbers have been reported 7.54 and 8.23, respectively. For this simulation study we have assumed a Nusselt number of 8.0 [46]. Classical analysis of the effective conductivity of packed beds provides that k_e can be written in terms of the porosity of the packed bed (ε), the conductivity of the reactant fluid and the catalyst [46].

$$k_e = \varepsilon k_{f,3} + (1 - \varepsilon) k_{cat} \tag{3.29}$$

In this case, we only have to solve two (2)-first order differential equations for the temperatures (T_1 and T_3) in each channel and one for the reaction progress. So, for this case, we have solved total three (3)-first order differential equations using the MATLAB Ordinary Differential Equations toolbox.

3.2. DEVELOPMENT OF MATHEMATICAL MODEL OF MMCR

3.2.1. Mathematical model development

For the Mathematical model development of WGS Membrane micro-channel reactor, we have considered reaction channel consists of two concentric tubes as shown in Fig. 3.3, the outer tube is the shell and the inner tube is the Palladium membrane. The catalyst is packed in the shell side, because this configuration is more efficient for the heat exchange, allowing better catalyst exploitation and also the membrane area has a good utilization. The mathematical models are written to describe the behavior of a non-isothermal WGS membrane micro-channel reactor in the stationary state.

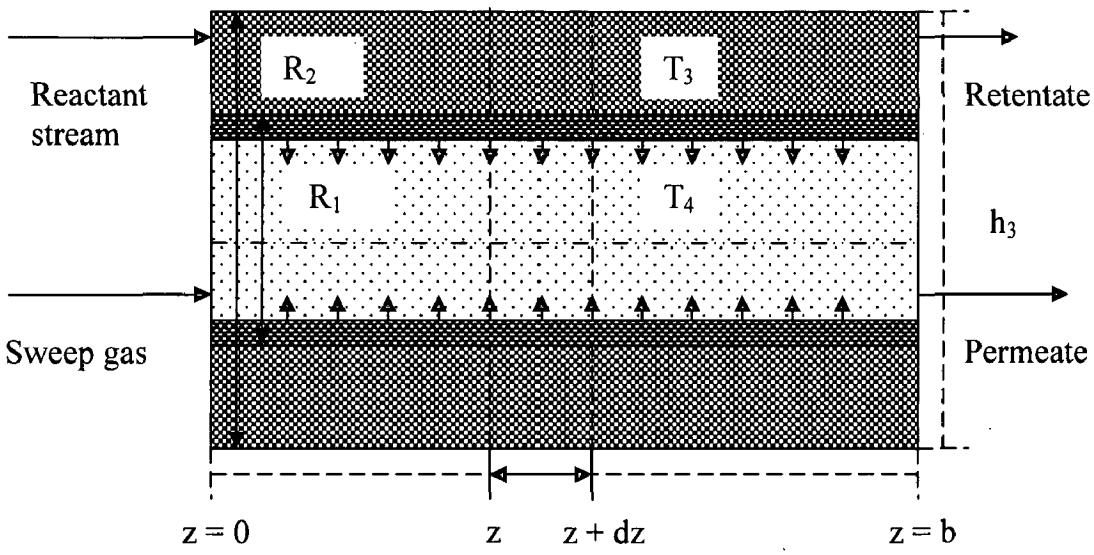

Fig.3.3. Schematic diagram of the membrane micro-channel reactor model

3.2.2. Assumptions

In addition of assumption, we have taken for development of mathematical model of WGS micro-channel reactor with consideration of heat conduction through the wall-channel, following assumptions also considered for development of this model.

1. Only H_2 is removed through the membrane, the Pd membrane shows an infinite selectivity versus H_2 compared with other species.

2. Plug flow in retentate and permeate streams. This assumption is justified by a very thin annulus, where the dispersion and radial profiles can be neglected with the respect to the axial ones.
3. Constant pressure on the permeate side.

3.2.3. Material balance

3.2.3.1. Feed (shell) side

Based on the volume element from z to $z+\Delta z$, the material balance for gas species i can be expressed as

In − Out + Generation = Accumulation (3.30)

$$F_z - F_{z+\Delta z} + \left(\upsilon_i r\left(c_i, T_3\right) A\right) - \left(2\Pi R_1 J_i\right) = 0 \tag{3.31}$$

Dividing both sides of Eq. (3.31) by Δz and taking the limit as $\Delta z \rightarrow 0$ gives

$$\frac{dF_i}{dz} - \left(\upsilon_i r\left(c_i, T_3\right)\Pi\left(R_2^2 - R_1^2\right)\right) - \left(2\Pi R_1 J_i\right) \tag{3.32}$$

where, υ_i are positive for the products and negative for the reactants.

In the material balance Eq. (3.32), the first term represents the convective flux variation of i^{th} species along the reactor length, the second the reaction and the third the hydrogen permeation through the membrane. The permeation rate of component i except hydrogen is zero (Ji = 0) because Pd membrane allows only hydrogen to permeate.

3.2.3.1. Sweep (lumen) side

Similarly, the material balance on the sweep or tube side is carried out, and the resulting equation is

$$\frac{dF_i}{dz} = \left(2\Pi R_1 J_i\right) \tag{3.33}$$

The equations of the permeate side are constituted of the same terms as at the reaction side, without that relative to the chemical reaction. The term of the permeating flux through the membrane has a positive sign because in this case the H_2 enters in the permeation volume.

3.2.4. Energy balance

In this section, we have derived the energy balance equations for the reaction-channel with membrane inside the tube and catalyst packed in the shell side as shown in Fig. (3.3). In addition of these energy balance equations, we also have to consider energy balance (heat transfer) Eq. (3.10) and Eq. (3.16) for the cooling-channel and for the wall-channel respectively as mention in section of WGS micro-channel reactor with heat conduction through the wall-channel.

3.2.4.1. Feed (shell)) side

We carried out the energy balance on the volume element of the membrane micro-channel reactor from z to $z+\Delta z$ by considering the heat of the reaction, the heat transfer through the membrane, and the energy carried by permeating gases. By taking the limit as $\Delta z \rightarrow 0$, we get the following differential equations.

$$\sum F_i C_{pi} \frac{dT_3}{dz} = -U_3(T_3 - T_2)w_3 + \left(\Pi\left(R_2^2 - R_1^2\right)\Delta Hr(c_i, T_3)\right) - \left(U^M\left(2\Pi R_1\right)\right)(T_3 - T_4) \tag{3.34}$$

In the energy balance Eq. (3.34), the first term represents the convective flux of energy in the shell side along the reactor length, the second term the heat exchanged through the wall-channel, the third term the heat production by chemical reaction and fourth term the heat exchanged with the permeation side.

3.2.4.1. Sweep (lumen) side

Similarly, the energy balance on the sweep or tube side is carried out, and the resulting equation is

$$\sum F_i C_{pi} \frac{dT_4}{dz} = \left(U^M\left(2\Pi R_1\right)\right)(T_3 - T_4) \tag{3.35}$$

In the energy balance Eq. (3.35) on permeates side, the heat produced by reactions is not present and the first term represents the convective flux of energy in the tube side along the reactor length, second term the heat exchanged with the permeation side.

The major resistance for the heat exchange between the annulus and the lumen side is the conductivity through the membrane support. In this work, a Palladium membrane is

used in the simulations, therefore, an overall heat transfer coefficient similar to that of the stainless steel shell is used for U^M [200 W/m^2 K] [17].

3.2.5 Boundary conditions

In order to solve the system we have to supply following boundary conditions:

$$F_{i(z=0)} = F_i^{\,0} \tag{3.36}$$

$$T_{4(z=0)} = T_{10} \tag{3.37}$$

Here, we have taken inlet permeation temperature as the same as inlet reaction temperature. Where, first conditions are the inlet molar flow rate of the reactant gas stream and second condition relate to inlet temperature of the permeation stream.

In addition of these boundary conditions, we also have to consider boundary conditions Eq. (3.18), Eq. (3.19) and Eq. (3.20) for the reaction temperature, the cooling-medium temperature and for the wall-channel temperature respectively as mention in section of WGS micro-channel reactor with heat conduction through the wall-channel.

3.2.6 Permeating flux

A Palladium membrane (200 nm thick) is considered in the present simulation which has an infinite selectivity towards H_2 against any other species such as CO or CO_2. Therefore, no CO, CO_2, H_2O present in the system or other species (e.g. nitrogen often used as sweep but not in this case) are not expected in the permeate stream. The permeating flux of hydrogen gas through Palladium membrane follows Sievert's law and is given by [41]:

$$J = \left(\frac{Q}{\delta}\right)\left(\sqrt{P_{H_2}} - \sqrt{P_{H_2,SW}}\right) \tag{3.38}$$

where, Q is the permeation coefficient, δ the membrane thickness and P_{H_2} and $P_{H_2,SW}$ hydrogen partial pressures on both the sides of membrane.

The permeation coefficient is given by [41]:

$$Q = \left(\frac{D}{K}\right) = \left(\frac{D_0}{K}\right)\exp\left(-\frac{E_D}{RT}\right) \tag{3.39}$$

where, D is the diffusivity of hydrogen through palladium, D_0 the diffusivity pre-exponential coefficient, K Sievert's constant, E_D the activation energy for diffusion, R the universal gas constant and T the absolute temperature. For this simulation, we have considered the following permeation coefficient equation of Palladium membrane [32]:

$$Q = 2.19\times10^{-4}T^{-1.0358}\exp\left(-\frac{21700}{RT}\right) \tag{3.40}$$

Thus, the total flow of gas, F, through the membrane will be given by [41]:

$$F = J\times A = \left(\frac{D_O}{K\delta}\right)\exp\left(-\frac{E_D}{RT}\right)\left(\sqrt{P_{H_2}} - \sqrt{P_{H_2,SW}}\right)\times A \tag{3.41}$$

From this equation, it can be seen that the permeation of hydrogen through the micro-channel membrane increases if the membrane thickness is reduced and/or the hydrogen pressure gradient across the membrane is increased. It also suggests that if we increase the temperature of the micro-channel membrane, the hydrogen flow will increase. Thus, the membrane should withstand high temperatures without breaking or becoming brittle. A low membrane thickness is required in order to reduce the cost.

The partial pressures in the reaction side and sweep side can be determined as

$$P_i = y_i P \tag{3.42}$$

$$P_{H_2,SW} = given \tag{3.43}$$

The most important variable to be evaluated for describing the membrane micro-channel reactor is CO conversion which is calculated as follows [17]:

$$X_{co} = 1 - \frac{F_{CO}^{Reaction}}{F_{co}^{Feed}} = \frac{F_{CO_2}^{Reaction}}{F_{co}^{Feed}} \tag{3.44}$$

In this work, the permeating driving force is created only by the total feed pressure producing a pure H_2 stream as permeate, without requiring a further purification. The other method widely utilizes the sweep gas presence that implies the use of an inert gas, e.g. N_2, fed into the permeation side to improve the H_2 permeation reducing the H_2 partial pressure, but reducing also the purity of the H_2 recovered. However, a very low sweep gas flow rate of hydrogen ($F_{H_2}^{Sweep} = 10^{-5}F_{co}^{Feed}$) is used in the simulations for numerical reasons in order to fix the initial condition of integration system. The use of the same

permeating species as sweep also means a stream on permeate side consisting only of hydrogen [17].

For the study of WGS reaction in membrane micro-channel reactor, we have considered the following three cases:

CASE-1: WGS Membrane micro-channel reactor with neglecting the heat conduction through the wall-channel without heat exchange stream

This is the special case of the problem under consideration. For this, we have to solve five (5)-material balance equations for the reaction in membrane micro channel and two (2)-energy balance equations: one for the reaction and second one for the permeation. So, we have solved total seven (7)-first order differential equations simultaneously using the MATLAB Ordinary Differential Equations toolbox.

CASE-2: WGS Membrane micro-channel reactor with neglecting the heat conduction through the wall-channel with heat exchange stream

This is also the special case of the problem under consideration. For this, with addition of seven (7)-first order differential equations as mention in case-1, we have to consider energy balance equations for heat exchange stream [cooling-channel]. So, we have solved total eight (8)-first order differential equations simultaneously using the MATLAB Ordinary Differential Equations toolbox.

CASE-3: WGS Membrane micro-channel reactor with heat conduction through the wall-channel with heat exchange stream [channel-1]

In this case, with addition of eight (8)-first order differential equations as mention in case-2, we have to consider heat transfer equations for the wall-channel. So, we have solved total ten (10) - first order differential equations simultaneously using the MATLAB Ordinary Differential Equations toolbox.

3.3. REACTION RATE

For this work, the commercial 5 wt. % copper on alumina catalyst is used. The reaction rate for this catalyst is given by the following equation [58]:

$$r' = k_3 P_{CO} P_{H_2O} \left(1 - \frac{P_{CO_2} P_{H_2}}{K_3 P_{CO} P_{H_2O}}\right) \text{in(mol/g-cat.s)} \tag{3.45}$$

$$\text{where, } k_3 = 0.00225 \exp\left(\frac{-50,000}{RT}\right) \text{in(mol/g-cat.s.kpa}^x\text{)} \tag{3.46}$$

$$K_3 = 9.543 \times 10^{-3} \exp\left(\frac{39876}{RT}\right) \tag{3.47}$$

Crushed catalyst particle size used in the experiment ranged from 0.25 mm to 0.5 mm. For this work, particle diameter and the bulk catalyst density are assumed to be 0.3 mm and 10^6 g/m3, respectively [58]. So, rate expression in terms of (mol/ m^3 s) is given by

$$r = r' \rho_b \text{ in (mol/m}^3\text{s)} \tag{3.48}$$

Since the reactant is assumed to follow the ideal gas law, the concentration change due to temperature variation results in variation of the reactant density.

$$\rho_3 = mw \sum C_i = mw \left(\frac{P}{RT}\right) \tag{3.49}$$

3.4. OPERATING CONDITIONS

Model geometries and physical parameters are summarized in Table 3.1 [46]. Constant properties are assumed for the heat exchange stream-cooling medium i.e. air. For the reactant, volume averaged values at 600 K are used for k_3 and $Cp_{,3}$. For the heat exchange fluid, values for ρ_1, $k1$ and $Cp_{,1}$ are taken at 400 K for the air [46].

A typical exit stream composition of a steam reformer (SR) or auto-thermal reactor (ATR) consists of 25–75% H_2, 1–15% CO, 5–20% CO_2, 10–60% N_2 and a water-to-CO mole ratio between 2 and 15 [43]. The inlet conditions of the Reactant gas composition and feed flow rate, which we have used in this work, are summarized in Table 3.2 [46].

Table 3.1: Model geometry and physical parameters [46]

Model geometry	**Value**
Channel width, b (mm)	40
Fin thickness, b_2 (mm)	20
Channel length, Z (mm)	40
Cooling channel height, h_1 (mm)	0.5
Wall channel height, h_2 (mm)	1
Reaction channel height or inside diameter of shell, $h_3 = R_2$ (mm)	0.5
Outside diameter of the tube, R_1 (mm)	0.25
Membrane thickness, δ (nm)	200
Physical parameters	
Bulk catalyst density, ρ_b (g/m^3)	10^6
Catalyst conductivity, k_{cat} (W/m K)	0.4
Reactant thermal conductivity, $k_{f,3}$ (W/m K)	0.1181
Air density, ρ_1 (kg/m^3)	0.883
Air thermal conductivity, $k_{f,1}$ (W/m K)	0.0331
Air heat capacity, $C_{p,1}$ (J/kg K)	1009
Air velocity, u_1 (m/s)	0-5
Inlet reactant temperature, T_3 (K)	710
Inlet air temperature, T_1 (K)	400
Inlet pressure, P (kPa)	303
Permeate pressure, $P_{H_2,SW}$ (kPa)	10

Table 3.2: Reactant gas composition and feed flow rate [46]

Component	**Gas composition (%)**	**Molar flow rate (mol/s)**
CO	6	1.56×10^{-5}
H_20	25	6.5×10^{-5}
CO_2	10	2.6×10^{-5}
H_2	29	7.54×10^{-5}
N_2	30	7.8×10^{-5}

The temperature dependence of heat capacity is given by the following equations according to the thermodynamics:

$$\frac{Cp_i}{R} = A + BT + CT^2 + DT^{-2} \tag{3.50}$$

where, either C or D is zero, depending on the substance considered. Since the Cp/R is dimensionless, the units of Cp are governed by the choice of R. Heat capacity constants values of components are summarized in Table 3.3.

Table 3.3: Heat capacity constants values

Component	A	$B\times10^3$	$C\times10^6$	$D\times10^{-5}$
CO	3.376	0.557	--	-0.031
H_2O	3.470	1.450	--	0.121
CO_2	5.457	1.045	--	-1.157
H_2	3.249	0.422	--	0.083
N_2	3.280	0.593	--	0.040

The temperature dependence of heat of reaction is given by the following equations according to the thermodynamics:

$$\Delta H^0 = \Delta H_O{}^0 + \langle \Delta Cp^0 \rangle_H (T - T_0) \tag{3.51}$$

where, ΔH^0 and $\Delta H_O{}^0$ are heat of reaction at temperature T and at reference temperature T_0 respectively. For this work, we have taken 25^0C as reference temperature T_0.

$\langle \Delta Cp^0 \rangle_H$ is the mean heat capacity change of reaction, which is given by the following equations:

$$\frac{\langle \Delta Cp^0 \rangle_H}{R} = \Delta A + \frac{\Delta B}{2} T_0 (\tau + 1) + \frac{\Delta C}{2} T_0^2 (\tau^2 + \tau + 1) + \frac{\Delta D}{\tau T_0^2} \tag{3.52}$$

$$\text{where, } \tau = \frac{T}{T_0},\ \Delta A = \sum \upsilon_i A_i,\ \Delta B = \sum \upsilon_i B_i,\ \Delta C = \sum \upsilon_i C_i,\ \Delta D = \sum \upsilon_i D_i \tag{3.53}$$

υ_i is positive for products and negative for the reactant.

CHAPTER 4

RESULTS AND DISCUSSION

4.1 STUDY OF WGSR IN MCR

4.1.1. Model Validation

For the model validation, the effect of step number on the WGS micro-channel reactor without heat conduction through wall-channel has been considered. For this, all the parameters used are given in the Table 3.1 and number of steps of 50 has been used. We obtained the same trend as given in G. Y. Kim et.al. (2005). However, we observed that this number of steps of 50 is not an optimized step for micro-channel reactor. Therefore, in order to optimize the number of steps, we have studied WGS reactor temperature performance by taking different number of steps: 10, 20, 30, 40, 50, 100, 200, 300, 400 and 500 [Figs. 4.1.(a)-(j)]. We found that at smaller step-number, reaction temperature is going to be decreased immediately and CO conversion is increases fast in the starting, then slowly along the length of the micro-channel reactor and there is no effect of step-number on heat exchange stream temperature profile. With increasing the step-number, reaction temperature is first increases from 710 to 740 K, then going to be decreased and CO conversion is increases faster in the starting, then slowly along the length of the micro-channel reactor. We observed that step-number of 500 is an optimized step and we have taken this step-number for all further results. WGS reaction is a fast exothermic in nature, reaction temperature increases fast in the starting and then decreases due to exchange of heat with heat exchange stream i.e. air. CO conversion is also increases fast in the starting and then it increases slowly. Exit temperature of the reactant stream and heat exchange stream is same that is 550 K as obtained by G. Y. Kim et.al. (2005).

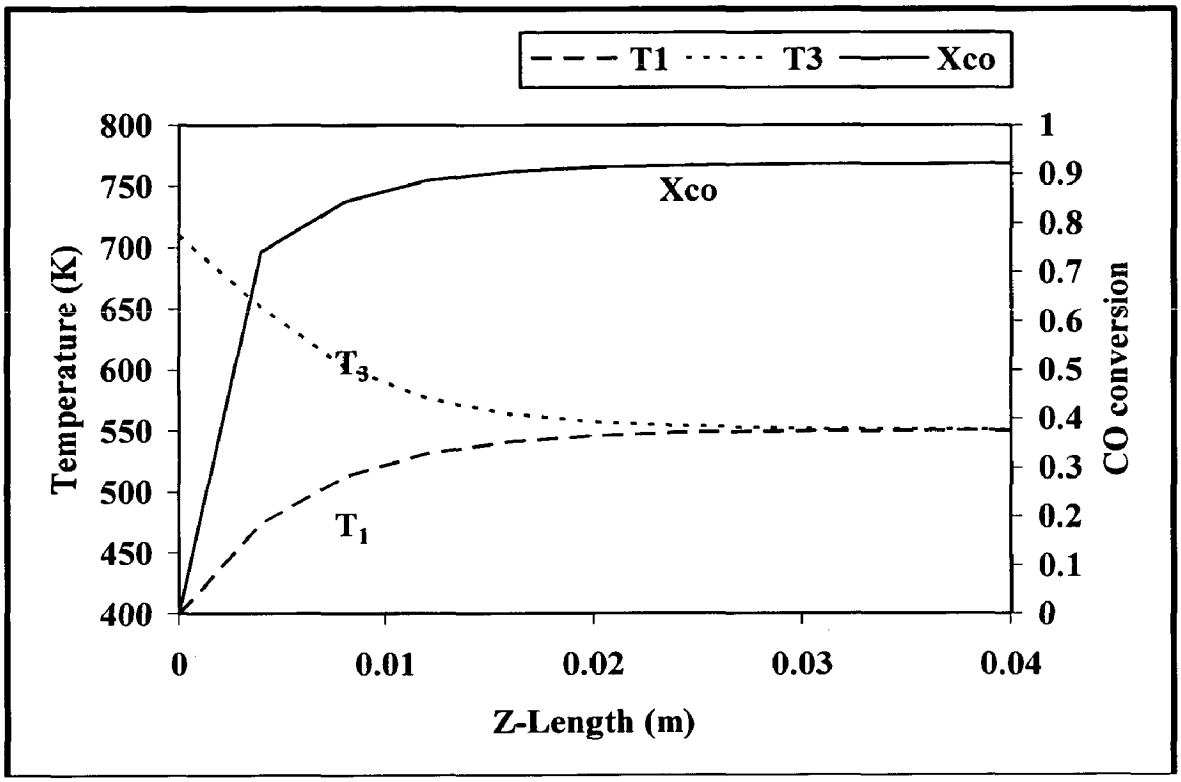

Fig.4.1(a). WGS reactor temperature profile [step-number: 10]

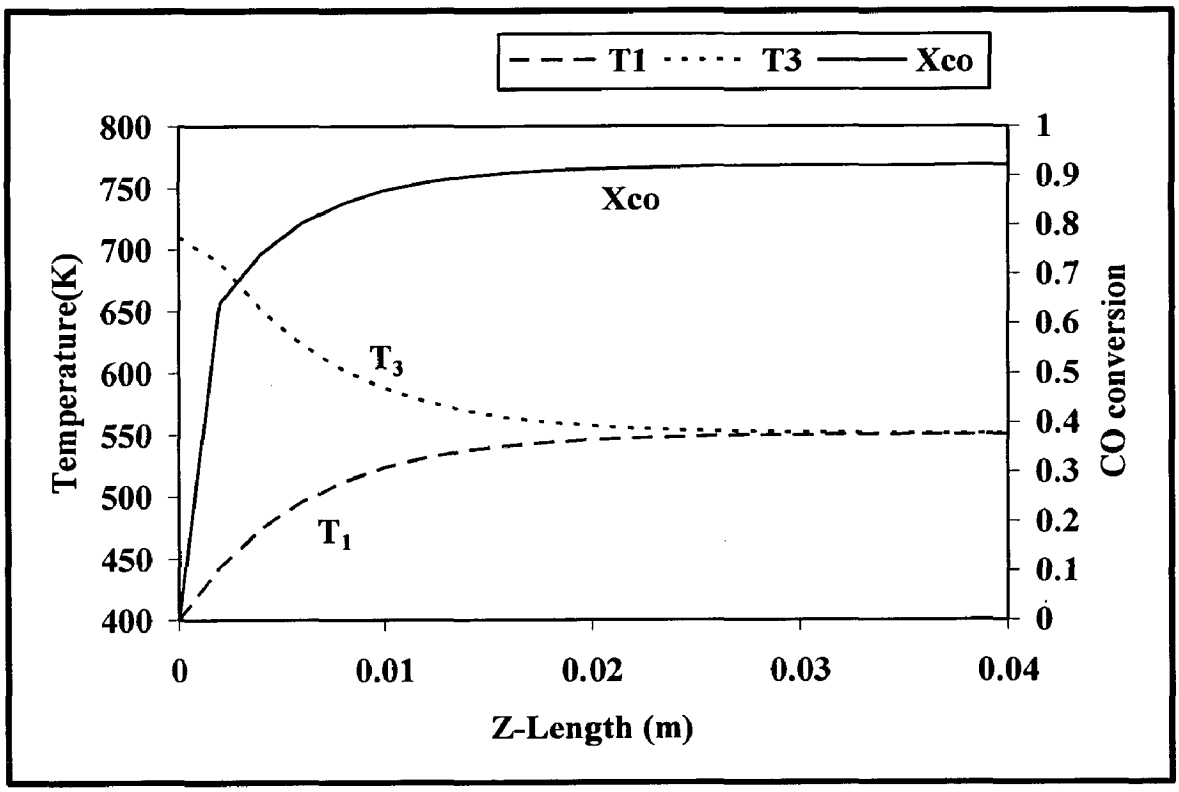

Fig.4.1(b). WGS reactor temperature profile [step-number: 20]

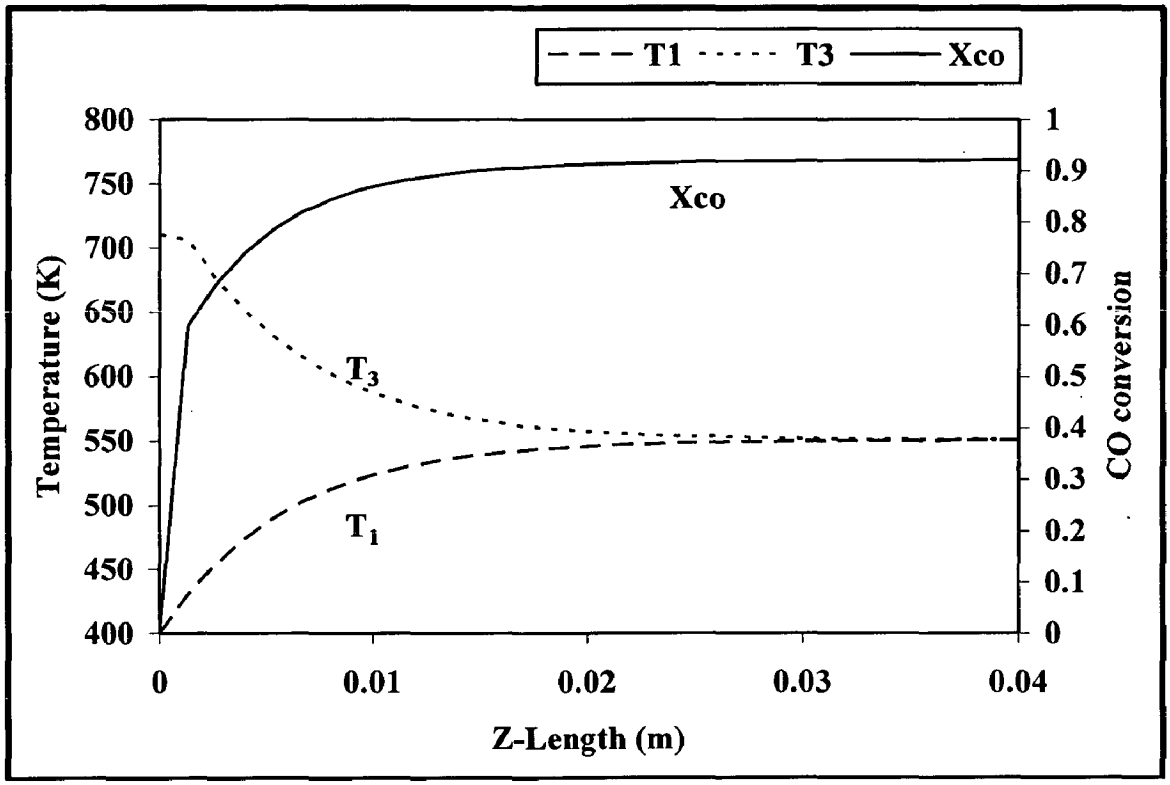

Fig.4.1(c). WGS reactor temperature profile [step-number: 30]

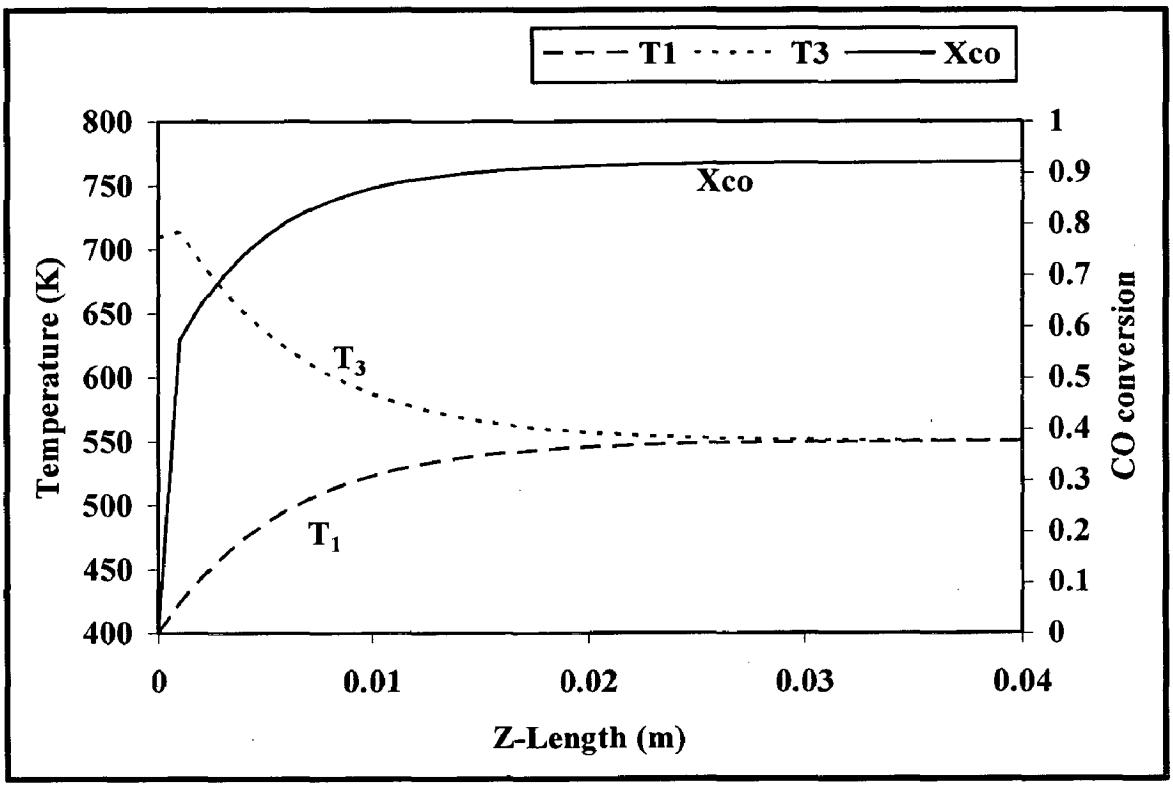

Fig.4.1(d). WGS reactor temperature profile [step-number: 40]

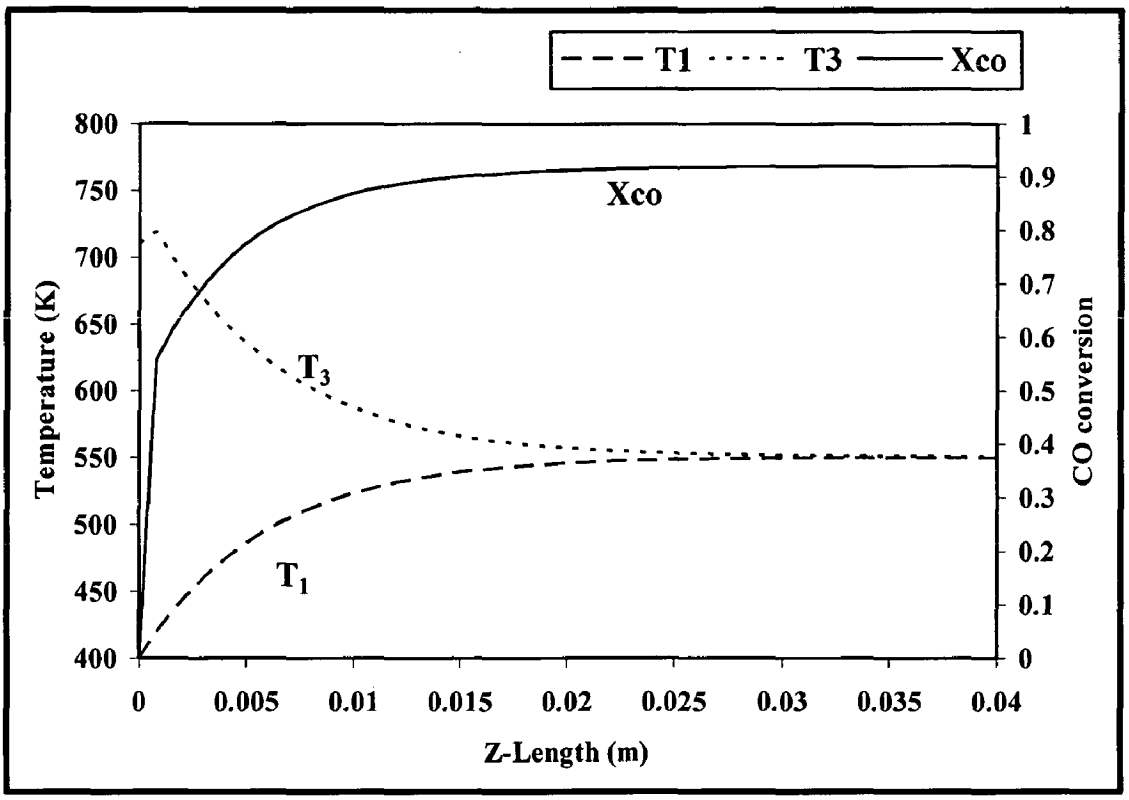

Fig.4.1(e). WGS reactor temperature profile [step-number: 50]

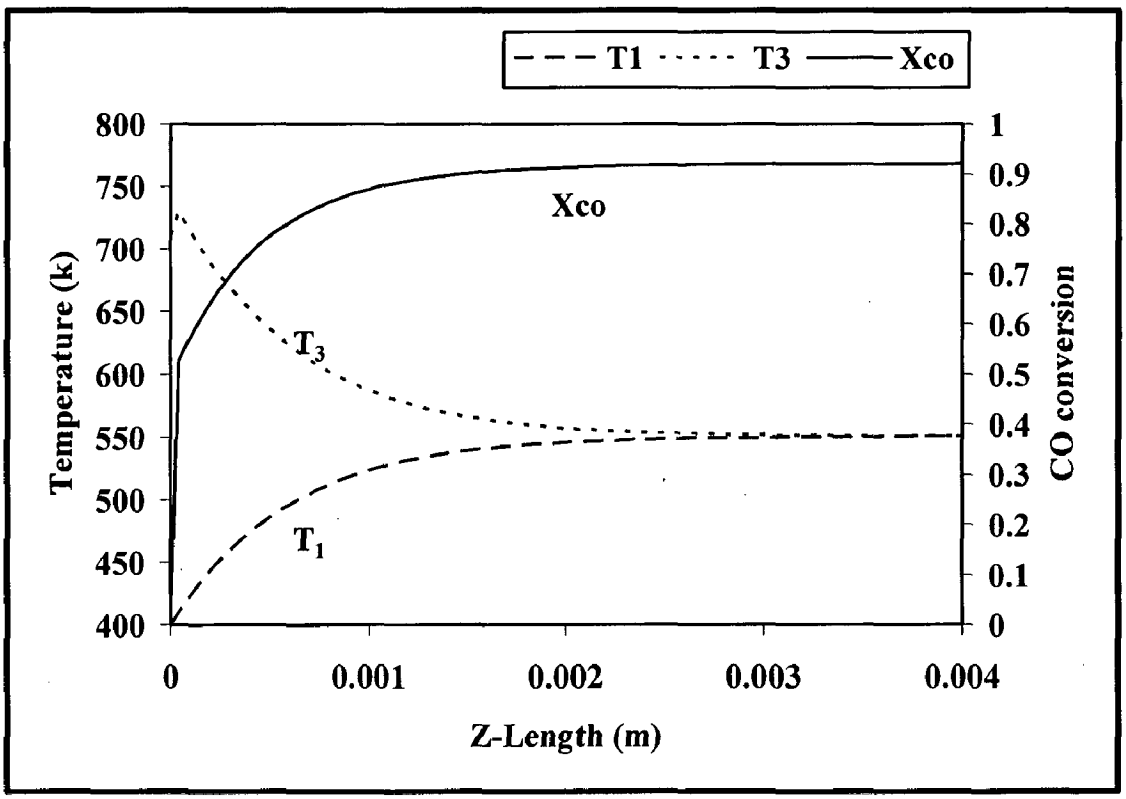

Fig.4.1(f). WGS reactor temperature profile [step-number: 100]

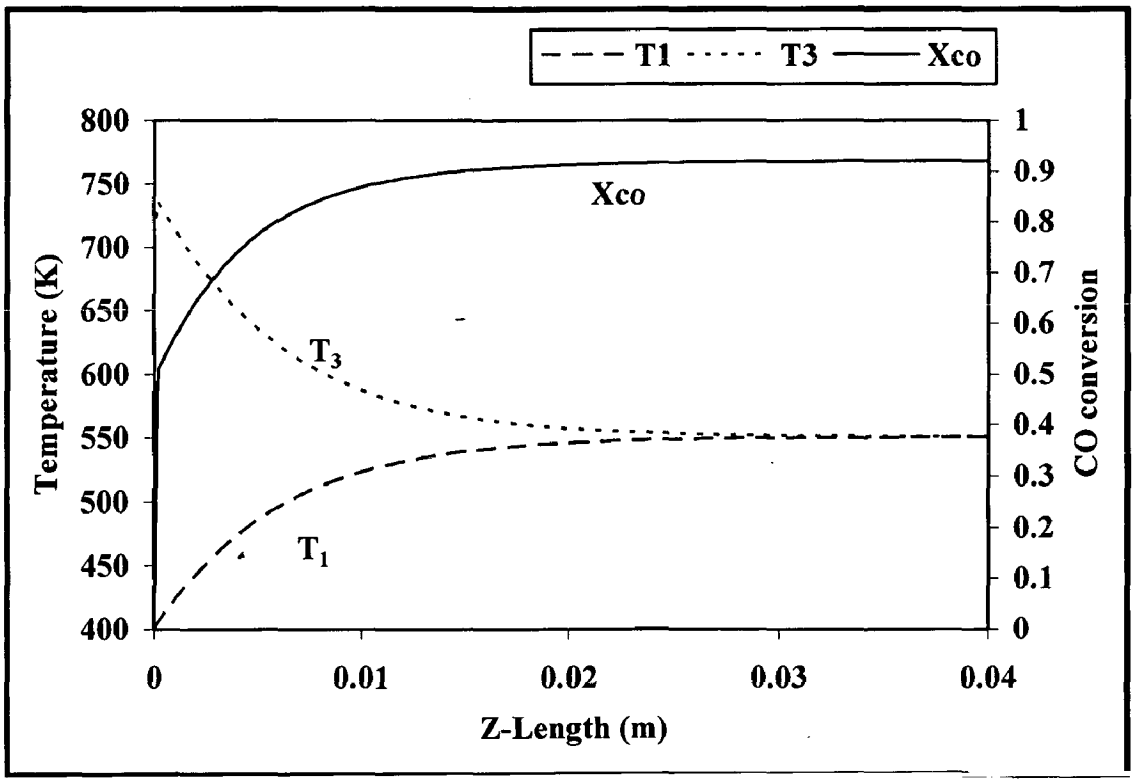

Fig.4.1(g). WGS reactor temperature profile [step-number: 200]

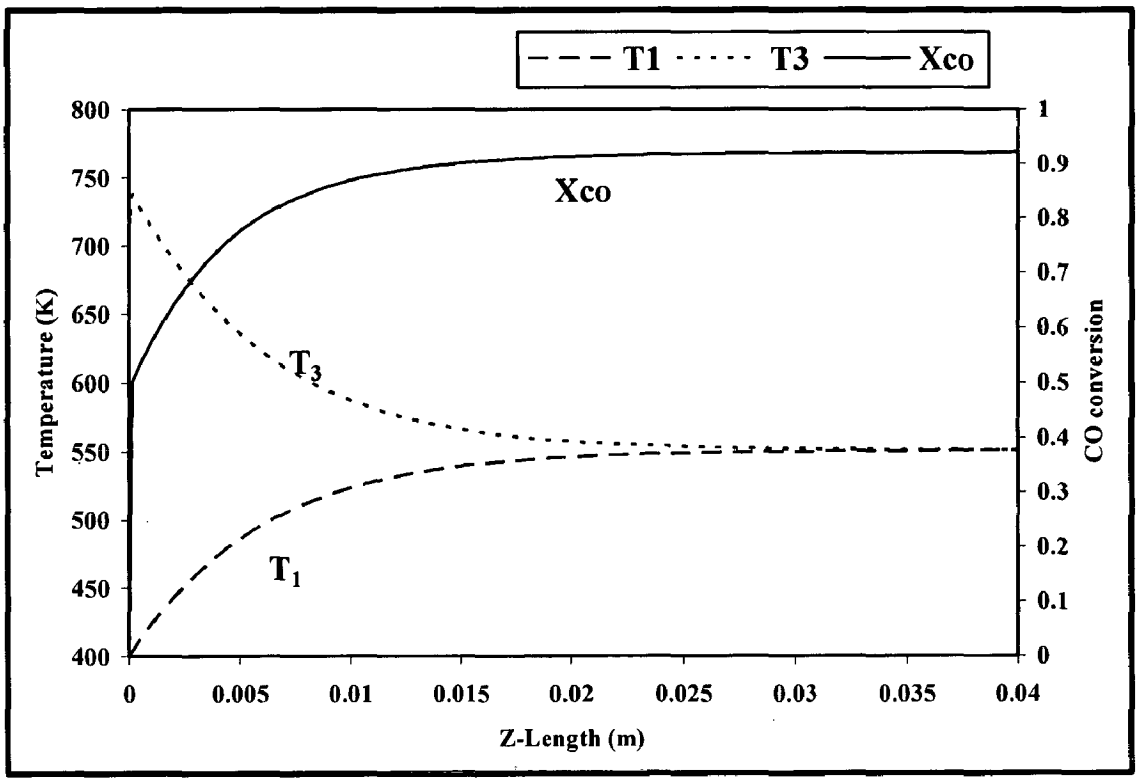

Fig.4.1(h). WGS reactor temperature profile [step-number: 300]

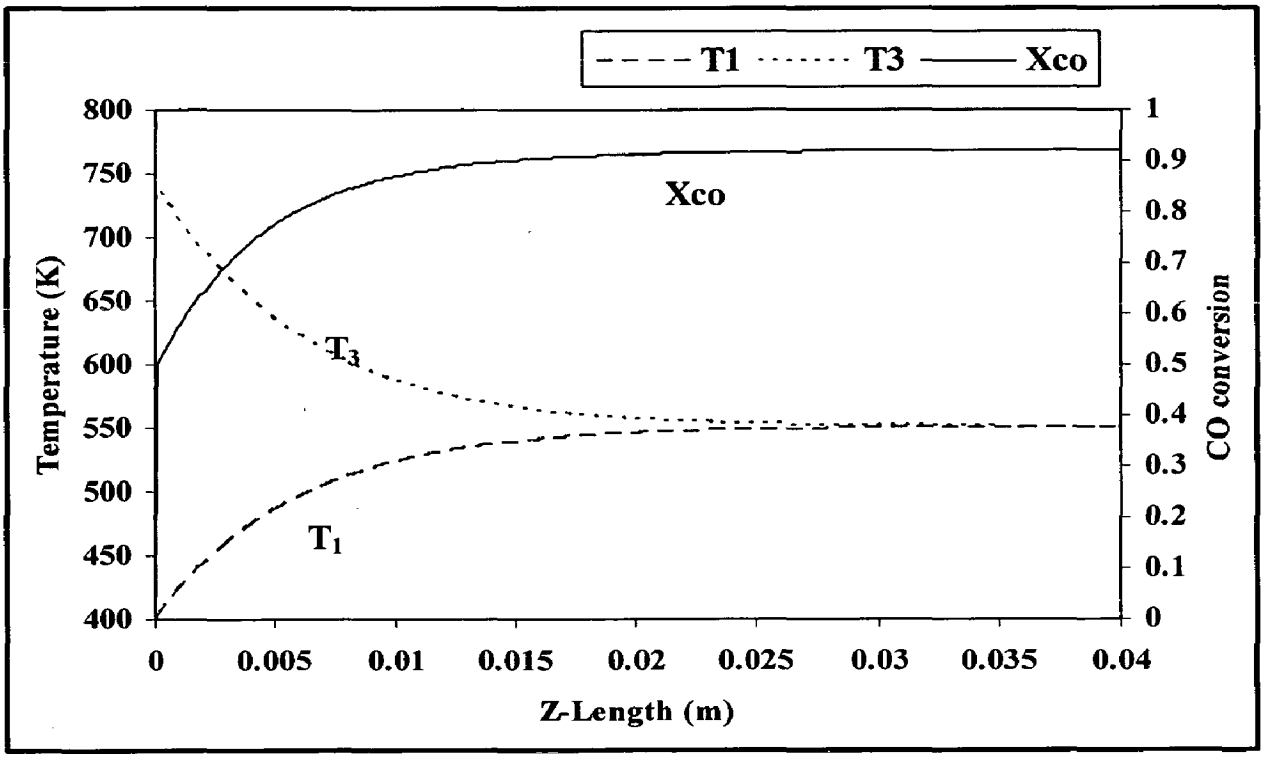

Fig.4.1(i). WGS reactor temperature profile [step-number: 400]

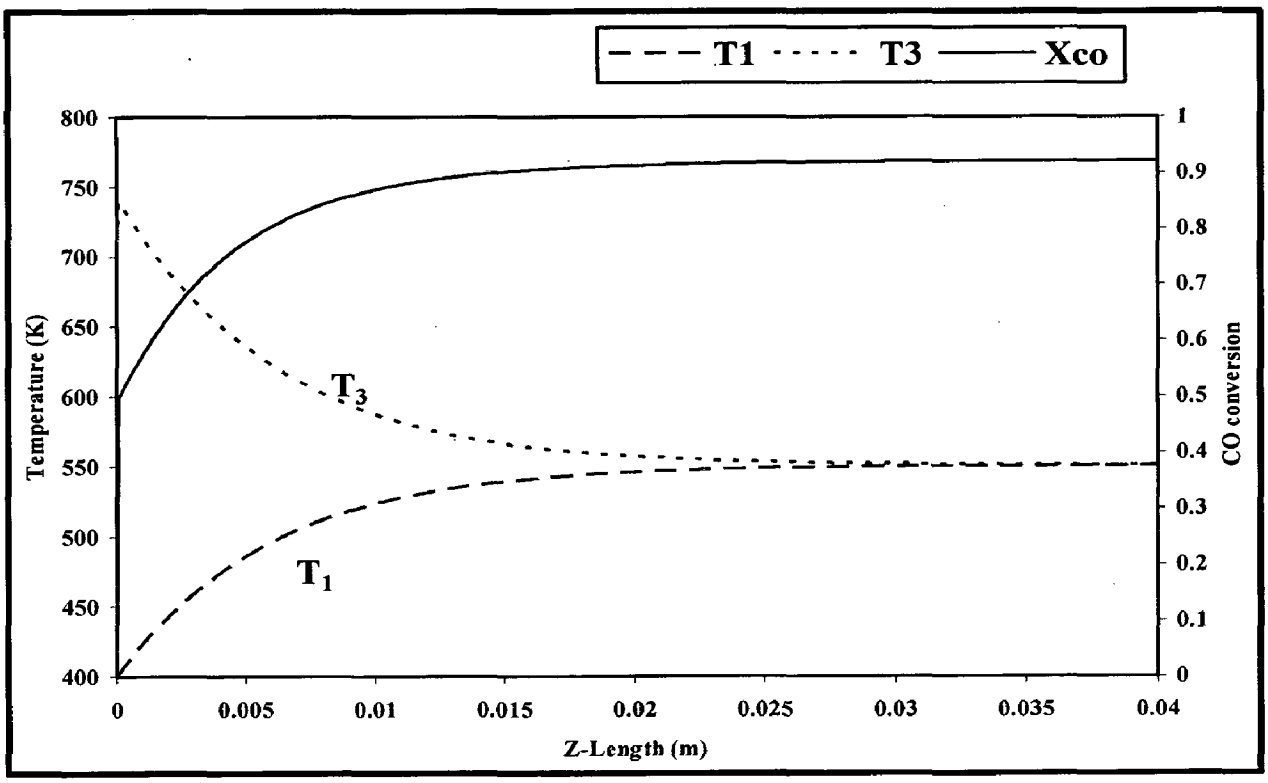

Fig.4.1(j). WGS reactor temperature profile [step-number: 500]

4.1.2. Effect of micro-reactor length (Z)

With consideration of the heat conduction through the wall-channel in micro-channel reactor, initially we have taken all parameters same as given in the Table 3.1. For this, we have optimized the micro-reactor-length by taking different micro-reactor-length (m): 0.04, 0.02, 0.01, 0.005, 0.004, 0.003 and 0.002 [Figs. 4.2.(a)-(g)] and seen their effect on the WGS reactor temperature. From these figures, we can observe that for a micro-reactor smaller than 0.005 m, the deviation between temperature of reactant stream, heat exchange stream and wall-channel is large. Since the reported exit temperature of 550 K of reactant stream, heat exchange stream and wall-channel has been achieved for the reactor length of 0.005 m, therefore we can say that micro-reactor-length of 0.005 m is optimized and we have used this length for the generation of the further results in this case.

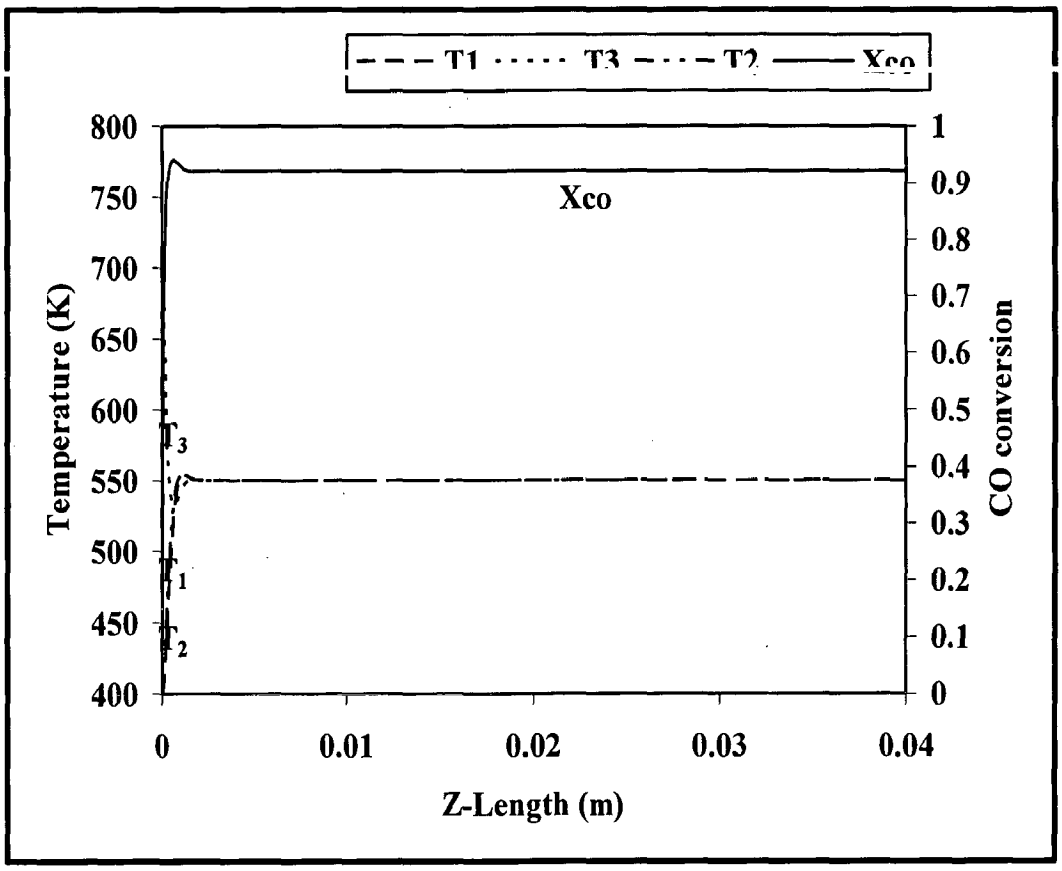

Fig.4.2(a). WGS reactor temperature profile [Z: 0.04 m]

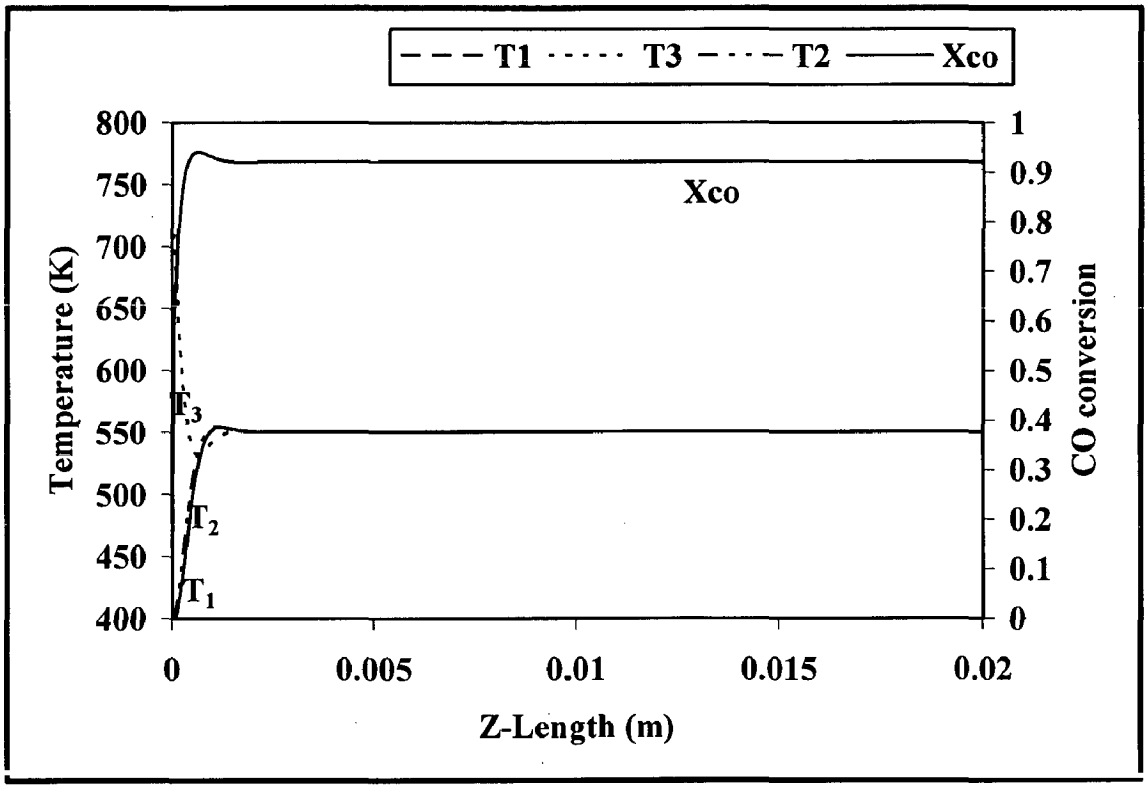

Fig.4.2(b). WGS reactor temperature profile [Z: 0.02 m]

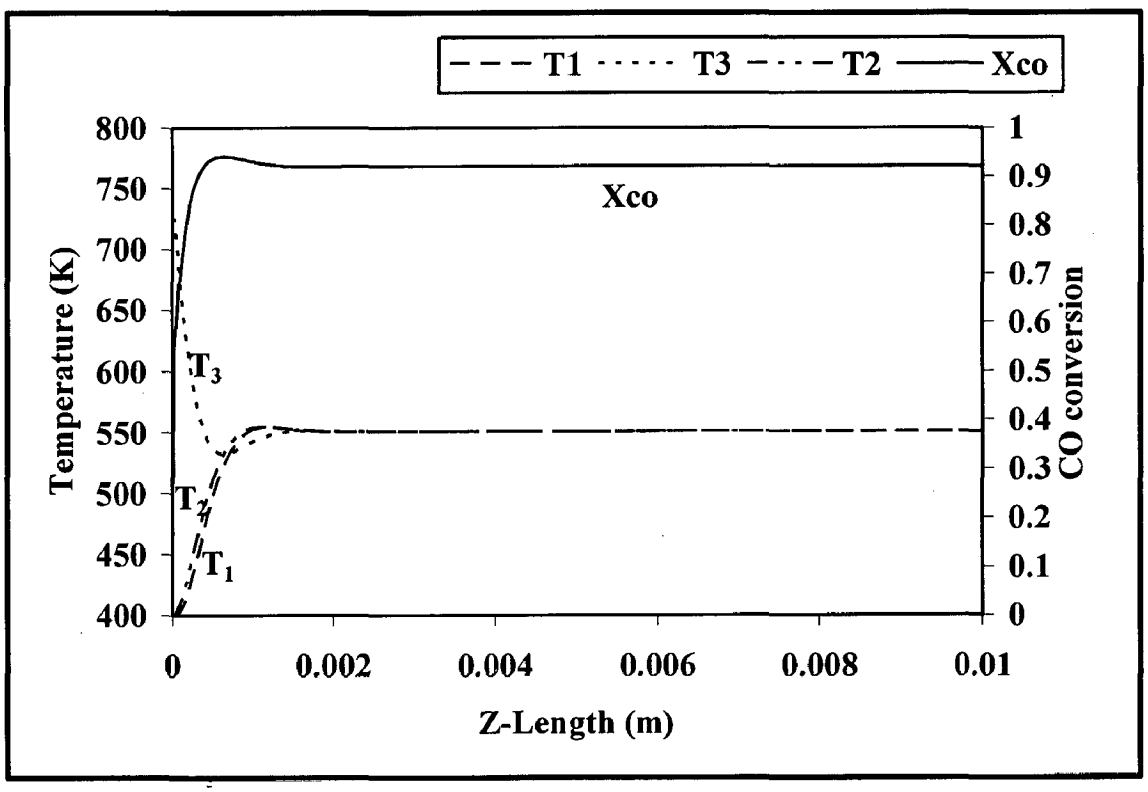

Fig.4.2(c). WGS reactor temperature profile [Z: 0.01 m]

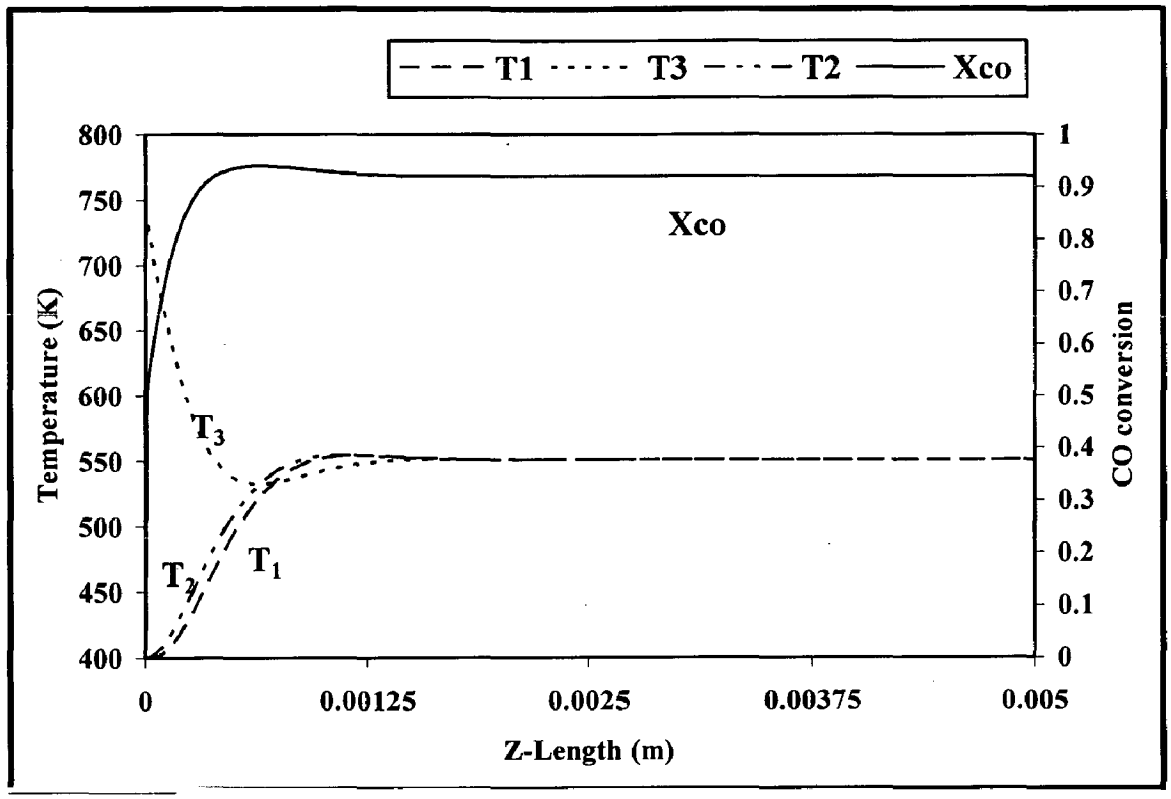

Fig.4.2(d). WGS reactor temperature profile [Z: 0.005 m]

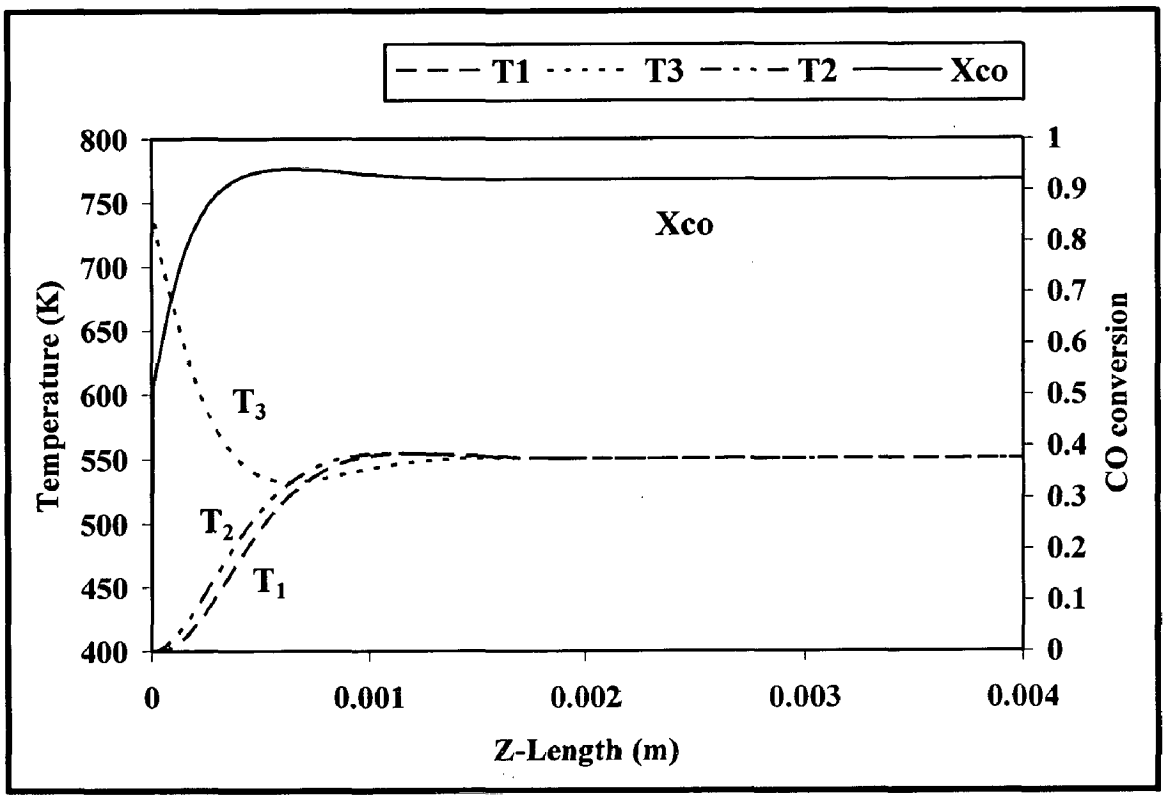

Fig.4.2(e). WGS reactor temperature profile [Z: 0.004 m]

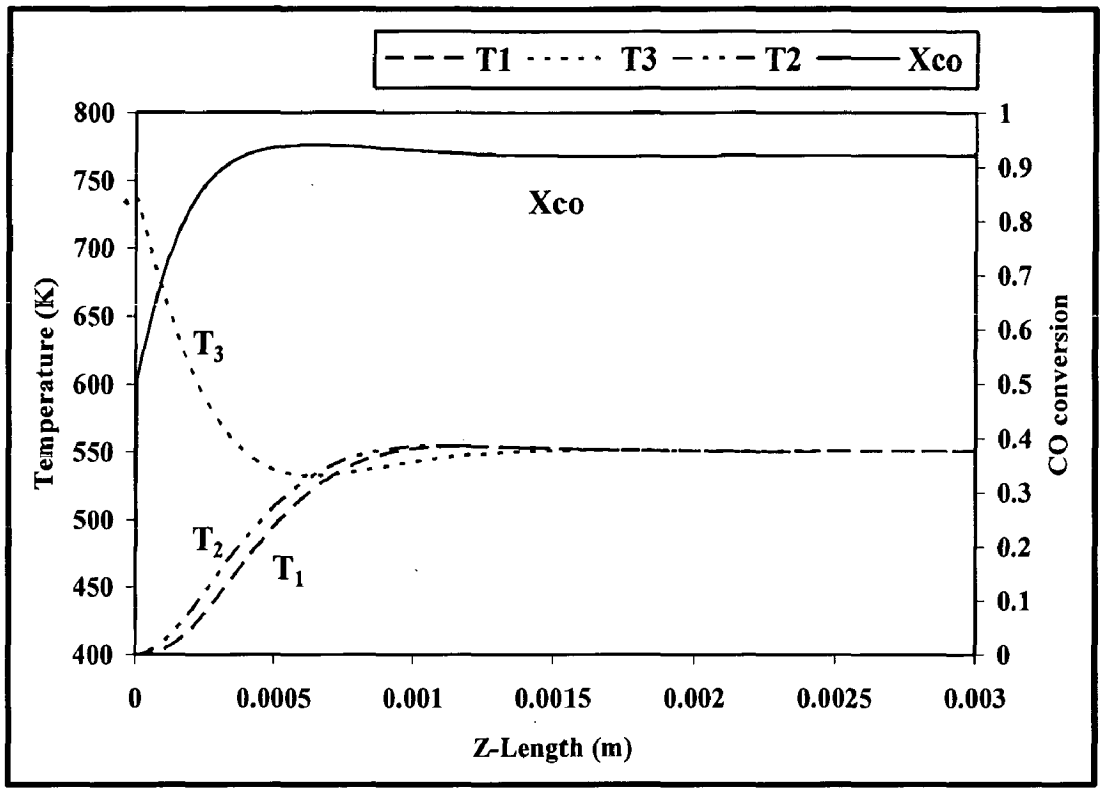

Fig.4.2(f). WGS reactor temperature profile [Z: 0.003 m]

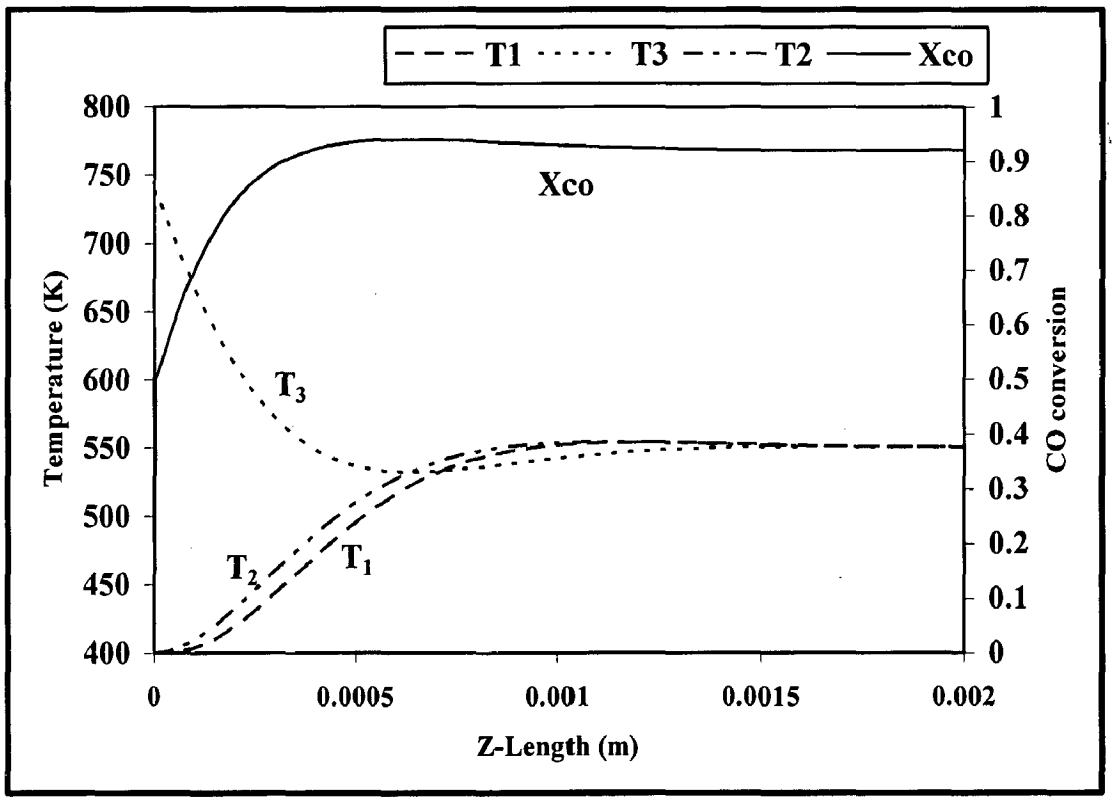

Fig.4.2(g). WGS reactor temperature profile [Z: 0.002 m]

In the next section, we have studied the effect of different parameters such as reaction-channel height (h_3), heat-exchange-channel height (h_1), wall-channel thickness (h_2), and wall-thermal conductivity (λ_2) for WGSR with and without heat conduction through the wall-channel. Also the effect of channel-width (b) for the heat conduction through the wall-channel case has been studied. For this, we have studied and compared the effect of reaction-temperature (T_3), heat exchange stream temperature (T_1) and heat exchange stream velocity (u_1) on the exit CO conversion with and without heat conduction through the wall-channel cases. In Table 4.1, we have summarized all these optimized parameters for two cases, which have obtained from our result.

Table 4.1: Optimized parameters

Parameters	**Case-1: Without heat conduction**	**Case-2: With heat conduction**
Step-number	500	500
Micro-reactor length, Z (m)	0.04	0.005
Reaction-channel-height, h_3(m)	0.0005	0.0007
Heat exchange stream channel height, h_1 (m)	0.0005	0.002
Wall-channel height, h_2 (m)	0.001	0.0025
Wall-thermal conductivity, λ_2 (W/ m K)	0.03	0.03
Channel width, b (m)	0.04	0.04
Reaction temperature, T_3 (K)	710	710
Heat exchange stream temperature:air, T_1 (K)	400	400
Heat exchange stream velocity: air, (m/s)	0.73	0.73

4.1.3. Effect of reaction-channel height (h_3)

From this, we observed that there is no significant effect of reaction-channel height on exit WGSR temperature and exit CO conversion for the case-1 [Fig.4.3(a)]. But for the case-2 [Fig.4.3(b)], with increase of reaction-channel height, exit CO conversion is decreases and deviation between the exit temperature of reactant stream, heat exchange stream and wall-channel is increases.

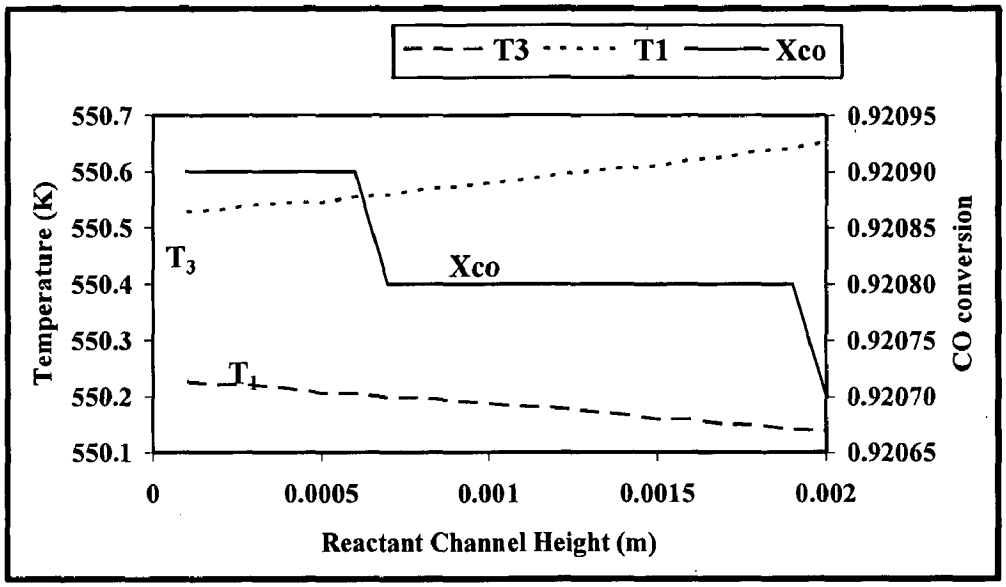

Fig.4.3(a). Effect of reaction-channel height (h_3) without heat conduction

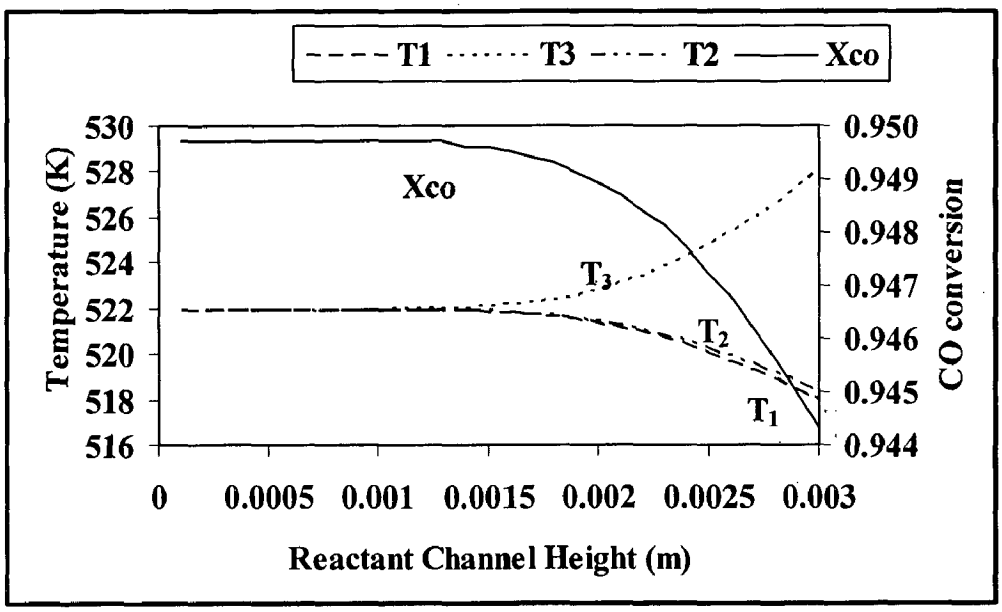

Fig.4.3(b). Effect of reaction-channel height (h_3) with heat conduction

4.1.4. Effect of heat-exchange-channel height (h_1)

From this, we observed that with increase of heat-exchange-channel height, exit CO conversion is increases fast in the starting and then slowly for the case-1 and case-2 both [Fig.4.4(a)-(b)]. With increase of heat-exchange-channel height, deviation between the exit temperature of reactant stream and heat exchange stream is increases for the case-1 [Fig.4.4(a)]. While for the case-2, there is no significant effect of heat-exchange-channel heights, on the exit temperature of reactant stream, heat exchange stream and wall-channel [Fig.4.4(b)].

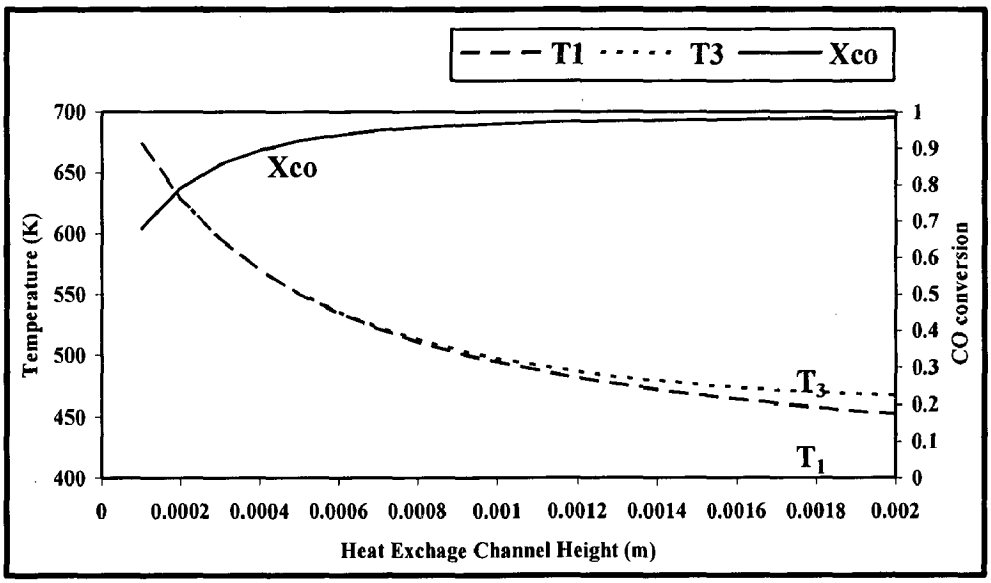

Fig.4.4(a). Effect of heat-exchange-channel (h_1) height without heat conduction

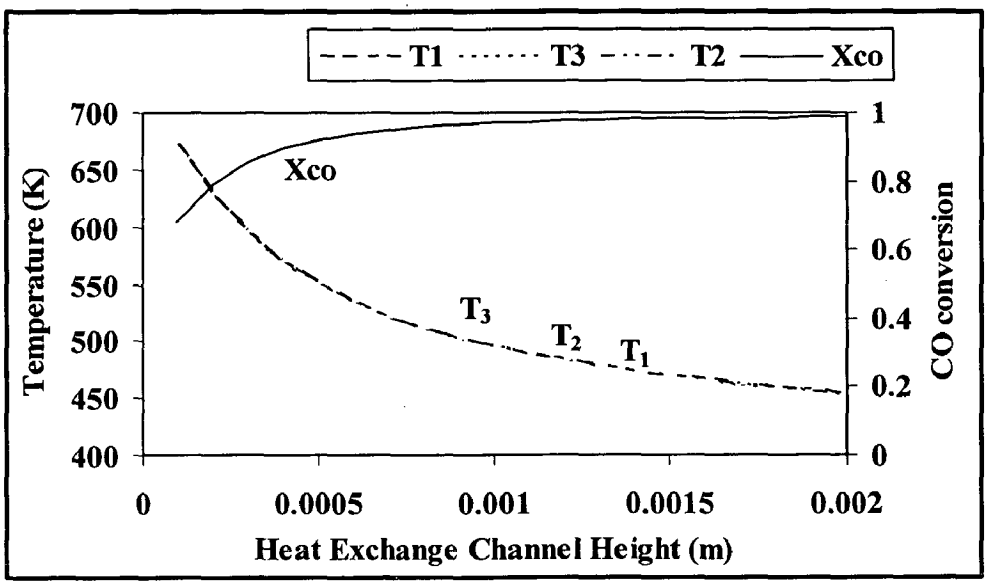

Fig.4.4(b). Effect of heat-exchange-channel (h_1) height with heat conduction

4.1.5. Effect of wall-channel height (h_2)

From this, we observed that with increase of wall-channel height, exit CO conversion is decreases and deviation between exit temperature of reactant stream and heat exchange stream is increases for the case-1 [Fig.4.5(a)]. While, for the case-2, with increase of wall-channel height, exit CO conversion is increases, exit temperature of reactant stream is decreases and exit temperature of heat exchange stream and wall-channel is increases almost together [Fig.4.5(b)].

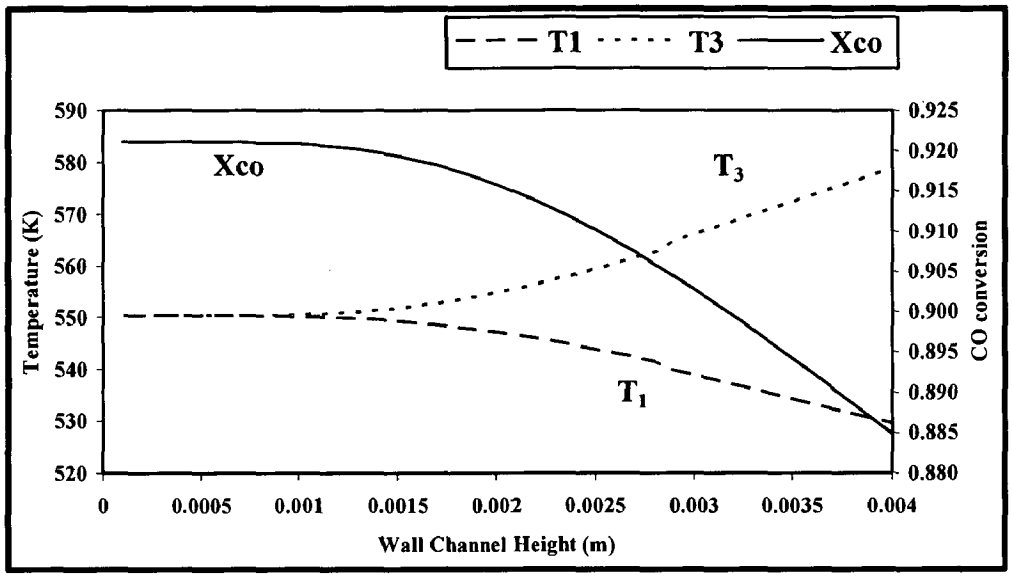

Fig.4.5(a). Effect of wall-channel height (h_2) without heat conduction

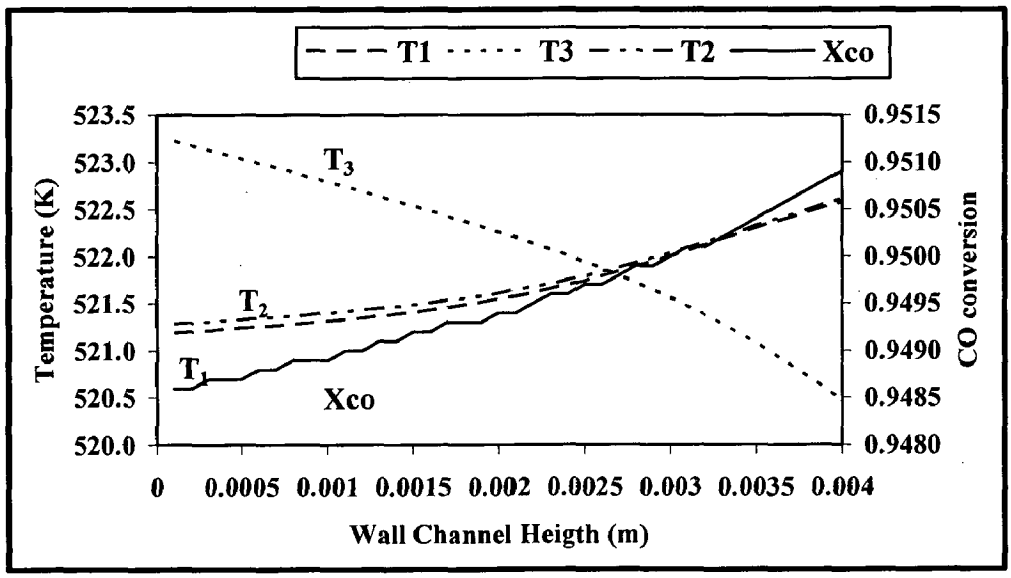

Fig.4.5(b). Effect of wall-channel height (h_2) with heat conduction

4.1.6. Effect of wall-thermal conductivity (λ_2)

From this, we observed that with increase of wall-thermal conductivity, exit CO conversion is increases for the case-1 and case-2 [Fig.4.6(a)-(b)]. For the case-1, with increase of wall-thermal conductivity, deviation between the exit temperature of reactant stream and heat exchange stream is decreases [Fig.4.6(a)]. While, for the case-2, exit temperature of heat exchange stream and wall-channel is an increase in starting and then decreases [Fig.4.6 (b)].

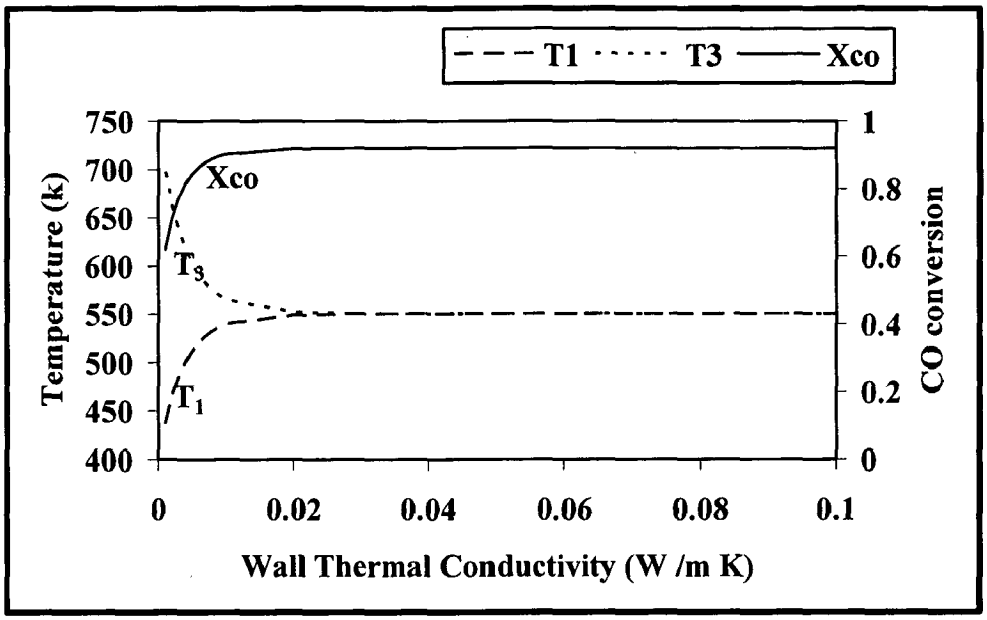

Fig.4.6(a). Effect of thermal conductivity (λ_2) without heat conduction

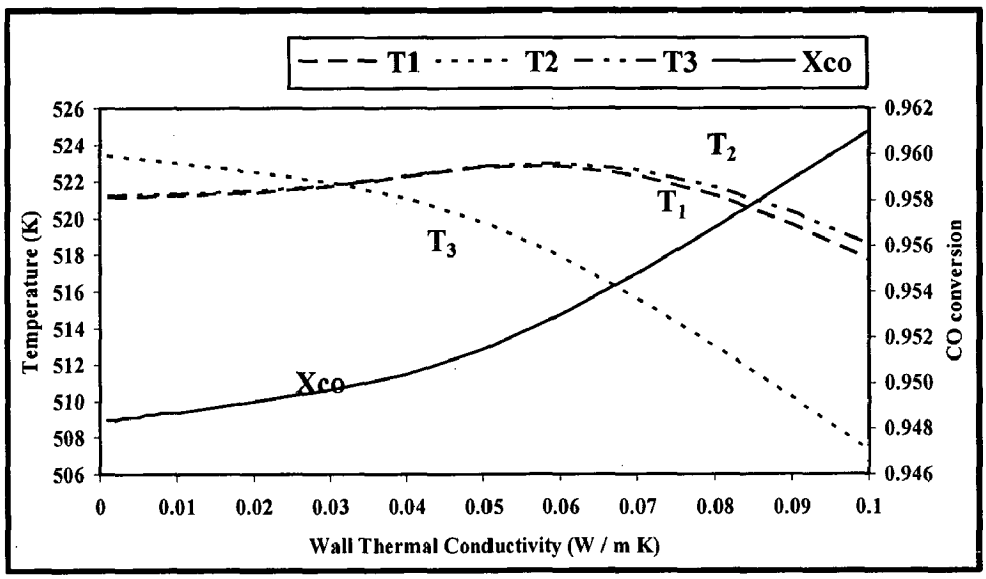

Fig.4.6(b). Effect of thermal conductivity (λ_2) with heat conduction

4.1.7. Effect of reaction-temperature (T_3) on CO conversion

From this, we observed that with increase of reaction-temperature, exit CO conversion is decreases fast for the case-1 fast and slow for case-2 and exit CO conversion is higher for the case-2 as compared to case-1 [Fig.4.7].

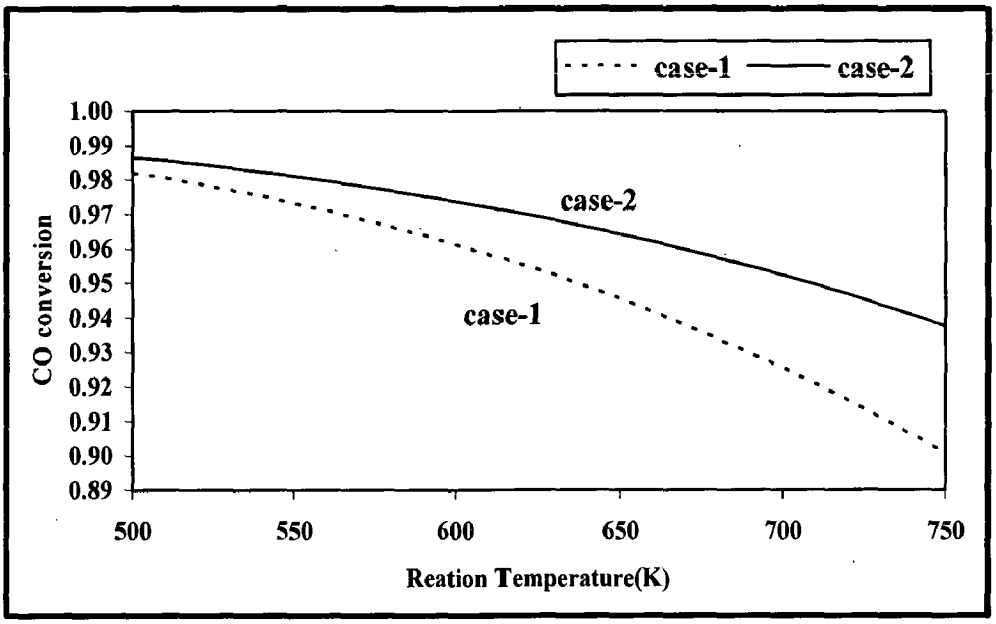

Fig.4.7. Effect of reaction-temperature (T_3) on CO-conversion

4.1.8. Effect of heat-exchange-temperature (T_1) on CO conversion

From this, we observed that with increase of reaction-temperature, exit CO conversion is decreases for the case-1 and case-2 both [Fig.4.8].

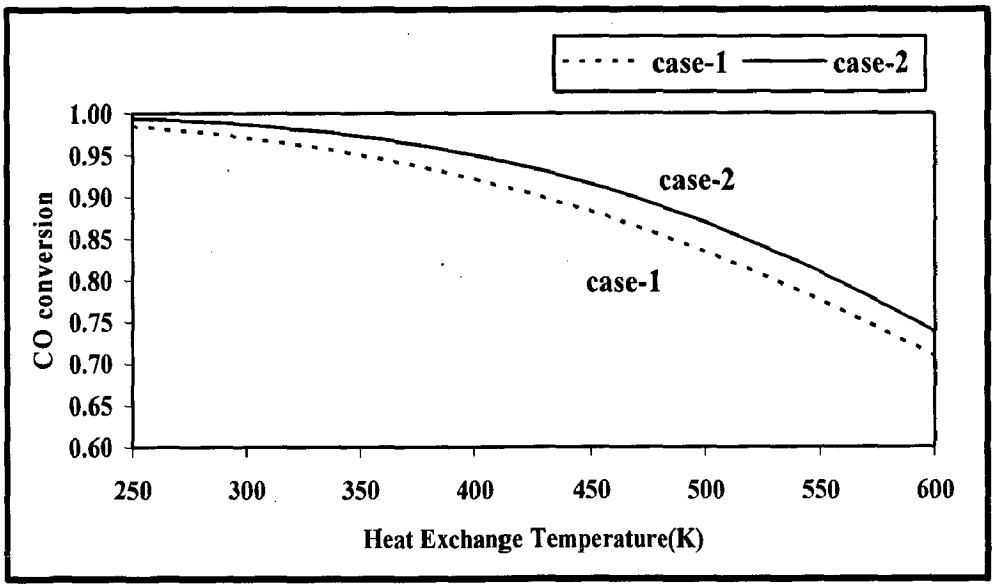

Fig.4.8. Effect of heat-exchange-temperature (T_1) on CO-conversion

4.1.9. Effect of heat-exchange-velocity (u_1) on CO conversion

From this, we observed that with increase of heat-exchange-velocity, exit CO conversion is increases for the case-1 and case-2 both and exit CO conversion is higher for the case-2 as compared to case-1 [Fig.4.9].

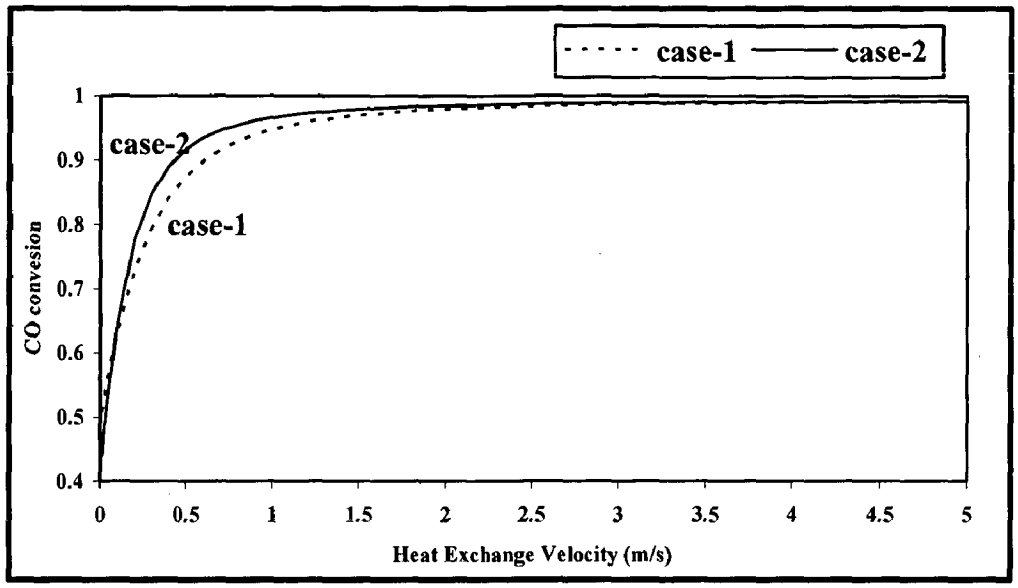

Fig.4.9. Effect of heat-exchange-velocity (u_1) on CO-conversion

4.1.10. Effect of channel-width (b)

From this, we observed that with increase of channel-width, exit CO conversion is increases and deviation between exit temperature of reactant stream, heat exchange stream and wall-channel is decreases [Fig.4.10].

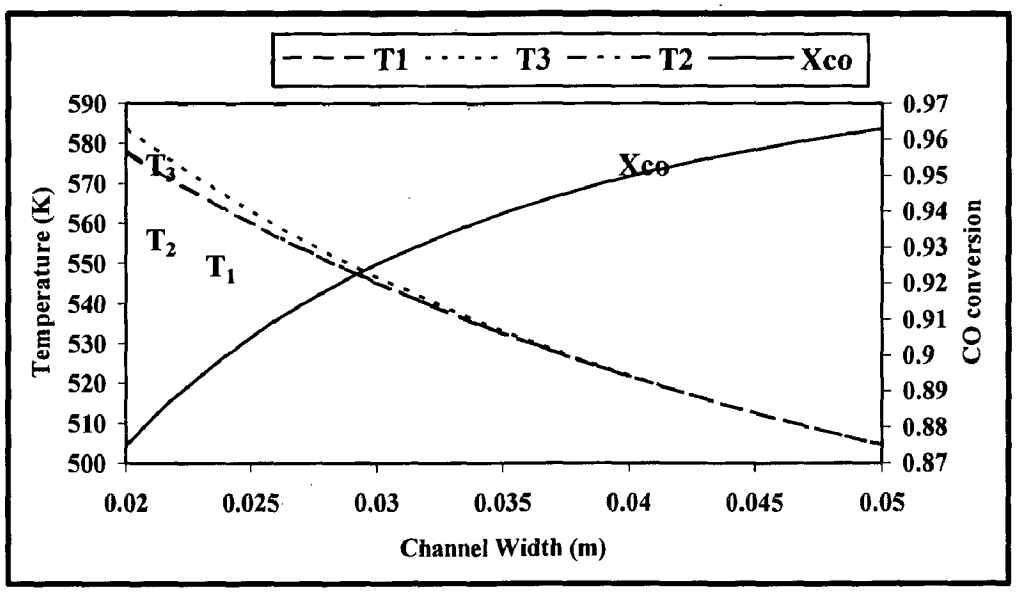

Fig.4.10. Effect of channel-width (b) with heat conduction

4.1.11. Optimized WGSR temperature profile

This is a WGS reactor temperature profile with all optimized parameters as mention in Table 4.1 for the case of heat conduction through wall-channel [Fig.4.11].

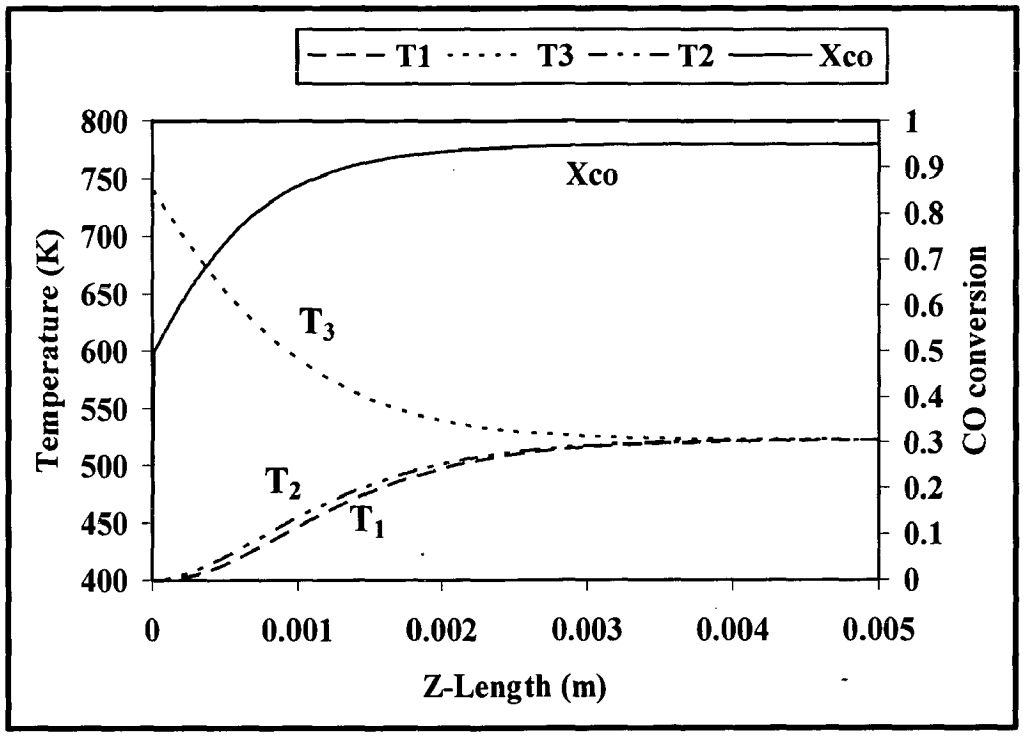

Fig.4.11. Optimized WGS reactor temperature profile

4.2 STUDY OF WGSR IN MMCR

For the membrane micro-channel reactor, we have considered the three cases as with and without heat conduction through the wall-channel and with and without the heat exchange stream-cooling medium i.e. air. For this three cases, we have study molar fraction profiles for all species (CO, CO_2, H_2O, and H_2) along the z-axis and also WGS reactor temperature profile.

CASE-1: Without the heat conduction and heat exchange stream

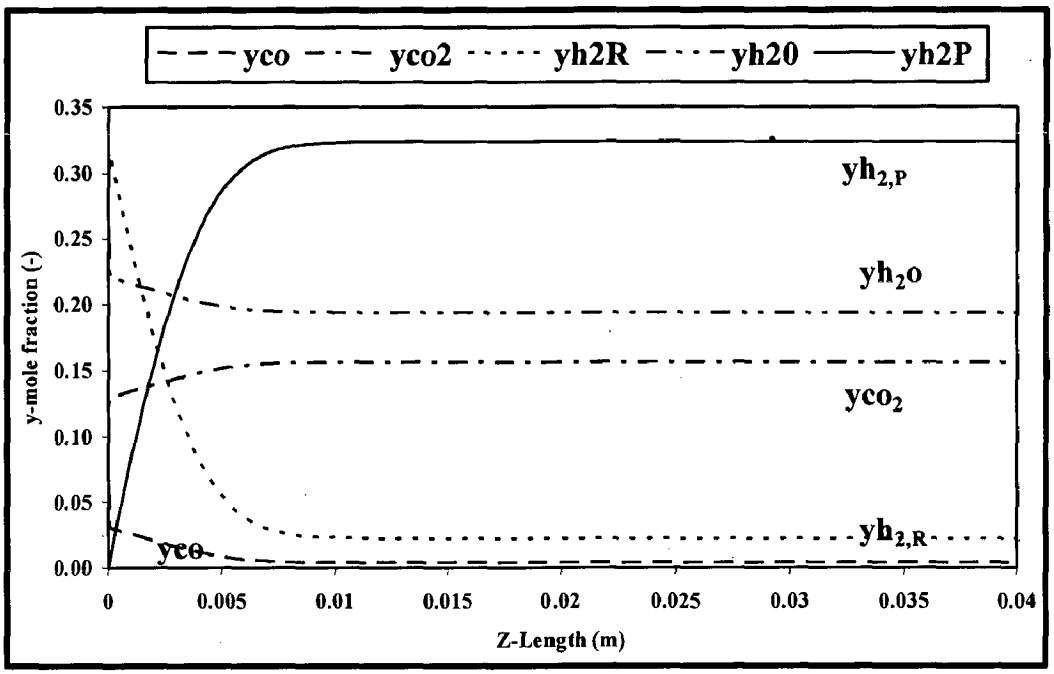

Fig.4.12. Mole fraction of the reaction species vs. axial co-ordinate

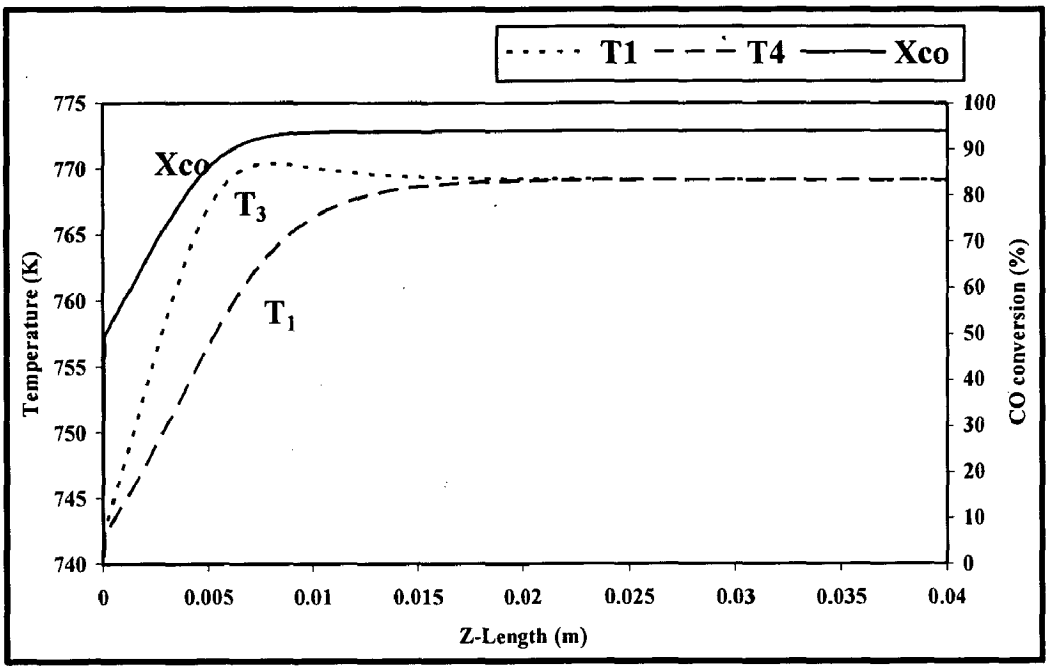

Fig.4.13. WGS reactor temperature profile

CASE-2: Without the heat conduction and with heat exchange stream

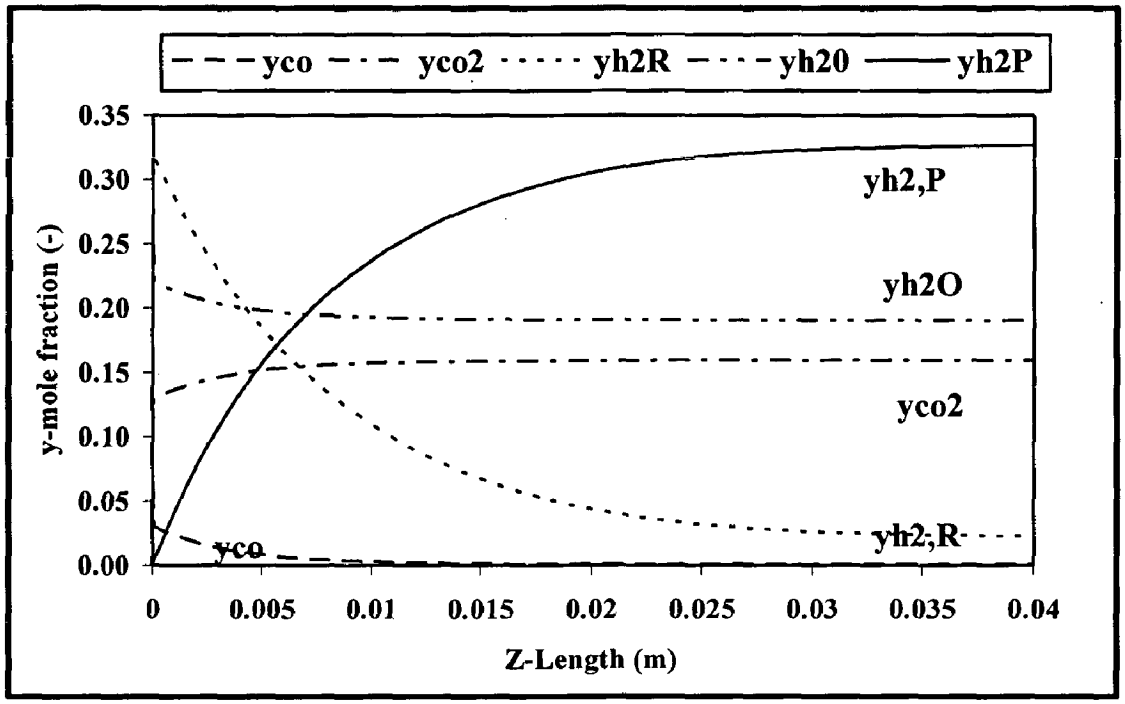

Fig.4.14. Mole fraction of the reaction species vs. axial co-ordinate

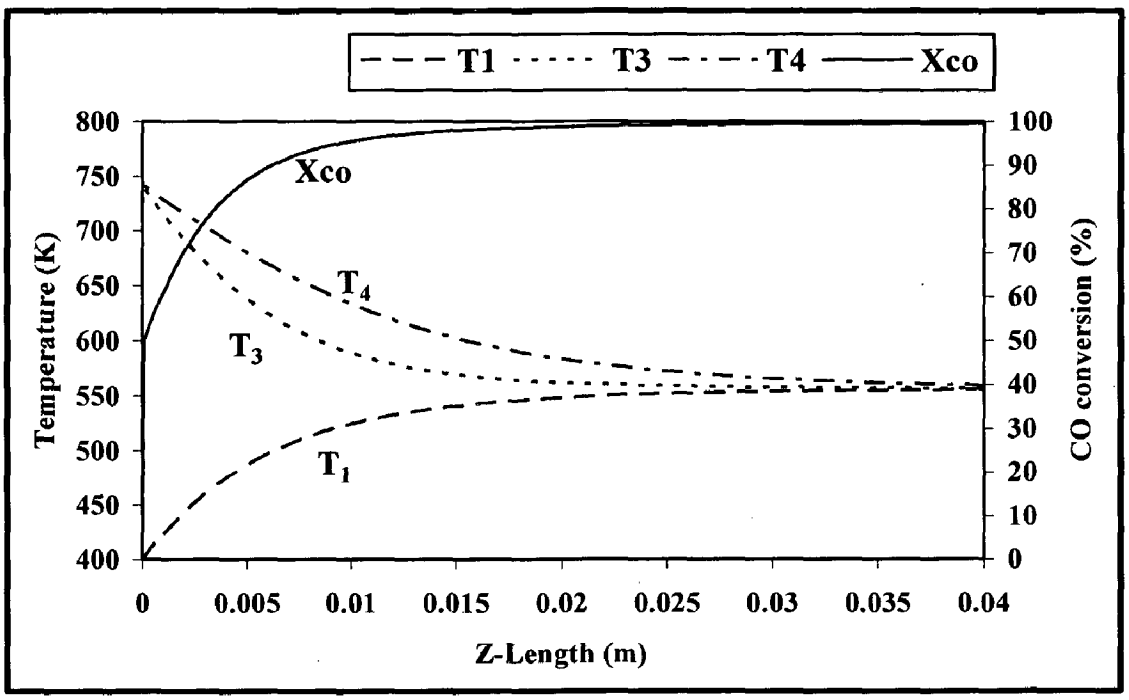

Fig.4.15. WGS reactor temperature profile

CASE-3: With heat conduction and heat exchange stream

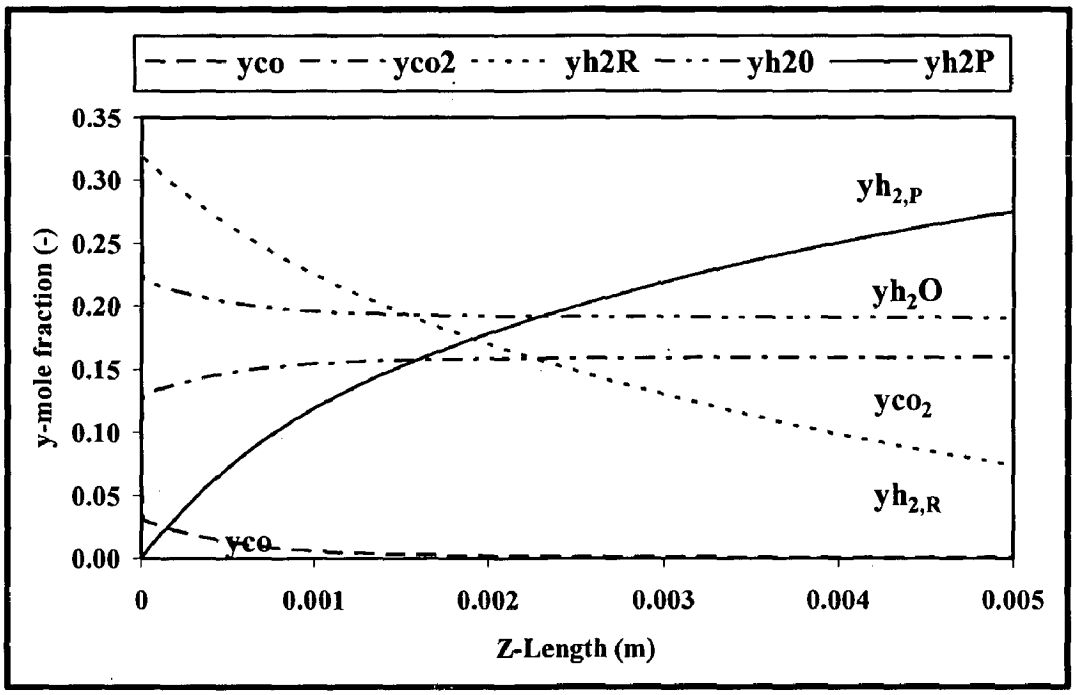

Fig.4.16. Mole fraction of the reaction species vs. axial co-ordinate

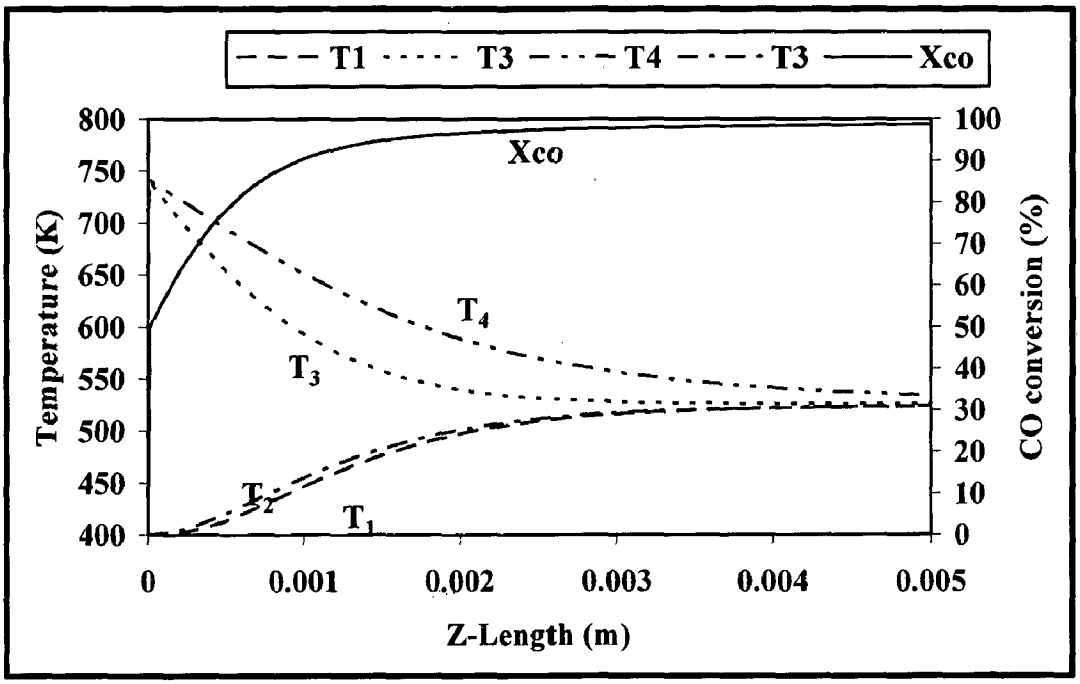

Fig.4.17. WGS reactor temperature profile

CHAPTER 5

CONCLUSIONS AND RECOMMENDATIONS

5.1 CONCLUSIONS

The water gas shift (WGS) reaction is widely used in the clean up process for the removal of carbon monoxide from the reformate gases. This study has introduced and integrated heat exchange and reaction design for micro-channel reactor with and without heat conduction through the wall-channel. The integrated design enables the integration among various components in a system through a heat exchange medium. The model has been utilized to perform a parametric study on WGS reaction to characterize the integrated micro-channel reactor performance.

The study investigated the sensitivities of micro-channel reactor design parameters such as micro-reactor length (Z), reaction-channel height (h_3), heat-exchange-channel height (h_1), wall-channel height (h_2), wall-thermal conductivity (λ_2), channel-width (b) and the optimized operating parameters are identified for the both case of micro-channel reactor. We also studied the effect of reaction-temperature (T_3), heat-exchange-temperature (T_1), heat-exchange-velocity (u_1) on CO conversion.

From this study, we observed that micro-reactor length (Z) for the micro-channel reactor with heat conduction through the wall-channel [0.005 m] that is smaller than the case of the micro-channel reactor without heat conduction through the wall-channel [0.04 m]. We also found the higher CO conversion for the micro-channel reactor with heat conduction through the wall-channel than without heat conduction through the wall-channel.

We also considered membrane micro-channel reactor with and without the heat conduction through the wall-channel and also with and without heat exchange stream-cooling medium (air). We used palladium as membrane for this study because its offer high perm-selectivity for hydrogen as compare to other species. For this reactor, we have used the optimized operating parameters that are identified in the micro-channel reactor and we studied the water gas shift temperature profile and mole fraction profile of each species for the three case of membrane micro-channel reactor. We also found the higher CO conversion for the membrane micro-channel reactor with heat exchange medium than

without heat exchange medium in case of without heat condution through the wall-channel. We also found the same CO conversion for the membrane micro-channel reactor with heat exchange medium with and without heat conduction through wall-channel.

5.2 RECOMMENDATIONS FOR FUTURE WORK

- For this study, we have taken the reactant gas composition and feed flow rates from Kim et al.(2005), typical exit stream compositions of a steam reformer (SR) or auto-thermal reactor (ATR) is used as the feed gas compostion for WGSR. Therefore, instead of using the data from published paper, we should use the industrial data in order to optimize the performance of these reactors.
- Here, we have calculated the heap capacity of each species and heat of reaction according to the thermodynamic property. We should study these parameters in the laboratory and then can be applied at industrial scale.

REFERENECES

1. Acres, G.J.K., Recent advances in fuel cell technology and its applications, J. Po. Sou., 2001, 100, 60–66.
2. Alfadhel, K.A., and Kothare, M.V., Microfluidic modeling and simulation of flow in membrane microreactors, Chem. Eng. Sci. 2005b, 60, 2911 – 2926.
3. Alfadhel, K.A., and Kothare, M.V., Modeling of multicomponent concentration profiles in membrane microreactors, Ind. Eng. Chem. Res., 2005a, 44, 9794-9804.
4. Alonso-Amigo, M.G., Polymer microfabrication for microarrays, microreactors and microfluidics, J. Asso. Lab. Auto., 2000, 5(6), 96-101.
5. Amadeo, N.E., and Laborde, M.A., Hydrogen production from the low-temperature water-gas shift reaction: kinetics and simulation of the Industrial Reactor, Int. J. Hyd. Ene., 1995, 20(12), 949-956.
6. Andreeva, D., Idakiev, V., Tabakova, T., Ilieva, L., Falaras, P., Bourlinos, A., and Travlos, A., Low-temperature water-gas shift reaction over Au/CeO_2 catalysts, Cat. Tod., 2002, 72, 51–57.
7. Aoki, N., Hasebe, S., and Mae, K., Mixing in microreactors: effectiveness of lamination segments as a form of feed on product distribution for multiple reactions, Chem. Eng. J., 2004, 101, 323–331.
8. Baier, T., and Kolb, G., Temperature control of the water gas shift reaction in microstructured reactors, Chem. Eng. Sci., 2007, 62, 4602 – 4611.
9. Barnett, B.M., and Teagan, W.P., The role of fuel cells in our energy future, J. Po. Sou., 1992, 37, 15–31.
10. Basheer, C., Shahitha, F., Hussain, J., Lee, H.K., and Valiyaveettil, S., Design of a capillary-microreactor for efficient Suzuki coupling reactions, Tetra. Let., 2004, 45, 7297–7300.
11. Basile, A., Chiappetta, G., Tosti, S., and Violante, V., Experimental and simulation of both Pd and Pd/Ag for a water gas shift membrane reactor, Sep. Purif. Tech., 2001, 25, 549–571.

12. Basile, A., Criscuoli, A., Santellab, F., and Driol, E., Membrane reactor for water gas shift reaction, Gas. Sep. Purif., 1996, 10(4), 243-254.

13. Basile, A., Paturzo, L., and Gallucci, F., Co-current and counter-current modes for water gas shift membrane reactor, Cat. Tod., 2003, 82, 275–281.

14. Bell, N.H., and Edgar, T.F., Modelling of a fixed-bed water-gas shift reactor 1. Steady-state model verification, J. Proc. Cont., 1991, 1, 22-31.

15. Bell, N.H., and Edgar, T.F., Modelling of a fixed-bed water-gas shift reactor 2. Variable catalyst, activity effects and dynamic testing, J. Proc. Cont., 1991, 1, 59-67.

16. Brown, L.F., A comparative study of fuels for on-board hydrogen production for fuel-cell- powered automobiles, Int. J. Hyd. Ene., 2001, 26, 381–397.

17. Brunetti, A., Caravella, A., Barbieri, G., and Drioli, E., Simulation study of water gas shift reaction in a membrane reactor, J. Mem. Sci., 2007, 306, 329–340.

18. Brunettia, A., Barbieria, G., Driolia, E., Granatob, T., and Leec, K.H., A porous stainless steel supported silica membrane for WGS reaction in a catalytic membrane reactor, Chem. Eng. Sci., 2007, 62, 5621 – 5626.

19. Choi, Y., and Stenger, H.G., Water gas shift reaction kinetics and reactor modeling for fuel cell grade hydrogen, J. Po. Sou., 2003, 124, 432–439.

20. Creer, J.G., Jackson, P., Pandy, G., and Percival, G.G., and seddon, D., The design and construction of a multichannel microreactor for catalyst evaluation, App. Cat. 1986 22, 85-95.

21. Damle, A.S., Gangwal, S.K., and Venkataraman, V.K., A simple model for a water gas shift membrane reactor, Gas sep. and Purif., 1994, 8(2), 101-106.

22. Dittmeyer, R., Hollein, V., and Daub, K., Membrane reactors for hydrogenation and dehydrogenation processes based on supported palladium, J. Mol. Cat. A: Chem., 2001, 173, 135–184.

23. Dongho, M., and Laud, C.R.F., Assessing high-temperature water-gas shift membrane reactors, Ind. Eng. Chemi. Res., 2003, 42(4), 711-717.

24. Dupont, N., Germani, G., Veen, A.C., Schuurman, Y., Schafer G., and Mirodatos, C., Specificities of micro-structured reactors for hydrogen production and purification, Int. J. Hyd. Eng., 2007, 32, 1443 – 1449.

25. Ernst, H., Rob, B., and Knoll, M., Characterisation and application of the electrochemical plate microreactor in analytical chemistry, Electrochim. Acta., 2002, 47, 1795–1800.

26. Ernst, K.H., Campbell, C.T., and Moretti, G., Kinetics of the reverse water-gas shift reaction over Cu(110), J. Cat., 1992, 134, 66-74.

27. Figueiredo, R.T., Ramos, A.L.D., Andrade, H.M.C., and Fierro, J.L.G., Effect of low steam/carbon ratio on water gas shift reaction, Cat. Tod., 2005, 107-108, 671–675.

28. Gavrilidis, A., Angeli, P., Cao, E., Yeong, K.K. and Wan, Y.S.S., Technology and applications of microengineered reactors, Trans I. Chem. E., 2002, 80(A), 3-13.

29. Gines, M.J.L., Amadeo, N., Laborde, M., Apesteguia, C.R., Activity and structure-sensitivity of the water-gas shift reaction over Cu-Zn-A1 mixed oxide catalysts, App. Cat. A: Gen., 1995, 131, 283-296.

30. Giunta, P., Amadeo, N., and Laborde, M., Simulation of a low temperature water gas shift reactor using the heterogeneous model/application to a pem fuel cell, J. Po. Sou., 2006, 156, 489–496.

31. Gorke, O., Pfeifer, P., and Schubert, K., Water gas shift reaction and selective oxidation of CO in microreactors, App. Cat. A: Gen., 2004, 263, 11–18.

32. Goto, S., Tagawa, T., Assabumrungrat, S., and Praserthdam, P., Simulation of membrane microreactor for fuel cell with methane feed, Cat. Tod., 2003, 82, 223–232.

33. Haswell, S.J., and Skelton, V., Chemical and biochemical microreactors, Tre. Analy. Chemi., 2000, 19(6), 389-395.

34. http://en.wikipedia.org/wiki/Microreactor

35. Huang, J., Azzami, L.E., and Winston, W.S.H., Modeling of CO_2-selective water gas shift membrane reactor for fuel cell, J. Mem. Sci., 2005, 261, 67–75.

36. Huang, J., Winston, W.S.H., Effects of system parameters on the performance of CO_2-selective WGS membrane reactor for fuel cells, J. Chin. Inst. Chem. Eng., 2008, 39, 129–136.

37. Hutchings, G. J., Copperthwaite, R. G., Gottschalk, F. M., Hunter, R., Mellor, J., Orchard, S. W. and Sangiorgio, T., A Comparative evaluation of cobalt chromium oxide, cobalt manganese oxide, and copper manganese oxide as catalysts for the water-gas shift reaction, J. Cat. 1992, 137, 408-422.

38. Iyoha, O., Enick, R., Killmeyer, R., Howard, B., Morreale, B., and Ciocco, M., Wall-catalyzed water-gas shift reaction in multi-tubular Pd and 80 wt% Pd–20wt%Cu membrane reactors at 1173 K, J. Mem. Sci., 2007, 298, 14–23.

39. Jensen, K.F., Microreaction engineering - is small better? , Chem. Eng. Sci., 2001, 56, 293-303.

40. Karim, A., Bravo, J., and Datye, A., Nonisothermality in packed bed reactors for steam reforming of methanol, App. Cat. A: Gen., 2005, 282, 101–109.

41. Karnik, S.V., Hatalis M.K. and Kothar, M.V., Towards a palladium micro-membrane for the water gas shift reaction: Microfabrication Approach and Hydrogen Purification Results, J. Microelectromech. Sys., 2003, 12(1), 93-100.

42. Keiski, R.L., Desponds, O., Chang, Y.F. and Somorjai, G.A., Kinetics of the water-gas shift reaction over several alkane activation and water-gas shift catalysts, App. Cat. A: Gen., 1993, 101, 317-338.

43. Keiski, R.L., Salmi, T., and Pohjola, V.J., Development and verification of a simulation model for a nonisothermal water-gas shift reactor, Chem. Eng. J., 1992, 48, 17-29.

44. Kenis, P.J.A, Ismagilov, R.F., Whitesides, G.M., Microfabrication inside capillaries using multiphase laminar flow patterning, www.sciencemag.org, Sci., 1999, 285, 83-85.

45. Keoschkerjan, R., Richter, M., Boskovic, D., Schnurer, F., and Lobbecke, S., Novel multifunctional microreaction unit for chemical engineering, Chem. Eng. J., 2004, 101, 469–475.

46. Kim, G. Y., Mayor, J. R., and Ni, J., Parametric study of microreactor design for water gas shift reactor using an integrated reaction and heat exchange model, Chem. Eng. J., 2005, 110, 1–10.

47. Kolb, G., Pennemann, H., and Zapf, R., Water-gas shift reaction in micro-channels—Results from catalyst screening and optimization, Cat. Tod., 2005, 110, 121–131.

48. Kroll, S., Meyer, L., Graf, A.M., Beutel, S., Glokler, J., Doring, S., Klaus, U., and Scheper, T., Heterogeneous surface modification of hollow fiber membranes for use in micro-reactor systems, J. Mem. Sci., 2007, 299, 181–189.

49. Lai, S.M., Ng, C.P., Aranda, R. M., and Yeung, K.L., Knoevenagel condensation reaction in zeolite membrane microreactor, Micropor. Mesopor. Mat., 2003, 66, 239–252.

50. Lei, Y., Cant, N.W., and Trimm, D.L., Activity patterns for the water gas shift reaction over supported precious metal catalyst, Cat. Let., 2005, 103(1-2), 133-136.

51. Lei, Y., Cant, N.W., and Trimm, D.L., Kinetics of the water–gas shift reaction over a rhodium-promoted iron–chromium oxide catalyst, Chem. Eng. J., 2005, 114, 81–85.

52. Lei, Y., Cant, N.W., and Trimm, D.L., The origin of rhodium promotion of Fe_3O_4-Cr_2O_3 cayalysts for the high-temperature water-gas shift reaction, J. Cat., 2006, 239, 227-236.

53. Ma, D. and Lund, C. R. F., Assessing high-temperature water-gas shift membrane reactors, Ind. Eng. Chem. Res., 2003, 42, 711-717.

54. Mann, R.F., Amphlett, J.C., Peppley, B., and Thurgood, C.P., A mechanistic model for the water gas shift reaction over commercial catalysts containing CuO/ZnO, Int. J. Chem. Rea. Eng., 2004, 2(A5), 1-17.

55. McCreedy, T., Fabrication techniques and materials commonly used for the production of microreactors and micro total analytical systems, Tre. Analy. Chemi., 2000, 19(6), 396-401.

56. Mears, D.E., Diagnostic criteria for heat transport limitation in fixed bed reactors, J. Cat., 1971, 20, 127–131.

57. Miyazaki, M., and Maeda, H., Microchannel enzyme reactors and their applications for processing, Tre. Biotech., 2006, 24(10), 463- 470.

58. Mizsey, P., Newson, E., Truong, T., and Hottinger, P., The kinetics of methanol decomposition: a part of autothermal partial oxidation to produce hydrogen for fuel cells, App. Cat. A: Gen., 2001, 213, 233–237.

59. Mukherjee, S., Hatalis, M.K., and Kothare, M.V., Water gas shift reaction in a glass microreactor, Cat. Tod., 2007, 120,107–120.

60. Okamotoa, H., Ushijima, T., and Kitoh, O., New methods for increasing productivity by using microreactors of planar pumping and alternating pumping types, Chem. Eng. J., 2004, 101, 57–63.

61. Ovesen, C.V., Clausen, B.S., Hammershoi, B.S., Steffensen G., Askgaard, T., Chorkendorff, J.K.N., Rasmussen, P.B., Stoltze, P., and Taylor, P., A microkinetic Analysis of the Water-Gas Shift Reaction under Industrial Conditions, J. cat., 1996, 158, 170–180.

62. Quiram. D.J, Hsing, I.M., Franz, A. J., Jensen, K. F. and Schmidt, M. A., Design issues for membrane-based gas phase microchemical systems, Chem. Eng. Sci. 2000, 55, 3065-3075.

63. Rebrov, E.V., Kuznetsov, S.A., Croon, M.H.J.M., and Schouten, J.C., Study of the water-gas shift reaction on Mo_2C/Mo catalytic coatings for application in microstructured fuel processors, Cat. Tod., 2007, 125, 88–96.

64. Salmi, T., Lindfors, L., and Bostrom, S., Modeling of the high temperature water gas shift reaction with stationary and transient experiments, Chem. Eng. Sci., 1986, 41, 929-936.

65. Sandoval A., Gomez-Cortes A., Zanella R., Diaz, G., and Saniger, J.M., Gold nanoparticles: Support effects for the WGS reaction, J. Mol. Cat. A: Chem., 2007, 278, 200–208.

66. Schonfeld, H., Hunger, K., Cecilia, R., and Kunz, U., Enhanced mass transfer using a novel polymer/carrier microreactor, Chem. Eng. J., 2004, 101, 455–463.

67. Shu, J., Grandjean, B.P.A., Neste, A.V., and Kaliaguine, S., Catalytic palladium-based membrane reactors: A Review, Can. J. Chem. Eng., 1991, 69, 1036-1060.

68. Sirkar, K.K., Shanbhag, P.V., and Kovvali, A.S., Membrane in a reactor: a functional perspective, Ind. Eng. Chem. Res., 1999, 38 (10), 3717-3737.

69. Srinivasa, S., Dhingrab, A., Im, H., and Erdogan, G., A scalable silicon microreactor for preferential CO oxidation: performance comparison with a tubular packed-bed microreactor, App. Cat. A: Gen., 2004, 274(1-2), 285–293.

70. Srinivasan R., Hsing, I.M., Berger, P.E., Jensen, K. F., Firebaugh, S.L., Schmidt, M.A., Harold, M.P., Lerou, J.J., and Ryley, R.F., Micromachined reactors for catalytic partial oxidation reactions, A.I.Ch.E. J., 1997, 43(11), 3059-3069.

71. Teekateerawej, S., Nishino, J., and Nosaka, Y., Design and evaluation of photocatalytic micro-channel reactors using TiO_2-coated porous ceramics, J. Photochemi. Photobio. A: Chemi, 2006, 179, 263–268.

72. Tiggelaar, R.M., Loeters, P.W.H., Maled, P., Oosterbroek, R.E., Gardeniers, J.G.E., Croon, M.H.J.M., Schouten, J.C., Elwenspoek, M.C., and Berg, A., Thermal and mechanical analysis of a microreactor for high temperature catalytic gas phase reactions, Sen. Act. A, 2004, 112, 267–277.

73. Tiggelaar, R.M., Male, P., Berenschot, J.W., Gardeniers, J.G.E., Oosterbroek, R.E., Croon, M.H.J.M, Schouten, J.C., Berg, A., and Elwenspoek, M.C., Fabrication of a high-temperature microreactor with integrated heater and sensor patterns on an ultrathin silicon membrane, Sens. Act. A, 2005, 119, 196-205.

74. Tomita, A., Hirabayashi, D., Nagao, M., Sano M., and Hibino, T., SOFC-type microreactors that generate hydrogen for PEFC applications, Solid State Ionics, 2004, 174, 9 –13.

75. Tonkovich, A.Y., Zilka, J.L., LaMont, M.J., Wang, Y., and Wegeng, R.S., Microchannel reactors for fuel processing applications. I. Water gas shift reactor, Chem. Eng. Sci., 1999, 54, 2947-2951.

76. Tosti, S., Basile, A., Chiappetta, G., Rizzello, C., and Violante, V., Pd–Ag membrane reactors for water gas shift reaction, Chem. Eng. J., 2003, 93, 23–30.

77. Wan, Y.S.S., Chau, J.L. H., Gavriilidis, A., and Yeung, K.L., et.al., Design and fabrication of zeolite-based microreactors and membrane microseparators, Microporous and Mesoporous Materials, 2001, 42, 157-175.

78. Worz, O., Jackel, K.P., Richter, and T., and Wolf, A., Microreactors, a new efficient tool for optimum reactor design, Chem. Eng. Sci., 2001, 56, 1029-1033.

79. Xue, E., Keeffe, M.O., and Ross, J.R.H., Water-gas shift conversion using a feed with a low steam to carbon monoxide ratio and containing sulphur, Cat. Tod., 1996, 30, 107-118.

80. Yahiro, H., Murawaki, K., Saiki, K., Yamamoto, T., and Yamaura, H., Study on the supported Cu-based catalysts for the low-temperature water–gas shift reaction, Cat. Tod., 2007, 126, 436–440.

81. Yamamoto, S., Hanaoka, T., Hamakawa, S., Sato, K., and Mizukami, F., Application of a microchannel to catalytic dehydrogenation of cyclohexane on Pd membrane, Cat. Tod., 2006, 118, 2-6.

82. Yeung, K.L., Zhang, X., Lau, W.N., and Aranda, R.M., Experiments and modeling of membrane microreactors, Cat. Tod., 2005, 110, 26–37.

83. Zerva, C., and Philippopoulos, C.J., Ceria catalysts for water gas shift reaction: Influence of preparation method on their activity, App. Cat. B: Env., 2006, 67, 105–112.